PREDICTING PRECISION NITROGEN SIDE-DRESS APPLICATIONS FOR MAIZE WITH A SIMULATION MODEL

by

ARIANNA TOFFANIN

(Under the Direction of George Vellidis)

ABSTRACT

Three fertilization strategies × three irrigation strategies were compared in replicated plot study designed to evaluate management strategies with the potential to improve water use efficiency (WUE) and nitrogen use efficiency (NUE) in the southeastern Coastal Plain of the USA. Scheduling irrigation using the SmartIrrigation Corn App and automated soil moisture sensor networks, and applying side-dress nitrogen using fertigation resulted in higher WUE and NUE. One fertigation treatment used the STICS crop growth model (INRA, France) to schedule side-dress applications. The model simulations matched field observations well for biomass, nitrogen in biomass and yield but did less well for soil water and nitrogen content. Fertigation scheduling with the model resulted in high yield but not in higher NUE than other fertigation scheduling approaches. Using models like STICS to predict the timing of N applications in maize has potential but additional research is needed to develop robust methodologies.

INDEX WORDS: irrigation scheduling, soil moisture sensors, checkbook method, SmartIrrigation, crop model, STICS, WUE, NUE

PREDICTING PRECISION NITROGEN SIDE-DRESS APPLICATIONS FOR MAIZE WITH A SIMULATION MODEL

by

ARIANNA TOFFANIN

BS, University of Padova, Italy, 2017

A Thesis Submitted to the Graduate Faculty of The University of Georgia in Partial Fulfillment of the Requirements for the Degree

MASTER OF SCIENCE

ATHENS, GEORGIA

2019

PREDICTING PRECISION NITROGEN SIDE-DRESS APPLICATIONS FOR MAIZE WITH A SIMULATION MODEL

by

ARIANNA TOFFANIN

Major Professor:	George Vellidis
	Maurizio Borin
Committee:	Miguel Cabrera
	Brenda Ortiz

Electronic Version Approved:

Ron Walcott
Interim Dean of the Graduate School
The University of Georgia
December 2019

ACKNOWLEDGEMENTS

I would like to thank the United States Department of Agriculture National Institute of Food and Agriculture (USDA NIFA) for providing the financial support for this research. I would also like to thank my major professors dr. George Vellidis for his guidance and support, and the other members of the committee members dr. Maurizio Borin, dr. Miguel Cabrera and dr. Brenda Ortiz for their precious advices. Thank you to the University of Padova, especially to dr. Francesco Morari for his foresight that led to the creation of this Dual Master's Degree opportunity and for having encouraged me into this adventure. Special thanks to the crew at the Stripling Irrigation Research Park for their professional experimental management and to Matthew A. Gruver for his excellent technical assistance and for all the music. Thank you to my colleagues and friends Anna and Dimitris, my roommate Kathleen and all the new friends I met in Tifton. Finally, I want to thank you my mum and dad, Damiano, and Giacomo for their support, patience, and love even five thousand miles away.

TABLE OF CONTENTS

LIST OF TABLES

LIST OF FIGURES

CHAPTER 1

INTRODUCTION AND LITERATURE REVIEW

Introduction

The world is approaching a food supply tipping point. The population is growing and expected to reach 10 billion by 2050. We will need to increase yields substantially to feed that many people. For most crops, nitrogen (N) is a critical crop input required to produce high yields. It needs to be properly managed because even short periods of deficiency can permanently decrease crop yield potential. N is an essential nutrient for plants and at the same time is the most difficult to manage among the mineral nutrients. This is because several biological and chemical processes that take place in the soil transform N applied as fertilizer to species of N that may lead to environmental side-effects of N application. Modern agriculture depends almost exclusively on inorganic manmade N fertilizers to produce the food and fiber that the world consumes.

Nitrogen is typically applied as dry or liquid sources that contain NH_4^+ (ammonium), NO_3^- (nitrate), urea, or a combination of these forms. Through biological and chemical processes in the soil, these compounds are transformed to produce two ionic forms of N that are biologically available to plants. These critical ions are NH_4^+ and NO_3^-. For plants to absorb these ions, they must be available in the soil solution - the water found in the pores or the soil matrix - or must be easily exchangeable from soil particles. Plant roots have a negative charge and can exchange cations directly with negatively charged soil particles. In the soil, NH_4^+ is quickly converted to NO_3^- by bacteria through the process of nitrification. Nitrate (NO_3^-) is highly soluble in water and easily transported below the crop root zone by rain or excess irrigation. This process is called

leaching. Fertilizers that escape the root zone by leaching become environmental contaminants. Fertilizers at or near the soil surface can also be lost to the environment with surface runoff generated by rain or excess irrigation affecting surface water quality and creating problems of eutrophication. The denitrification process can reduce N from the nitrate form (NO_3^-) up to the nitrous oxide (N_2O) form (a reactive greenhouse gas) or N^2 gas. Moreover, at high pH conditions ammonia volatilization occurs. N loss is a natural process due mainly to the mineralization of soil organic matter, but in the recent years it was greatly accelerated by agricultural practices, especially the addition of external N sources, resulting in harmful human health and the environmental effects. The United Nations Food and Agricultural Organization (FAO) estimates that N fertilizer use increased 25% over the past 10 years, exceeding 100 million tons in 2018.

N source, type and timing of application, and soil characteristics are factors affecting N losses that farmers should consider when planning the management in order to increase the overall performance of the cropping system while minimizing nutrient losses.

Maize – the world's most productive crop

Maize (*Zea Mays* L.) is the world's most productive crop in terms of yield and the most cultivated crop in the United States of America with about 33 million hectares harvested in 2018. The State of Georgia cultivates an average of about 128,500 harvested hectares, steady since 2008, recording an average production of 10,000 kg ha^{-1}.

Maize is an intensively cultivated crop with high nutritional requirements that overcome the soil replenishment capacity, thus relies on external inputs. Among the mineral nutrients, N is the most relevant; in Iowa N applications cost averages 18% and 13% of the variable costs in a maize-maize and maize -soybean rotation, respectively. N is taken up in the form of NO_3^- or NH_4^+

available in the soil solution; however, its dynamic nature often makes it the most limiting factor in maize production. Therefore, the fraction of applied N fertilizer that is absorbed and used by the plant, called nitrogen use efficiency (NUE), is at best around 50%. This means that more than half on the N applied may be lost to the environment or is immobilized in the soil organic fraction.

Managing N applications

N is therefore the most challenging nutrient to manage and to sustainably intensify agricultural systems. N availability and maize response to fertilization are mainly determined by the weather pattern during the growing season and are thus difficult to predict because of spatial and temporal variability among and within fields. Soil test analysis to assess and schedule N fertilization is ineffective due to the difficulty of collecting representative samples and the unreliability of it in case of rainfall near the time of sampling that would lead to under or overestimation of the real soil N availability, especially in sandy soils where N retention is low. The methods commonly used to determine the optimum N rate are based on the yield goal method, where the recommendation is made according to historical series of yield data. However, the lack of relationship between the economical optimum N rate and the yield level was clearly demonstrated, so these methods have low reliability. To overcome this problem, starting in the 1980s, dynamic models have been developed to account for interactions between management and environmental conditions to estimate N balance and fertilization requirements. The agricultural community is showing growing interest in these mathematical models that predict soil N. One of the best known is ADAPT-N, developed at Cornell University. However, this model was licensed and requires a considerable spending to be applied. What farmers need are inexpensive models that could increase N fertilization efficiency. The benefits provided by these systems has been widely

assessed and increase when the use is widespread across the agricultural community. Most of the maize models used in the United States of America are effective just for the mid-west, which is the leading area of maize production in the country. Among the several existing soil-crop simulation models, *STICS* (Simulateur mulTIdisciplinaire pour les Cultures Standard) was selected to be adapted to the Georgia Coastal Plain for the simulation of N availability in the soil. This model is capable of simulating the effect of climate, soil and crop management on the main dynamics of the soil-crop environment that influence plant development and the ecology of the system. Its strengths are the generality and ability to simulate a wide range of different processes, including the development and growth of the crop, and water, carbon and N balances in the soil-plant environment.

Fertigation

Alongside with agricultural models, fertigation is a further strategy that could be used to increase NUE. With this system, liquid fertilizer is applied with the irrigation water allowing small doses to be applied during the growing season. This increases the potential that applied N will be used by the crop and not lost to the environment. Models could therefore help scheduling fertigation interventions. Tools like STICS that estimate the amount of biologically available N in the root zone and that could give N scheduling information would allow growers to make conscious management decisions to move towards sustainable intensification of our agricultural production systems.

Nitrogen use efficiency

Beginning in the 1940s, average maize production started to increase boosted by the adoption of more productive hybrids and by the use of inorganic N (Christianson, et al.) fertilizer (Pruitt, 2016). Since then, the annual average yield in the United States of America has increased from about 2 Mg ha^{-1} (Kucharik, et al., 2005) to about 15 Mg ha^{-1}. From the 1980s, average N application rates have plateaued at about 155 kg N ha^{-1}, but maize yields have continued to increase by over 135 kg ha^{-1} per year. This indicates that N use efficiency (NUE) was increasing significantly. NUE is the total biomass or grain yield produced per unit of applied N fertilizer (kg grain (kg $N)^{-1}$). It is an integration of N uptake efficiency (NUpE) and N utilization efficiency (NUtE) which are the capacity of plant roots to acquire N from the soil, and the fraction of plant-acquired N to be converted to total plant biomass or grain yield, respectively (Xu, et al., 2012). NUE increased as a result of improvements in both hybrid genetics and agronomic practices. Although there are large differences in NUpE and NUtE among different maize lines and hybrids (Hirel, et al., 2011), the need for continuous improvement in N use efficiency is clear, since NUE in maize has been estimated to be less than 50% on average (Raun, et al., 1999). Low N use efficiency in most cases is a result of faulty timing of fertilization in respect to maize N uptake (Cassman, et al., 2002) (Raun, et al., 1999) (Shanahan, et al., 2008).

Nitrogen in the plant

N is an essential macronutrient for plant growth and development. Being the basic building block for enzymes and other proteins in the vegetative tissues and the grain, each unit of N supports 6.25 units of protein production. Besides this, N is an integral part of chlorophyll, whose basic structure, called porphyrin ring, is composed of 4 N and 16 C atoms. Thus, an adequate supply of N is

associated with high photosynthetic activity, vigorous vegetative growth, and a dark green color (Vos, et al., 2005). The extent of photosynthesis during grain filling also strongly influences maize grain yield (Muchow, 1988) and can be affected by many factors, including maize variety, climatic condition, CO_2 level, and temperature, as well as the available N level of the soil (Jaaffar, et al., 1988).

Maize plants contain 1 to 6% N by weight and absorb N as both nitrate (NO_3^-) and ammonium (NH_4^+). Both forms move to plant roots by mass flow and diffusion, so drought conditions can reduce plant growth, reducing N transport to plant roots and resulting in low N recovery efficiency in dry years (Kim, et al., 2008). Generally, in moist, warm, well-aerated soils, NO_3^- in the soil solution is greater than NH_4^+, thus it is absorbed in higher amounts. The high rate of NO_3^- uptake causes an increase in rhizosphere pH due to an increase in anion (HCO_3^-, OH^- and organic anions) transport out of cells (P.H., 1981). Nitrate is absorbed from the external environment into the roots by nitrate transporters (NRT1s and NRT2s).

Once in the plant, NO_3^- is reduced through an energy-requiring process that uses 1 NADH and 1 Fd (ferredoxin) for each NO_3^- reduced in protein synthesis (Sechley, et al., 1992). This process involves two reactions, the former occurring in the cytoplasm and being the reduction of NO_3^- to nitrite (NO_2^-) catalyzed by the enzyme nitrate reductase (NR), which has an activity that varies under the influence of light intensity, CO2 levels, temperature, water availability, and NO_3^- supply (Beevers, et al., 1969); under low light conditions, nitrate will be stored in the vacuole for future use. In the latter reaction, nitrite is further reduced in the chloroplast by the nitrite reductase (Kimball, et al., 2019) to produce ammonia (NH_3). Both reactions occur in series to avoid the accumulation of toxic nitrite, and the ammonia produced is immediately assimilated into amino acids by glutamine synthase (Morris, et al.)/glutamate synthase (GOGAT) using 1 ATP. The amino

acids are subsequently combined into proteins and nucleic acids. Compared to nitrate metabolism, ammonium requires one less reduction step (Havlin, et al., 2016). Although maize is capable of absorbing both nitrate and ammonium, a study from 1987 showed an increase in yield in terms of number of kernels per ear between 8% and 25% in maize fertilized with a mixture of NO_3^- and NH_4^+ compared to NO_3^- alone (Below, 1987). Beside its function as a nutrient, nitrate acts also as an important signal to regulate gene expression, plant growth, and development (Krouk, et al., 2010). Nitrate signaling can be divided into short-term, or primary nitrate response, and long-term effects. The primary nitrate response induces, in a matter of minutes, some genes involved in nitrate transport and reduction (Wang, et al., 2000) (Wang, et al., 2003) (Wang, et al., 2007) (Scheible, et al., 2004) (Gutiérrez, et al., 2007).

The long-term effects refer to the impact of nitrate on plant growth and development which includes effects on the morphogenesis of roots, plant flowering, seed dormancy, stomatal closure independent of abscisic acid, the circadian rhythm, and the transport of auxin (Alboresi, et al., 2005;Krouk, et al., 2010) (Roenneberg, et al., 1996) (Stitt, 1999) (Walch-Liu, et al., 2005) (Wilkinson, et al., 2007).

Uptake pattern and partitioning

N uptake follows a traditional sigmoidal (S-shaped) uptake pattern with two-thirds of the total plant uptake acquired by tasseling/silking (VT/R1) (Figure 1.1) (Bender, et al., 2013). Maize requires only a fraction of N during the seedling stage, but its needs escalate rapidly once it reaches the V8 growth stage. From V8, maize can reach the VT/R1 stage in about 30 days if temperature and moisture conditions are favorable. Such a rapid growth requires a large supply of N equal to more than half the total requirement to fulfill the demand of prolific green tissue development. N

uptake prior to flowering supports critical ear shoot development, kernel number and potential kernel size. However, is important to notice that the plant's needs for N do not end at tasseling, because N used for grain development originates from both remobilized N and continued N uptake from the soil, especially in the modern hybrids. Based on recent publications from experiments conducted in Illinois and Indiana, the amount of N remobilized from vegetative tissue averages 38% across different yield levels, which comes from about the 63% of the leaf N content (DeBruin, et al., 2013), and less than 20% of the stalk N as documented by further works by Pioneer. These studies point out that, as long as the N is available early, it can be stored in different tissues and remobilized during grain development. In Iowa, studies demonstrated that approximately 60% (134 kg N $acre^{-1}$) of total N is taken up by R1 for a high-yielding maize crop of about 15000 kg

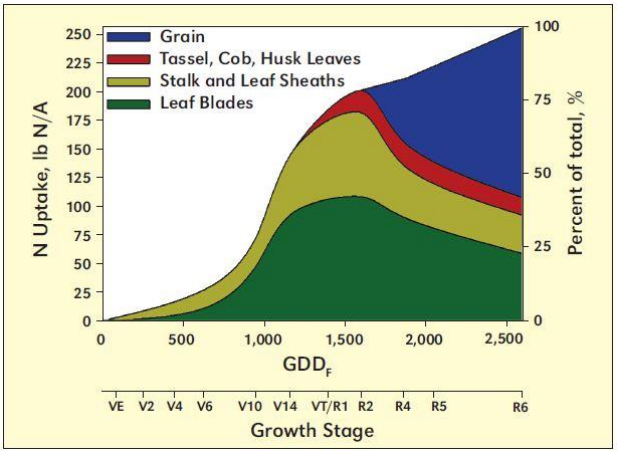

Figure 1.1 Total maize N uptake and partitioning in Illinois across four plant fractions: leaf, stalk, reproductive and grain tissues. GDD_F = growing degree days, Fahrenheit. (Bender et al., 2013)

ha^{-1} maize, while the remaining 40% is taken up post-flowering (Abendroth, et al., 2011). In 2012, a further work by Ciampitti and Vyn summarized 100 scientific reports covering old (1940 to 1990) and new (1991 to 2011) hybrids showing that, on average, new hybrids took up 29% more N post flowering than old hybrids (Ciampitti, et al., 2012). As a result, researchers, agronomists and growers may need to re-evaluate recommendations for timing of N applications to maintain adequate N supply throughout maize's reproductive stages.

Deficiency

N deficiency is characterized by the yellowing, or chlorosis, of the lower leaves because of the loss of protein N from chloroplasts. Under severe N deficiency, the chlorosis turns to necrosis that begins at the leaf tip and progresses along the midrib until the entire leaf is dead. The location of the symptoms indicates the mobility of N in the plant: as soon as the roots are unable to absorb enough N, protein in the older leaves are converted to soluble N and translocated to the active meristematic tissue to be reused in the synthesis of new protein (Havlin, et al., 2016). N deficiency significantly reduces a plant's capacity to photosynthesize (Boussadia, et al., 2010) by reducing the rates of leaf photosynthesis and new leaf area expansion. N deficiency leads to the degradation of photosynthetic pigments and proteins, and reduces enzyme synthesis in plants (Polesskaya, et al., 2004). Earlier studies in several other crops have also indicated that N deficiency reduces ribulose bisphosphate carboxylase/oxygenase (Rubisco) activity (Heitholt, et al., 1991) and production. In addition, N deficiency impacts overall plant metabolism through wide reprogramming of primary and secondary metabolic pathways (Scheible, et al., 2004). Limited N supply causes reduced plant growth and morphological changes such as increased root growth relative to shoot growth to explore a larger soil volume. An adaptive mechanism that maize adopts as a response to N deficiency is to make better use of the absorbed N within the plant (Marschner,

2011). Concerning yield response to N deficiency, Jung et al. (1972) observed equivalent yields when a single N application was made from 5 to 8 weeks (V5 to V12 stages) after planting, with a decline when N application was delayed until the ninth week or later (Jung, et al., 1972). In contrast, Binder et al. (2000) found that maize yields can decline when N applications are delayed after 6 weeks (Binder, et al., 2000). The earliest stage they assessed to be associated with significant yield reduction was V6, but in different years they also recorded situations where a deficit up to VT didn't show any decrease in yield.

Determine optimum nitrogen fertilization rate

The determination of the optimum N rate is one of the biggest challenges for farmers being that this mineral nutrient undergoes several processes that cause it to be unavailable for crop uptake.

Pre-Sidedress Nitrate Test

The dynamic nature of N makes the assessment of its availability for the growing season more difficult compared to other mineral nutrients that can be easily determined with soil tests. However, many N soil tests have been developed during the years, the most important being Pre-Sidedress Nitrate Test (Magdoff, et al., 1984) whose intent is to adjust a side-dress N recommendation linking soil N content during the V4-V5 stage (about 30 days after planting) to a critical concentration of soil nitrate.

Limitations of this practice are (1) the common difficulty of collecting representative samples due to cost and likely adverse climatic conditions and (2) its unreliability due to rainfall near the time of sampling, which can cause leaching or denitrification of nitrate mineralized from organic sources with consequent under or over estimation of the real nitrate supply capacity of the soil

(Morris, et al., 2018). In general, soil N tests can reduce the uncertainty in predicting N requirement compared to pre-season evaluations (Bundy, et al., 1988) (Andraski, et al., 2002), but present weaknesses that classify these methods as slightly reliable.

Yield goal methods

The first generation of simulation models developed to predict the optimum N rate at the beginning of the growing season are classified as static, or steady-state. Steady-state models are usually developed on average N response across multiple years in different sites and environments. Thus, they generally perform well in regions where are developed, and may not be robust in other regions with different soil, climate and crop rotations. They do not account for spatial and temporal variation of organic matter mineralization, rainfall distribution, soil moisture, temperature, hydrology, tillage, landscape position, organic carbon, and soil water-holding capacity in N requirements during the growing season (Rutan, et al., 2017). These models are based on the Stanford`s equation that quantifies the N application rate (N_{fert}) as the difference between the total N uptake by the crop (N_{crop}) and the fraction of this amount provided by the natural soil fertility (N_{soil}), adjusted by the recovery efficiency (RE_N). Being very hard to evaluate roots N content, in the calculations N_{crop} and N_{soil} are replaced by U and U_0 respectively that consider the N content of the only aboveground plant portion (Eq. 1.1). This method is also called "yield goal method" because U is estimated primarily from the attended yield (Morris, et al., 2018).

$$N_{fert} = \frac{U - U_0}{RE_N} \qquad [1.1]$$

RE_N depends on the area. Lahda et al. (2005) estimated across several US regions an average RE_N for maize of 0.65 ± 0.03 indicating that the 65% of the N applied is used by the plant while the rest overcome different processes such as leaching, volatilization, denitrification, immobilization and

surface runoff (Ladha, et al., 2005). Stanford in 1973 suggested a simplified version of his own equation that became the calculation to set the base N recommendation in all yield-base methods historically used in the US Corn Belt (Stanford, 1973) (Eq. 1.2).

$$N_f = n(Y_{GOAL}) \quad [1.2]$$

Where Y_{GOAL} is the yield goal determined differently from state to state and *n* is an empirical factor known as the "internal N requirement" of maize obtained considering U_0 and RE_N as constants and U as directly proportional to yield, its value is usually between 1.79 and 2.14 x 10^{-2} kg N (kg grain)$^{-1}$. Georgia utilizes the latter.

A first expansion of the above equation consists in adjusting the calculation with the so called "credits" factors that accounts for other sources of N that contribute to the N uptake and that thereby reduce N_{fert} value (Eq. 1.3). These N sources accounting for fertilizer equivalents are previous legume crops (N_{LN}), residual N from earlier than the previous growing season (N_{RLN}), manure inorganic N from fresh application (Banger, et al.), manure organic N from fresh application (N_{MON}), soil nitrate (N_{SNO3}), soil organic matter (Qin, et al.), and residual soil nitrate (N_{RNO3}). All these values are empirically estimated, site specific and are subtracted from the base recommendation.

$$N_f = n\,(Y_{GOAL}) - N_{LN} - N_{RLN} - N_{MIN} - N_{MON} - N_{SNO3} - N_{SOM} - N_{RNO3} \quad [1.3]$$

N_{LN} in Georgia corresponds to 22 to 45 kg ha^{-1} when maize is rotated with soybean (*Glycine max* L.) or peanuts (*Arachis hypogaea* L.) (Noland, 2018). Although all these are clear conceptual models, they have many limitations. Indeed, yield-based approaches are questioned from early 2000s mainly for four reasons: (i) the assumption that U_0 and RE_N are constant across space and time while they vary greatly depending on soil properties, management practices and climatic conditions even through the growing season, (ii) the poor relationship between the recommended

N rate and the economic optimum N rate observed in N rate response trials (high maize yields are not indicative of high N fertilization need), (iii) lack of a standard methodology to pre-season determination of the yield goal, (iv) use of inappropriate adjustments for nonfertilizer N sources that should be adjusted for their efficiency factor, data rarely available (Sawyer, et al., 2006). As a general statement, all the models based on empirical data are subjected to this kind of problem being time consuming and expensive to obtain enough data to get enough accuracy for all conditions. However, these equations are the fundamentals of more detailed models, having some strength such as the soundness for farmers and the ease to be implemented in the simplest forms.

Maximum Return to Nitrogen - MRTN

In 2004 a new static method to determine the fertilizer N rate was first outlined by Nafziger et al. (Nafziger, et al., 2004). It is the MRTN (maximum return to nitrogen) nowadays calibrated and validated for seven states in the Corn Belt. The goal of this method was to standardize the guidelines to N rate recommendations across the different states and environments, making use of yield response data rather than crop yield. In this system trial data are fitted with the best response function and then uploaded to a database that hence provides the site response to N fertilization. The database is constantly updated allowing the application of recent research and being up to date with changing climatic conditions, maize hybrids, and crop production practices. This model requires state and region of interest, crop rotation, and N and crop price as input to return a graphical representation of the net return ($ acre^{-1}) at different N rates between 0 and 250 lb N acre^{-1} (0-280 kg ha^{-1}) highlighting the range of N rate application that allow maximum return to N in $ acre^{-1}. The net return is the value of maize production minus the cost of N used. The optimum rate range corresponds to the point of yield plateaus after which net returns starts diminishing.

However, this method has not been calibrated and validated in the state of Georgia that still uses the yield goal system, so we do not delve into the description.

Actual nitrogen recommendations in GA

The UGA College of Agricultural & Environmental Sciences recommends N fertilization in Georgia based on yield goals (Noland, 2018). The traditional fertilization method requires 1.2 pound (1.34 kg) of N per bushel (25.4 kg) of expected grain yield, which corresponds to a N rate of 300 lb N $acre^{-1}$ (336 kg ha^{-1}) in the average irrigated field with a yield goal of 250 bu/a. This rate should be reduced by 20 to 40 pounds per acre maize following peanuts and soybeans, and by 80 to 100 pounds per acre following alfalfa or a legume winter cover crop that is allowed to bloom. The total amount of N applied can be split in several applications. One approach is to apply 25 to 30% prior to or at planting, and the remainder as a side-dress application when the maize is about 50 cm high or applied through fertigation in 3 or 4 events at 7 to 10 days intervals from V6 on.

Dynamic models

As the name suggest, dynamic models account for the dynamic interactions between management and environmental conditions to estimate N fertilizer requirements (Setiyono, et al., 2011). The development of computer models that simulate natural processes and their interactions is currently one of the most promising strategies to predict and keep monitored N availability in the field. As stated by Holzworth (2014), simulation models provide benefits to the environment as well as to food security and to the overall farm management that are enhanced when the use is widespread across the agricultural community (Holzworth, et al., 2014).

History of agricultural systems modeling

Models are fundamental tools to conduct studies in the complex agricultural systems. Agricultural simulation models are defined by the USDA (United States Department of Agriculture) as approximations of the actual processes, process interactions, and matter and energy exchanges that take place in the real world. Process information have been translated into theories and mathematical models. These equations are implemented in computer simulation tools, which can then be tested, modified, and/or (in)validated against new experimental data (Köhne, et al., 2009). Although models are imperfect abstractions of the real world, they are useful for understanding and predicting performances of the agro-ecosystem. Agricultural simulation models play increasingly important roles in the development of sustainable land management across different conditions, especially because data collection might be tedious and impracticable in many situations. However, data are needed to develop, run, and evaluate models. Beside research, models are promising tools for land managers and policymakers to identify management options that maximize sustainability.

Models are used in Decision Support Systems (DSSs), which are computer software programs that, through models and other information, make site-specific recommendations for different disciplines, including general crop and land management (Plant, 1989) (Basso, et al., 2013). Models can apply from farm level to landscape-scale, national and global level depending on the interested target.

Modeling aims to provide agricultural information to the general public, assist in research and in the development of investment decisions, and to informs specific public policy design and implementation.

Brief history

The first use of models in agriculture is dated 1950 and was related to economical predictions of the effect of policies and to optimize the decisions at farm scale (Heady, 1957;Heady, et al., 1960) (Heady, 1957). Soon after, the International Biological Program (IBP) was created with the goal of creating research tools to study the complex behavior of ecosystems as affected by a range of environmental drivers (Worthington, 1975) (Van Dyne, et al., 1976). This was the turning point in implementing the use of models into research to gain insight into natural systems because IBP contributed strongly to the evolution of conceptual and mathematical modeling for studying natural processes and their interactions in managed systems (Coleman, et al., 2004). Models of agricultural production systems were first conceived in the 1960s. Two scientists are considered the pioneers of modeling agricultural systems: de Wit and Duncan. The former is a physicist from Wageningen University, who in the mid- 1960s believed that agricultural systems could be modeled by combining physical and biological principles and developed early computational analyses of plant photosynthesis and growth, and soil processes. W. G. Duncan is a chemical Engineer who began creating some of the first crop-specific simulation models for maize, cotton, and peanut (Duncan, 1971). These works inspired many scientists and engineers who started developing and using crop models. In 1969, a regional research project was initiated in the United States of America to develop and use production system models in cotton production. Thus, some of the first crop models were developed as new ways of studying agricultural systems that differed from traditional reductionist approaches, and inspiring others to get involved in a new, risky research approach. During this early time period, most agricultural scientists were highly skeptical of the value of models.

A global price increase of wheat and global shortages in 1972 boosted crop model development thanks to a new research program funded in the United States to create crop models for predicting the production of major crops that were grown anywhere in the world and traded internationally (Pinter Jr, et al., 2003). This led to the development of the CERES-Wheat and CERES-Maize crop models by Joe Ritchie and his colleagues in Texas (Ritchie, 1985) (Jones, et al., 1986) that are still used as implemented in the DSSAT model. At that time, the scientific community lacked a common environment to share scientific advances in this area of interdisciplinary agro-ecosystem research. I was in response of this need that Spedding, in 1976, founded the journal *Agricultural Systems* (Spedding, 1976). This tool boosted the knowledge about agricultural system modeling and represented a support tool for modelers, creating a collection of scholarly work about models and their methods of analysis. During the 1980s there were other notable government-funded initiatives in the U.S., Netherlands, and Australia that led to major developments of crop, livestock, and economic models. This includes the 1980 US Soil and Water Conservation Act that led to development of the EPIC model that is still in use today (Williams, et al., 1983) (Williams, et al., 1989) and the USAID-funded IBSNAT project that led to the creation of the DSSAT suite of crop models that incorporated the CERES and CROPGRO models (Boote, et al., 1998;Boote, et al., 2010;Jones, 1993) (Hoogenboom, 2012) (Jones, et al., 2003).

In the early 1990s, a major milestone was the establishment of the first fully funded, multidisciplinary crop modeling-oriented research group in Australia that led to the development of the APSIM suite of cropping system models that is currently one of the most widely-used suites of models (Keating, et al., 2003) (McCown, et al., 1996).

Alongside, a major event in the development of crop models is the development and diffusion of computers in the 1980s. Afterward, individual researchers could work with agricultural system

models that were being made available on personal computers or develop their own models. This revolution concerned even other fields that contributed to modeling of agricultural systems, such as computer graphics, statistical analysis, GIS, and other software being made available on several platforms (PC, smartphone, etc...). In addition, the development of the internet and world-wide web started a new era of communication and technologies that led to greater collaboration among scientists, more rapid development of agricultural models, and improved access to data. About 10 years later, another important concept was developed: open source software. This notion fits perfectly in the scientific community of agricultural system models that is constantly evolving. Already, at least two cropping system models (APSIM and DSSAT) allowed free access to model source code to enable community-based development of model components for possible inclusion in official model versions. In parallel to funded initiatives, scientists started creating consortia and networks to enhance collaboration for specific purposes. In 2010 an initiative called AgMIP (Agricultural Model Intercomparison and Improvement Project) was created with the goal of comparing and improving crop models and using the improved models to assess impacts and adaptations to climate change and climate variability at local to global scales. This work led various modeling groups to develop models that represent CO_2, water and GHG fluxes.

The continued dedication to develop reliable models has been one of the main features of many agricultural modeling efforts for cropping systems, livestock, and economics (Jones, et al., 2017).

Selection of the crop simulation model

Differences in crop simulation models (CSMs)

The long history of crop modelling has produced a large number of models, most of which have evolved from a few milestones such as CERES and EPIC (Williams, et al., 1989) (Jones, 1986) in

the USA. CSMs usually contain a relatively complete suite of biogeochemical processes, often made of sub-models that interact with each other to describe cycles of water, C and N for target ecosystems, thus any change in the environmental factors collectively affect a group of biogeochemical reactions (Brilli, et al., 2017).

CSMs are very diverse, depending on the schools of thought behind them, their history, or even the programming language in which they are written (Muller, et al., 2019). Crop models differ according to their choice of relationships and hypotheses regarding process functioning and feedback loops, and their combinations of mechanistic components (e.g. photosynthesis, soil water transport) and functional components (also termed phenomenological; e.g. radiation use efficiency, stomatal conductance) (van Ittersum, et al., 2003) (Parent, et al., 2014). In other words, a typical process can be described by using different approaches, resulting in different final outputs.

Selection of the model

For the purpose of this research we needed a crop simulation model reflecting the following characteristics: (i) publicly available, (ii) run field scale simulation, (iii) ability to simulate maize growth, (iv) ability to simulate real-time N availability in the soil-plant environment, (v) easy to calibrate, (vi) robust model giving good results in different environments and (vii) ability to make in-season N recommendations and the optional ability to (viii) simulate N leaching to quantify the N losses. In order to find the most suitable model we reviewed the capability of some of the most commonly used to fit our requirements (Table 1.1). A brief description of the models considered is provided below.

(i) **ADAPT-N** was developed at Cornell University as a combination of LEACHN model (Hutson, 20003) and a maize N uptake, growth, and yield model (Sinclair, et al., 1995). It provides field-specific, locally-adjusted side-dress N recommendations for maize production that incorporates the effects of local early-season weather, as well as basic soil, management and crop information.

(ii) **APSIM** (The Agricultural Production Systems sIMulator) (Keating, et al., 2003) developed in Australia, simulates several systems through the interaction among plants, animals, soil, climate and management. The model allows the analysis of the whole-farm system, including crop and pasture sequences and rotations, and livestock.

(iii) **CropSyst** (Cropping Systems Simulation Model) is a multi-year, multi-crop, daily time step crop growth simulation model, developed at the Washington State University (Claudio O.Stockle, 1994) CropSyst simulates the soil water and N balance, crop phenology, biomass production, crop yield, residue production and decomposition, soil erosion, and pesticide fate.

(iv) **DayCent** (Parton, et al., 1994) is the daily time-step version of the CENTURY biogeochemical model (Parton et al., 1994), able to simulate crop growth, soil C and N dynamics, N leaching and gaseous emissions (N_2O, NO, N_2, NH_3, CH_4 and CO_2) in crop fields, grasslands, forests, and savanna ecosystems. The model allows to simulate also several management practices and some external disturbances (i.e. fires) (Brilli, et al., 2017).

(v) **DNDC** (DeNitrification-DeComposition) (Li, et al., 1992) predicts crop growth, soil conditions of temperature and water content, soil C dynamics, N leaching, and trace gases emissions. From 2012 DNDC is capable of run biophysical processes of a whole-farm systems (Li, et al., 2012).

(vi) **DSSAT** (Decision Support System for Agrotechnology Transfer) (Jones, et al., 2003) integrates the effects of soil, crop variety, weather and management options of over 42 crops. DSSAT includes improved application programs for seasonal, spatial, sequence and crop rotation analyses. It can predict crop yield, resource dynamics such as for water, N and C, environmental impact (i.e. N leaching), evapotranspiration, SOM accumulation and assess the economic risks.

(vii) **EPIC** (Environmental Policy Integrated Climate) (Williams, et al., 1995) can simulate 80 crops. It can predict changes in soil, water, nutrient, pesticide movements, and crop yields due to effects of management decisions. Moreover, it can also assess water quality, N and C cycling, climate change impacts, and the effects of atmospheric CO_2. Is primarily designed to predict the effects of soil erosion on crop productivity.

(viii) **Maize-N** (Setiyono, et al., 2011) combines the Hybrid-Maize model for estimating yield (Yang, et al., 2004) with a soil organic matter mineralization scheme and empirical method for predicting the response of maize yield to N uptake.

(ix) **QUEFTS** (Janssen, et al., 1990) was developed in Wageningen, focusing on tropical conditions. The model allows N recommendations based on soil fertility status and economic profitability while fewer details are provided on mechanisms of soil N cycling within a growing season.

(x) **STICS** (Simulateur mulTIdiscplinaire pour les Cultures Standard) (Brisson, et al., 1998) is a soil-crop model which is built on a generic framework for plant description. The selection of adequate options and parameters values allows to simulate a wide range of plants. The model simulates plant growth as well as water, C and N fluxes. It allows to consider the effect of a large range of management options on agronomic and environmental outputs.

(xi) **SWAT** (Soil and Water Assessment Tool) is a small watershed to river basin-scale model used to simulate surface and ground water and predict the environmental impact of land management practices and climate change. It is widely used in assessing soil erosion, non-point pollution and regional management (Arnold J. G., 2007).

Among the models described above, only ADAPT-N, Maize-N and QUEFST provide in-season N recommendations. However, no one of these fits the selection criteria. Only QUEFTS is

Table 1.1 Status of the crop models to estimate crop-growth and environmental tradeoffs

Model	Spatial Scale	Publicly available	Corn growth	CV	Real-time N availability	In-season N recommendation	Leaching
ADAPT - N	Point	-	+	+	+	+	+
APSIM	Point	+	+	+	+	-	+
CropSyst	Point	+	+	+	+	-	+
DAYCENT	Point	+	+	-	+	-	+
DNDC	Point, regional	+	+	+	+	-	+
DSSAT	Point	+	+	+	+	-	+
EPIC	Watershed	+	+	-	+	-	+
Maize-N	Point	-	+	-	-	+	-
QUEFTS	Point	+	+	+	+	+	-
STICS	Point	+	+	+	+	-	+
SWAT	Watershed	+	+	+	+	-	+

available in the public domain, but this has been developed primarily for tropical soils which do not match our experimental conditions, and in addition it does not predict leaching and yield.

According to the simulation scale, EPIC and SWAT are more recommended for bigger areas like watersheds. Moreover, the parameterization of SWAT and DSSAT were considered too much challenging for the scope of the work. Sansoulet conducted a comparison between STICS, DayCent and DNDC simulations in spring wheat and demonstrated that STICS and DNDC provided good biomass and plant N predictions for all sites, whereas the results with DayCent were not as good, even if they were satisfactory. In the same experiment, STICS was the most effective in estimate evapotranspiration and N in the plant under rainfall excess due to its function for water excess affecting production (Sansoulet, et al., 2014).

Overall, STICS was selected as the most suitable for the intent of the research because, beside the ability to provide in-season N recommendations, it fits all the criteria of selection. Moreover, it stands out for its adaptability due to the modular structure, the minor inputs requirement compared to similar models and the robustness of its formalisms. Even though it is important to recall that N cycling strongly depends on interactions among plant growth processes, soil water dynamics and soil N dynamics that are highly non-linear and thus difficult to predict with simple approaches (Brilli et al., 2017). STICS is a crop-oriented model developed and mainly validated in continental France but tested in different locations like Guadeloupe (French West Indies) (Sierra, et al., 2003) and Eastern Canada (Sansoulet, et al., 2014) (Jégo, et al., 2011) giving promising results.

STICS

The process-based crop simulation model STICS (Simulateur mulTIdisciplinaire pour les Cultures Standard), was created at INRA, the French National Institute for Agricultural Research, in 1996

on initiative of Nadine Brisson (1998). It is a dynamic model that runs in real-time with a daily time step using readily available input data and can integrate temporal variabilities for successive crops. It is an 'engineering' model in the meaning given by Passioura (1996) because it aspires to provide management advices to farmers and sounds predictions to policy makers (Passioura, 1996). STICS's strengths are the generality and capability to simulate the effect of climate, soil and crop management on a wide range of different processes as the development and growth of the crop, and water, carbon and N balances in the soil-plant environment. STICS has a modular structure, where every module represents a set of eco-physiological processes occurring in the system and is composed of sub-modules dealing with specific mechanisms. The modules are (i) crop development, (ii) shoot growth, (iii) yield component, (iv) root growth, (v) water balance, (vi) N balance, (vii) microclimate, (viii) crop management and (ix) environment and heat, water and nitrate transfers. This design makes it a generic model easy to adapt to different crops; therefore, the model is currently adapted for nearly 30 species, including annual, perennial, herbaceous and woody plants. STICS is written in FORTRAN 77 and can be run under Windows, or any PC compatible microcomputer. The creators built it by bringing together different minor models: the GOA (Plant), BYM (water), and LIXIM (nitrogen) models, which had also been produced by INRA.

STICS incorporates robust formalisms of a generic nature that lie on known analogies or on the simplification of more complex ones. The model simulates the behavior of an average plant characterized by its aboveground biomass, leaf area index (LAI), and the biomass of harvested organs. The soil is considered as a succession of horizontal layers, each one characterized by its content of water and N at the start of the simulation, and its field capacity (Janssen, et al.), bulk

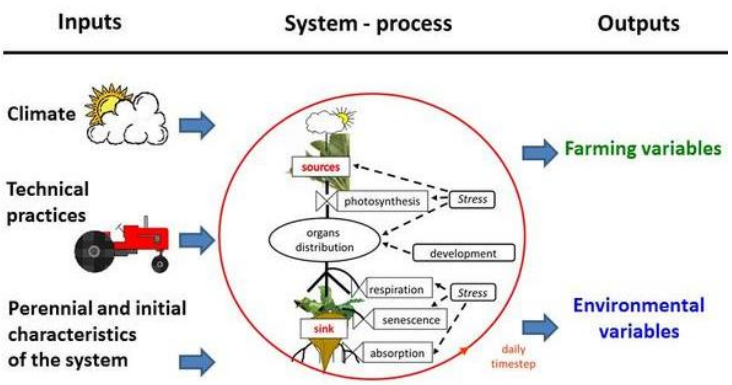

Figure 1.2 STICS model functioning principles

density, infiltrability and moisture content at permanent wilting point (PWP). Plant roots are defined with their length distribution in the soil profile.

The atmosphere is represented by a set of climate variables required as input and with a forcing function. Other inputs required are management information such as sowing date, fertilizer types and rates, and irrigation records and efficiency necessary to simulate the effect of agricultural practices. The outputs of STICS reflect the objectives of the model's creation (Figure 1.2).

Crop development

In STICS the developmental stages correspond to changes in the trophic or morphological strategy of the crop that influences the evolution of LAI or grain filling rather than organogenetic stages defined in classical agronomic scales. This module drives crop growth by organizing, throughout the cycle, the opening and closing of sinks, the establishment of the photosynthetically active system and the activation of remobilization to the storage organs. STICS uses daily updated degree-days to control the development. This method permits to consider fluctuations in growth rate due to the temperature. The radiation intercepted by the photosynthetically active system,

characterized by leaf are index, is transformed into biomass. In other words, plant growth is driven by the carbon balance. However, Ong (1983) and Pararajasingham and Hunt (1991) argued that the phasic chronology may be better simulated using a temperature closer to the plant (soil or organ) rather that the air temperature (Ong, 1983) (Pararajasingham, et al., 1991). Thus, STICS offers the possibility to adopt the idea of Idso et al. (1978) to drive the development by crop temperature (Idso, et al., 1978). The conversion from air temperature is assumed to be the arithmetic mean of the maximum crop temperature and the minimum crop temperature, these two values calculated with an energy balance of respectively the maximum and minimum values of the fluxes of net radiation (MJ m^{-2}), soil heat (°C) as a function of wind speed and net radiation, evapotranspiration (mm) and aerodynamic resistance (s m^{-1}) which requires wind speed (m s^{-1}), crop high (m) and bare soil roughness (m).

Crop development is divided into seven stages expressed in degree-days: (i) emergence, (ii) maximum acceleration of leaf growth, (iii) maximal leaf area index, (iv) beginning of grain filling, (v) beginning of net senescence, (vi) physiological maturity, and (vii) harvest. Emergence is simulated as dependent from three main factors: temperature, sowing depth, and water status of the soil that occur to be particularly important as first demonstrated by Bouaziz and Bruckler (1989) that linked a good emergence simulation to the good simulation of soil water status in the surface soil layers (Bouaziz, et al., 1989). STICS considers three subphases of emergence: (i) seed imbibition, (ii) germination, and (iii) shoot elongation. Germination failure is not considered, and plant density introduced as an input parameter corresponds to the density of emerged plants (Brisson, et al., 2003). Moreover, some plant-dependent sensitivity parameters can be used to simulate the effect of water and N stress that can generate delay during maize growth.

Shoot growth

The plant sub-system is characterized by its shoot biomass and leaf area index (LAI). The leaf growth (m^2 m^{-2} d^{-1}) is simulated at a canopy scale as a function of the phasic development (m^2 $plant^{-1}$ $degree\text{-}day^{-1}$), the effective crop temperature (degree-days) and the plant density (plant m^{-2}) combined with an inter-plant competition factor characteristic for the variety (Singels, et al., 1991) and the stress indices. The evolution of LAI is in four stages: two of growth, one of stability and one of senescence. The leaf area growth rate (m^2 $plant^{-1}$ $degree\text{-}day^{-1}$) is related to the phenological stages and is driven by a leaf development unit, values being 1 at emergence and 3 at the maximum LAI, when the growth stops. The main role of LAI in the model is the interception of radiation, on which depends the simulation of crop development, thus the accuracy is especially important during early growth and senescence; slightly lower accuracy is acceptable during the stability phase because the interception has reached its maximum. Shoot senescence only concerns leaves: dry matter and LAI. The concept of leaf lifespan is used for the simulation (Duru, et al., 1995) and dependents on the evolution of temperature, phenology and stresses are applied to the leaf area, that is considered lost through senescence once the lifetime has elapsed.

The interception of the photosynthetically active radiation (PAR) is estimated using an optical analogy, a type of Beer's law that demonstrated better predictions for homogeneous crops having leaves randomly distributed over the area than for canopies in rows, but since maize covers the row middles quickly (at V7 stage, about 30 days after emergence), we assume the formalism is applicable. The objective is to estimate, on a daily time step, the fraction of radiation intercepted by the crop and that transmitted to the soil. The radiation intercepted (MJ m^2) is function of LAI, of a daily extinction coefficient and of the ratio of PAR to the global radiation.

The daily production of shoot biomass (t ha^{-1} d^{-1}) relies on the radiation use efficiency (RUE), defined as the slope of the parabolic relationship between accumulated biomass and radiation intercepted by the crop (Monteith, 1972), in other words RUE indicate the aboveground dry weight increase per unit of intercepted PAR (Kiniry, et al., 1999). This parameter is widely employed in crop models (Jeuffroy, et al., 1999), because it synthesizes with just a few parameters the photosynthesis process. Accumulation of shoot biomass involves a maximum value of RUE that differs based on the crop growth stage. From the juvenile to the vegetative and reproductive stages the model simulates the preferential migration of assimilates towards the roots at the beginning of the cycle. The reduction of RUE for high radiation explain the parabolic shape of the relation.

Only abiotic stresses are accounted in STICS and considered independent one from each other, unless they impact the same process, situation where just the more severe is considered. Stresses are considered as indices varying from 0 to 1 to apply to the RUE function (Sinclair, 1986) that reduce plant processes according to the value of related variables such as soil available water content for water stress and the N nutrition index (INN) for N stress. INN is the ratio of actual N concentration and critical concentration referred to the same biomass. The latter comes from a 'critical dilution curve': a diagnosis tool of N nutrition so that plants below the curve experienced N deficiency and plants above it have an optimal growth. Inside the same stress, there are different indices according to the developmental stage affected.

Yield component

Yield is defined as the weight and the quality of the grain. For determinate crops like maize, STICS apply the approach of the 'dynamic harvest index' (ratio of grain biomass to total shoot biomass), inspired by Spaeth and Sinclair (Spaeth, et al., 1985). This approach assumes a linear variation of

the carbon harvest index (g grain (g plant^{-1})) as a function of time up to a threshold set to avoid simulating unrealistic yield, from the onset of grain filling to maturity. The number of grains is fixed during a critical period between 20 and 30 days before and after flowering and the mass of each grain is then calculated as the ratio of the total mass to the number of grains. The concept of harvest index is extended to N (Jérémie Lecoeur, 2001), simulated as an increasing proportion of the quantity of N in the biomass (N grain (N plant^{-1})). Both the harvest indices are calculated on a daily time step and sensitive only to the duration of grain filling to include the effect of thermal stress; water or N stresses are not accounted. The yield module is affected by almost all the STICS's modules, especially root growth, N balance, water balance, mineralization and the interaction rooting-water balance.

Root growth

Roots act as water and mineral N absorbers and are described by their growth in depth and density profile, separately. Root growth is proportional to temperature (Hunt, 1995) and dependent on water stress indices and bulk density; it starts at germination and stops when the leaf growth stops. The root profile effective for absorption is calculated with a method for high density crops called 'standard profile' that at each depth reached by the root system associates a profile of effective root density with a sigmoid shape, which represent the assumption of an exponential decrease of roots with depth (Gerwitz, et al., 1974). The growth rate of the root front is set between 0.1 and 0.2 cm by growing degree-day for maize. A threshold of 0.5 cm (cm soil^{-3}) is set as the optimal root density that permits maximal exploitation of the available water (Bonachela, 1996). In the upper layer, the effective root density can reach, but not exceed, this threshold. Thus, the profile of effective root density is simulated by a logistic function in the model.

Water balance

The water balance has the purpose of estimating soil water content, water fluxes and water stress indices. Weather variables used to compute it are rainfall, that with irrigation represent the water inputs, and evapotranspiration (EVT). EVT is composed of soil evaporation and plant transpiration. Soil evaporation is calculated in two steps: (i) potential evaporation related to the energy available at the soil level and to LAI, and (ii) actual evaporation related to water availability (Brisson, et al., 1991). Potential evaporation is calculated with a Beer's law equivalent which uses the reference potential EVT and is linked to the 'crop coefficient (K_c) approach' for estimating plant requirements. After a rain event, soil evaporation is assumed to be potential up to a threshold (mm), and then decrease according to the weather, especially wind speed, and soil type.

On a daily basis, transpiration equals absorption and is calculated in two steps, using potential EVT as the driving variable: potential crop transpiration with no water limitations and relative transpiration. The former is a logistic function of LAI which involves the maximum K_c attained when LAI is almost 5. The latter is expressed as the ratio of actual to maximal transpiration, is a bilinear function of the available water content. Such a formalism assumes that maize can uptake water at a maximal rate until the soil water content falls below a threshold determined according to root characteristics, stomatal functioning and evaporative demand (Slabbers, 1980) and tends to stabilize from a certain root depth.

Nitrogen balance

The inorganic N pool in the soil can be replenished by the addition of fertilizers, by rainfall (50% NH_4^+ and 50% NO_3^-) or by irrigation water as NO_3^-. The N balance in the soil-plant system depends on the main N transformations (mineralization, immobilization, nitrification and

denitrification) and the mineral N uptake of the crop. These processes depend mainly on soil temperature and water content. The net mineralization is the sum of the mineralization of stabilized organic matter (OM), also called basal mineralization, and of organic residues. The former is calculated as the fraction of active soil organic N times the actual mineralization rate (K2 in kg N d^{-1}). The active organic N (t ha^{-1}) is the product of organic N content in the upper layer (%), the proportion of active organic N (default value 0.35), BD (g cm^{-3}) and mineralization depth (cm). K2 is equal to the potential mineralization rate (kg N d^{-1}) at reference conditions times water content and temperature effects. These two effects are a linear function (higher water content, higher the effect) and a logistic function (over 25°C the rate slows down), respectively. Net mineralization from organic residues is assumed to follow the first order kinetics depending on the C/N ratio of the residue, soil temperature, water content and available soil N in the vicinity of the residues. The NH_4^+ derived from mineralization is rapidly transformed to nitrate through the process of nitrification that is assumed to occur in the biologically active layer (maximum depth of mineralization) according to soil temperature, soil water content and soil pH (low pH, lower nitrification and higher NH_4^+ concentration), factors that don't interact with each other. Denitrification is calculated as affected by soil temperature and prop erties like water content at FC, BD, NO_3^- content and actual water content (Hénault, et al., 2005). Both nitrification and denitrification are accompanied by N_2O emissions, considered a constant proportion of the nitrified NH_4^+ in satisfactory aerobic conditions, and constant ratio with total denitrification, respectively. Once in its mineral forms, N can be taken up by plants in an amount equal to the minimum between crop demand and soil supply. The daily N demand (kg N ha^{-1} d^{-1}) is derived from the 'critical N' curve, which value decreases as time and plant biomass increase. It is calculated as the product of the crop growth rate (t ha^{-1} d^{-1}) and the derivative of the maximal crop N content (%) relative to

the plant biomass (t ha^{-1}). Soil N supply equal to the minimum between the transport flux of nitrate from a point in the soil to the closest root via convection and diffusion, and the sink flux as the active absorption by the roots according to plant's capacity to absorb, root density and NO_3^- concentration.

Transfer of heat, water and nitrate

STICS accounts for heat transfer: daily thermal amplitude (°C) and soil temperature at depth Z (°C) are calculated using the daily thermal amplitude at the surface (difference between maximum and minimum crop temperature) and a soil thermal diffusivity coefficient (m^2 s^{-1}) (McCann, et al., 1991). Water and NO_3^- transport are simulated by a reservoir-type model for which microporosity is the mandatory compartment that has to be described. Water fills the layers by downward flow down to the bottom of the profile or to the layer in which the water content remains below FC. Soil layers affected by evaporation can dry until they reach the residual soil water content, while in deeper layers, the water is only extracted by the plant and therefore is always above PWP. The amount of NO_3^- above a certain threshold, is assumed to mix completely with the water of the layer and to drain with it. Upwards nitrate movements occur via plant uptake only (Beaudoin, et al., 2009).

The FACETS Project

The Floridian Aquifer Collaborative Engagement and Sustainability (FACETS) project is funded by a grant from the Unites States Department of Agriculture, National Institute of Food and Agriculture (USDA NIFA) and involves the University of Florida, University of Georgia, Albany State University and Auburn University (floridanwater.org). The Floridian aquifer system extends

from South Carolina and South Georgia to the all Florida and parts of Alabama and Mississippi. It is the primary source of drinking and irrigation water for most cities and rural areas in central and northern Florida as well as eastern and southern Georgia, for a total of nearly 10 million people (Marella, et al., 2005).

The problem of water pollution caused by agricultural practices raised concerns, especially related to the most fragile environments, such as rivers and springs, with which the Floridian aquifer is particularly rich (Figure 1.3). The FACETS project recognizes this problem and aims to achieve economic sustainability of agriculture and silviculture in North Florida and South Georgia while

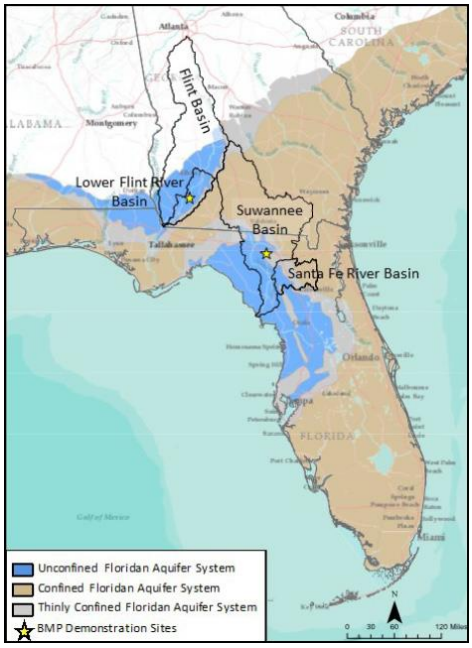

Figure 1.3 Map of the Floridan aquifer with more susceptible area highlighted (unconfined system)

protecting water quantity, quality, and habitat. This goal is being pursued through three main objectives:

1. Build a comprehensive modeling platform to predict the impacts of alternative land use and production practices on the water in the area;
2. Engage stakeholders to understand changes needed to achieve economic sustainability through their involvement in exploring different scenarios;
3. Conduct innovative agricultural Best Management Practice (BMP) research and demonstration projects. Develop and deliver digital decision toolkit and training programs for stakeholders.

My research addresses the third objective of the FACETS project and involves developing the ability to schedule N applications in maize with a simulation model for the digital decision toolkit. The simulation model will be incorporated into a smartphone app to help farmers with scheduling N fertilization applications. This type of tool is particularly important in sandy Coastal Plain soils of this area where N is very mobile. In this area, excessive rainfall or excessive irrigation events easily lead to N leaching.

Hypotheses

1. We hypothesize that the yield of the treatments where side-dress N fertilization is applied will be higher than the traditional fertilization approach;
2. We hypothesize that the simulation run with the STICS model will be accurate and representative of the real observed conditions;
3. We hypothesize the predictions to be consistent through spatial and temporal variability.

Objectives

1. Adapt, calibrate, and validate the STICS model for maize production in the Coastal Plain soils of Georgia.
2. Use the STICS model to predict the timing of nitrogen side-dress applications
3. Evaluate the performance of the model and provide recommendations on whether it is appropriate for use in the digital decision toolkit.

CHAPTER 2

MATERIALS AND METHODS

Experimental site

The experiment was carried out at the University of Georgia's C.M. Stripling Irrigation Research Park (SIRP) near Camilla, GA (31° 16' 55.2"N, 84° 17' 38.04"W). Geographically, SIRP is located in the Lower Flint River Basin within the southeastern Coastal Plain. The average annual air temperature is 19.4 °C and the mean annual rainfall is 1314 mm. The soil is deep, well-drained, moderately permeable and kaolinitic with 0 to 5 % slopes (Lucy series soil - USDA Natural Resources Conservation Service). It is loamy sand on the upper layers and sandy loam, or sandy clay loam, in the deeper layers. The experiment began in 2018 and was carried out in three small fields cropped in a peanut-maize-cotton rotation. Each field was 1.2 ha, for a total of 3.6 ha site. Each field was divided into 27 plots of about 98 m^2 (14 m long × 7 m wide) each one composed of 8 crop rows and surrounded by buffer zones as shown in Figure 2.1. The treatment structure was a factorial of three irrigation treatments and three N fertilization strategies (9 treatments in total) that were arranged in a completely randomized design with three replications. These treatments were used in each of the three fields described above, with the difference that each field had a different crop sequence (Figure 2.1). The sequence of crops in 2018/2019 was maize/cotton in one field, peanuts/maize in the second field, and cotton/peanuts in the third field.

All crops were preceded by a rye cover crop (*Secale cereale*) established in November and terminated the following spring using herbicides. For maize, rye was killed around the end of

February. Maize was sown using strip tillage at the end of March. Tillage and sowing were performed concurrently. Maize cultivar P1870 (Pioneer) was sown at a plant density of about 80 000 seeds ha^{-1} (0.91 m between rows, 0.125 m within rows) on March 29th and March 27th in 2018 and 2019, respectively. This is a yellow maize cultivar with good performance in both irrigated and higher yielding non-irrigated environments.

In 2018, N application was uniform among treatments at pre-planting and planting and differed among treatments for side-dress applications. The pre-planting application used a dry urea based pre-plant fertilizer application about three weeks before planting at 56 kg N ha^{-1}. At sowing, additional 50 kg N ha^{-1} was applied as 50% of a 28-0-0-5 fertilizer and 50% of a 20-17-0-2.5 formulation. Side-dress N applications used a liquid urea-based of grade 28-0-0-5, in different

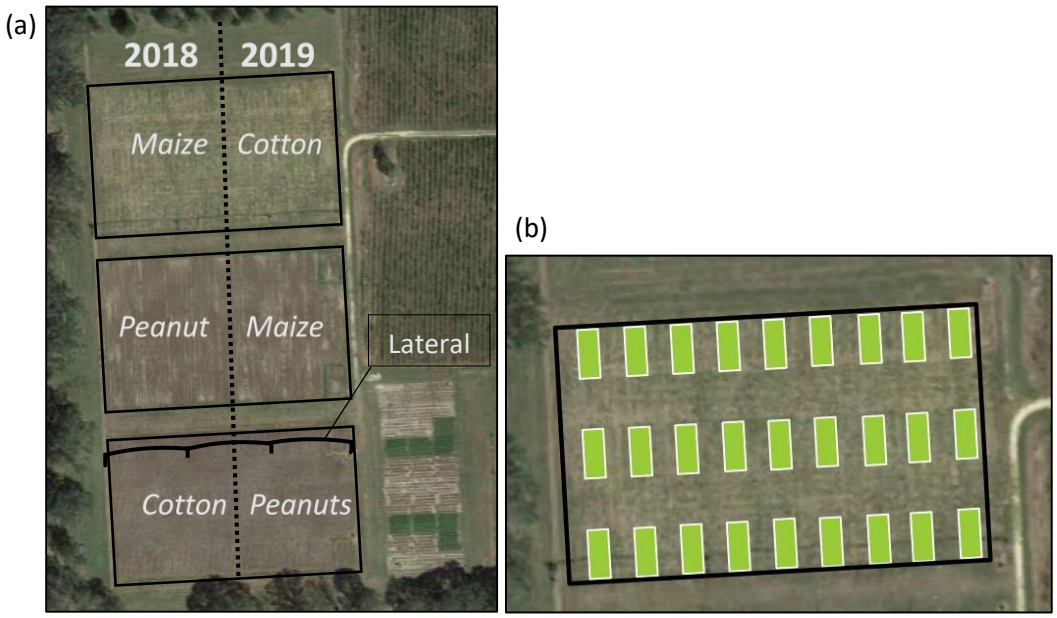

Figure 2.1 Crop grown in each of the blocks during 2018 and 2019 (a), and experimental layout of the 27 plots of each field (b)

amounts among treatments. Similar applications took place in 2019 with 57 kg N ha^{-1} applied at pre-planting, 34 kg N ha^{-1} at planting, 56 kg N ha^{-1} as a common first side-dress application and successive applications different in amount and timing among treatments (Table 2.1).

Weed control was performed using glyphosate herbicide applications before and after emergence (total of 7.60 l ha^{-1} in 2018 and 7.02 kg ha^{-1} in 2019). Rainfall, solar radiation, minimum and maximum air temperature, air humidity and wind speed were recorded daily at a standard weather station located 550 m from the plots. Maize was harvested on August 21st in 2018 and August 26th in 2019.

Irrigation strategies

The experimental site was irrigated with a lateral irrigation system equipped with variable rate irrigation controls. Each of the plots shown in Figure 2 can be irrigated with unique application rates. The irrigation strategies evaluated in 2018 and 2019 were a combination of standard / traditional strategies and emerging strategies with potential to improve irrigation water use efficiency (WUE). The three irrigation strategies tested were (i) the traditional checkbook method, (ii) the University of Georgia Smart Sensor Array (UGA SSA) and (iii) the SmartIrrigation Corn App. In this study, the University of Georgia Corn Checkbook method was considered a standard / traditional strategy and is recommended by the University of Georgia Extension Services. It was developed from a historical average of evapotranspiration (ET). It recommends weekly applications of irrigation water based on historical average ET minus rain received during the week. This method is designed to ensure that the crop is never water-stressed and as a result is conservative and during normal to high precipitation years, often leads to over-irrigation (Noland, 2018).

The UGA SSA is an irrigation scheduling system that makes irrigation recommendations based on soil water tension (SWT) readings. The soil water tension (in kPa) indicates the suction force required from a plant to extract water from the soil. The more negative this value, the drier the soil, while values close to 0 kPa indicates saturated conditions (Vellidis, et al., 2013). This system is composed of nodes, each one incorporating a sensor circuit board powered by two 1.5 V batteries that acquires values from three Watermark® soil moisture sensors (Irrometer, Riverside, California, USA) (Thomson, et al., 1987) (Shock, et al., 2003) measuring SWT at three different depths (0.20, 0.40, and 0.60 m below soil surface for maize). Nodes send sensor data through radio transmission to the base station located in a strategic position (usually at the center pivot point). This is designed to receive all sensor data at regular intervals defined by the operator (Liakos, et al., 2015). Then the data are sent to a server and displayed in a dedicated website where a graphical interface informs real-time field conditions to the user (Vellidis, et al., 2008). Default thresholds are set to trigger irrigation.

The SmartIrrigation Corn App is one of several smartphone applications included in the SmartIrrigation Apps Suite and is still under development. It uses a simplified daily soil water balance that considers field capacity, rooting depth, evapotranspiration (ETc), rainfall, maximum allowable depletion, and irrigation system characteristics to estimate a daily plant available root zone soil water deficit. Evapotranspiration is estimated from a reference ET (ETo), which is calculated with the Penman-Monteith equation multiplied by a crop coefficient (Kc). Meteorological data (daily mean temperature, wind speed, relative humidity, and solar radiation) are obtained from the closest weather station. Daily Kc values are extracted from a crop coefficient curve. The Corn App model sends notifications to the user when the root zone soil water deficit (%) exceeds established thresholds. Based on the deficit, the user can manage the irrigation treatment to balance the deficit. A default notification deficit threshold of 50% is suggested from

emergence to prior to tasseling (611 GDDs). From tasseling to the end of the dough growth stage (1214 GDDs), the default notification deficit is reduced to 33%. Finally, the default notification deficit is set back to 50% from the beginning of dent to maturity. The notification thresholds may be changed by the user.

Nitrogen fertilization treatments

The treatments tested in 2018 were a combination of standard/traditional practices and emerging practices with potential to improve nitrogen use efficiency (NUE). The traditional practice was to use the UGA Extension Service recommendation of multiplying yield goal in bu ac^{-1} by 1.2 to calculate the N application rate. Based on prior yields at the field, the yield goal was set to 250 bu ac^{-1} and the associated N application rate was 300 lb N ac^{-1} or 336 kg N ha^{-1}.

The emerging practice evaluated was fertigation, or the application of fertilizer through the irrigation system. This practice was selected because it can be used to apply side-dress nutrients

Table 2.1 Total N rate of the fertilization treatments of maize of 2018 and 2019 with specifics on the timing of application

Year	Fertilization Strategy	N rate kg ha^{-1}	N applied (kg ha^{-1})				
			Preplant	Planting	Side-dress		
					common	kg ha^{-1} /event	no. events
2018	Traditional	336	56	50	-	226	1
	Fertigation high	336	56	50	-	57	4
	Fertigation low	280	56	50	-	43	4
2019	Traditional	337	57	34	56	95	2
	Fertigation Scheduled	280	57	34	56	27	5
	Fertigation Model	315	57	34	56	34	5

Table 2.2 Experimental treatments of growing season 2018 and 2019 for maize

Treatment no.	2018			2019		
	Irrigation Treatment		Fertilization Treatment	Irrigation Treatment		Fertilization Treatment
1	Corn App[1]	×	Fertigation[2] High[3]	Checkbook	×	Fertigation Scheduled[8]
2	Corn App	×	Traditional[4]	Corn App	×	Traditional[9]
3	Corn App	×	Fertigation Lower[5]	Corn App	×	Fertigation Model[10]
4	Checkbook[6]	×	Fertigation High	Checkbook	×	Fertigation Model
5	Checkbook	×	Traditional	Corn App	×	Fertigation Scheduled
6	Checkbook	×	Fertigation Lower	UGA SSA	×	Fertigation Scheduled
7	UGA SSA[7]	×	Fertigation High	UGA SSA	×	Fertigation Model
8	UGA SSA	×	Traditional	UGA SSA	×	Traditional
9	UGA SSA	×	Fertigation Lower	Checkbook	×	Traditional

[1] SmartIrrigation Corn App estimates daily plant available soil water deficit and recommends irrigation accordingly
[2] Application of fertilizer through the lateral irrigation system
[3] 336 kg N ha^{-1} applied as preplant (56), at planting (50), and four scheduled fertigation events (57 kg N ha^{-1} each for a total of 228 kg N ha^{-1})
[4] 336 kg N ha^{-1} applied as preplant (56), at planting (50) and as one side-dress application (226)
[5] 280 kg N ha^{-1} applied as preplant (56), at planting (50), and four scheduled fertigation events (43 kg N ha^{-1} each for a total of 172 kg N ha^{-1})
[6] Traditional irrigation method based on historical ET data
[7] Sensor-based irrigation strategy based on soil water tension (kPa) thresholds
[8] 280 kg N ha^{-1} applied as preplant (57), at planting (34), one common side-dress application (56) and five scheduled fertigation events (27 kg N ha^{-1} each for a total of 133 kg N ha^{-1})
[9] 336 kg N ha^{-1} applied as preplant (57), at planting (34) and as one side-dress application (226)
[10] 315 kg N ha^{-1} applied as preplant (57), at planting (34), one common side-dress (56) and five customized fertigation events (34 kg N ha^{-1} each for a total of 170 kg N ha^{-1})

in small doses throughout the growing season and theoretically should result in higher NUE as less N is likely to be lost via leaching. Fertigation was evaluated using both the 1.2 multiplication factor for determining the N application rate and a 1.0 multiplication factor. The lower multiplication factor resulted in an application rate of 250 lb N ac^{-1} or 280 kg N ha^{-1}, and it was selected because we hypothesized that higher NUE would require less N to achieve the same yield.

The three fertilization treatments used in the study were: (i) the traditional method with a total of 336 kg N ha^{-1} applied as preplant (56), at planting (50), and as one side-dress application (226),

(ii) 336 kg N ha^{-1} applied as preplant (56), at planting (50), and four scheduled fertigation events (57 kg N ha^{-1} each for a total of 228 kg N ha^{-1}), and (iii) 280 kg N ha^{-1} applied as preplant (56), at planting (50), and four scheduled fertigation events (43 kg N ha^{-1} each for a total of 172 kg N ha^{-1}). In 2019 the second fertigation treatment was replaced by scheduling side-dress N applications according to the STICS model predictions and resulted in 315 kg N ha^{-1} applied as preplant (57), at planting (34), one common side-dress (56) and five customized fertigation events (34 kg N ha^{-1} each for a total of 170 kg N ha^{-1}). The traditional fertilization method in 2019 was slightly different from 2018. The total of 336 kg N ha^{-1} was split in pre-planting (57), planting (34), one common side-dress application (56) and two side-dress of 95 kg ha^{-1} each. In Fertigation Schedule treatment of 2019, 280 kg N ha^{-1} were applied as preplant (56), at planting (50), one common side-dress application (56) and four scheduled fertigation events (27 kg N ha^{-1} each for a total of 133 kg N ha^{-1}). The treatments and associated N rates are presented in Table 2.1.

Table 2.2 presents the combination of irrigation and fertilization treatments for 2018 and 2019 and the treatment numbers they were assigned during each year.

Data collection and sampling procedures

Soil water tension

To monitor soil moisture continuously during the growing season, UGA SSA sensor nodes were installed at the center of each of the 27 experimental plots. SWT was recorded hourly at 0.2, 0.4, and 0.60 m for the entire growing season. Figure 2.2 is an example of a SWT data from plot 231-3 (App × App).

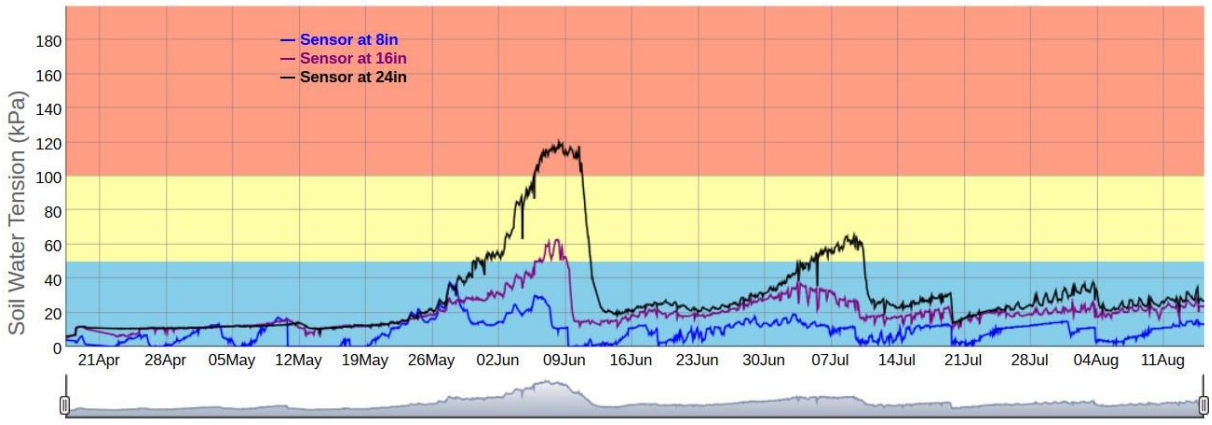

Figure 2.2 Soil water tension (SWT) readings in kPa for node 19 – Corn App × Fertigation model – of 2019 showing the trend of SWT over time at the three depths (0.20 m, 0.41 m and 0.61 m) of the Watermark® sensors

Soil sampling and analysis

A manual auger (76 mm or 3 in diameter) was used to collect soil cores from each plot at four depths: 0-0.15 m, 0.15-0.30 m, 0.30-0.60 m and 0.60-0.90 m. A first sampling of one core/plot was conducted in February, before the growing season began, to determine soil texture, soil moisture, and soil nutrient concentrations. Then, one core/plot was collected monthly during the growing season from April to July, and a final sampling was carried out in September, after harvest. Collected soil samples were used to calculate the soil gravimetric water content (θg) and pH, P, K, Mg, Ca, S, B, Zn, Mn, Fe and Cu content, CEC, % base saturation, and organic matter, Nitrate-N, Ammonia-N and TKN detection. Volumetric water content was determined by weighing soil before and after being dried at 80°C for 72 hours. The remaining variables were

determined by a commercial soil-testing laboratory (Waters Agricultural Laboratories, Camilla, Ga).

Because of budgetary limitations, in 2019, the number of sampling sites was reduced from 27 to 9 plots (three replications of three treatments), and the samples analyzed only for nitrate and ammonium content.

Biomass sampling and analysis

Prior to both maize growing seasons, a sample of the rye cover crop was collected from a 0.23 m × 0.46 m area and the tissue was analyzed for total Kjeldahl nitrogen (TKN) (Nelson, et al., 1973). To evaluate seasonal biomass and N accumulation in the aboveground maize biomass, plants in 0.91 m (a linear yard) of row were collected at five dates at V5 (vegetative leaf stage 5), V10 (vegetative leaf stage 10), V15 (vegetative leaf stage 15), R2 (reproductive blister), R4 (reproductive dough), and R6 (physiological maturity) stages. Plant stalks were cut at the soil surface, counted and separated into three components: stems (stalks and leaf sheaths), leaves (leaf blades) and ears. The components were oven dried at 80°C for 72 hours and the dry weight was collected. The samples were analyzed for TKN (%) by the Waters Agricultural Laboratories (Camilla, Georgia). In 2019, leaf area (cm^2) was also measured using a Leaf Area Meter (LI-COR 3100) and used to derive the leaf area index.

Statistical methods

The effects of irrigation and fertilization, and the interaction term irrigation × fertilization on yield, NUE and WUE were evaluated using a two-ways analysis of variance (ANOVA). A further ANOVA was performed including the layer effect on N content in the soil. When the ANOVA resulted in a significant test, further statistical evaluation was conducted using the Tukey-Kramer

HSD test. The relationships between continuous variables and categorical factors were examined using the Oneway platform and additional analysis of means comparison were performed using the Tukey-Kramer HSD test. The statistical analyses were conducted using JMP 14 (SAS Institute, Cary, NC).

Partial nutrient balance

To make an overall estimation of the impact of fertilizations on soil fertility, a partial nutrient balance (PNB) was calculated using equation 2.1. PNB is the simplest form of nutrient recovery efficiency and indicates the amount of nutrient take up in relation to the amount applied (Fixen, et al., 2015).

A PNB value close to 1 roughly indicates that plant uptake is approximately the same as fertilizer applied and that soil fertility is maintained at a steady state. A PNB well below 1 indicates excessive fertilization and avoidable losses. In contrast, PNB above 1 indicates that more N is taken up by the crop than applied.

$$PNB = \frac{aboveground\ biomass}{N\ rate} \qquad [2.1]$$

Model Parameterization

As described in the Introduction, the STICS model (version 9.1; 2019) was selected to perform the mathematical simulation of soil N during the maize growing season. The ultimate goal of the mathematical simulation was to use STICS to schedule fertigation applications as a function of soil N concentrations. To match the experimental data, ammonium and nitrate contents in the soil (kg ha^{-1}) were selected as the model's daily outputs. To estimate these parameters the model required the parameterization of six groups of variables: (i) general parameters, (ii) plant

parameters, (iii) initial conditions, (iv) soil parameters, (v) crop management information and (vi) weather data.

General parameters

The water stress option was deactivated because it was assumed that all the irrigation strategies maintained soil moisture at optimal levels during the growing season. Soil tillage and compaction effects were set to 0 to simulate conservation tillage as it is not included as an option in the model. All the other general parameters remained unchanged as default options.

Plant parameters

In STICS, crop parameters are divided into a set of common parameters and a set of cultivar-specific parameters (Figure 2.3). Crop development is a function of growing degree days (GDDs), calculated using equation 2.2, where Tmax and Tmin are the respectively maximum and minimum daily temperature, and Tbase the minimum temperature for phasic development, set for maize at 10°C. Any temperature below Tbase have no influence on development.

$$GDD = \frac{(Tmax+Tmin)}{2} - Tbase \quad [2.2]$$

The development was set to be driven by the temperature within the canopy derived from an energy balance with a daily time step. This method relies on the calculations of the sum of evaporative fluxes and net radiation. The latter is calculated using an albedo value of 0.25 typical of loamy sand soil and long wave radiation calculated using the Brutsaert formula (Brutsaert, 1982). The LAI option was chosen for driving leaf dynamics. The radiation interception of the canopy is calculated through a Beer's law optical analogy whose extinction coefficient is set to 0.7

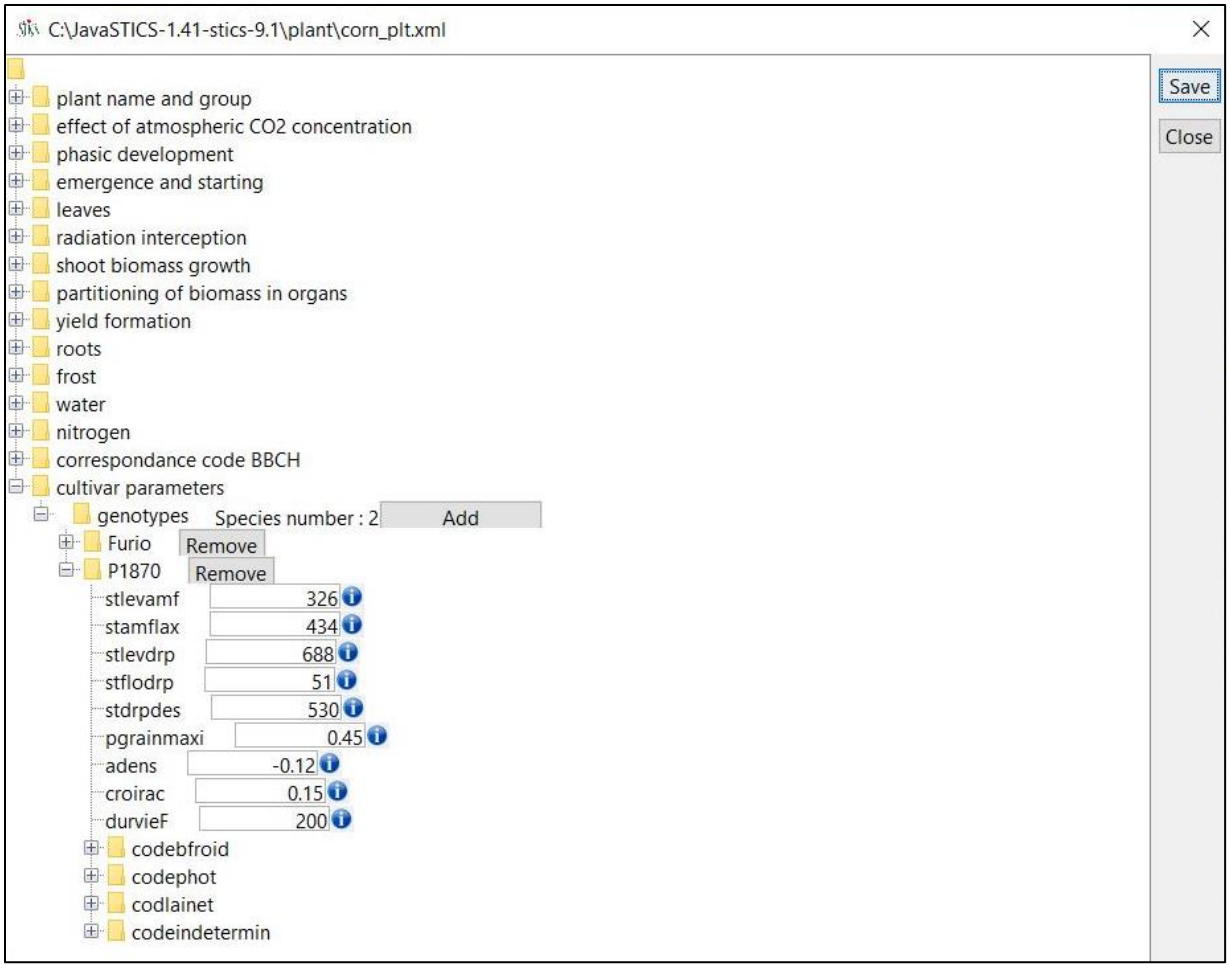

Figure 2.3 Screenshot of plant parameterization of the STICS model. Each folder contains a set of default parameters that can be edited by the user

(Beaudoin, et al., 2009). This option was selected for its simplicity compared to the radiation transfer method that requires the input of several critical parameters.

Root growth is simulated using the standard profile approach to get the profile of effective absorption and is assumed to take place up to a depth of 0.9 m and to stop at the end of the leaf growth stage.

Water uptake is simulated using the crop coefficient approach that is set as a maximum value of 1.20 according to FAO (Allen R.G., 1998). Default values were used for all the other water uptake parameters.

The critical N concentration curve parameters in STICS are defined as common parameters and they are not specific to cultivars. The calculation of parameters influencing the critical N concentration curve were optimized for the simulation to match values of N in the aboveground plant biomass.

In the crop module of STICS, a new maize variety was created and called P1870 because of the relatively large differences in yield between French cultivars included in the model and the cultivar used in the study. Crop development as a function of growing degree days was determined using the phenological stages prediction incorporated in the SmartIrrigation Corn App.

Soil

STICS considers the soil as a succession of horizontal layers, each one characterized by its moisture and N content at the start of the simulation, and its field capacity (Janssen, et al.), bulk density, infiltrability and moisture content at permanent wilting point (PWP). The profile was divided into three layers of 1-0.30 m, 0.31-0.60 m and 0.61-0.90 m, respectively. The soil texture at the field site was mainly loamy sand in the top layer and sandy loam or sandy clay loam below. A constant bulk density value of 1.6 g cm^{-3} (Henry F. Perkins, 1986) was used. Values of gravimetric water content at FC and PWP are estimated using the Van Genuchten model (Liang, et al., 2016). Gravimetric water content at FC was set between 14 and 23 % and at PWP between 4 and 8 %.

Default infiltration values suggested in the STICS manual were 45 mm d^{-1} in topsoil with coarse texture and 24 mm d^{-1} in subsoil of the same textural class (Beaudoin, et al., 2009). The macroporosity, capillary rise, nitrification and denitrification functions were activated.

Weather station and climate file

Input weather data files, including maximum and minimum temperature (°C), global radiation (MJ m^{-2}), precipitation (mm) and wind speed (m s^{-1}), were created using data from the local Georgia Weather Network weather station. The weather station is located at SIRP and is called "Camilla". The data files were then created and characterized in STICS as located at 31.2° N latitude and collecting data at a height of 2.5 m.

Potential evapotranspiration (PET) was calculated with the Priestley-Taylor method (Priestley, et al., 1972) because it is the least demanding method that doesn't require vapor pressure, value that the weather station do not provide on a daily basis. This function relies on a site-dependent coefficient that for many soil surface conditions is 1.26 and shows to give far better results in humid environments that in arid ones (Beaudoin, et al., 2009), which is the case of the humid subtropical climate of the experimental area. Inorganic N concentration in the rain was considered negligible according to the data of the National Atmospheric Deposition Program (NADP) from a site located in the Tift County, about 78 km from the experimental site.

Crop management and simulation initialization

Rye biomass remaining in the field before sowing was set to remain on the soil surface and quantified through rye tissue analysis as 0.5 t ha^{-1} with an 88 % of water on the fresh weight, 44

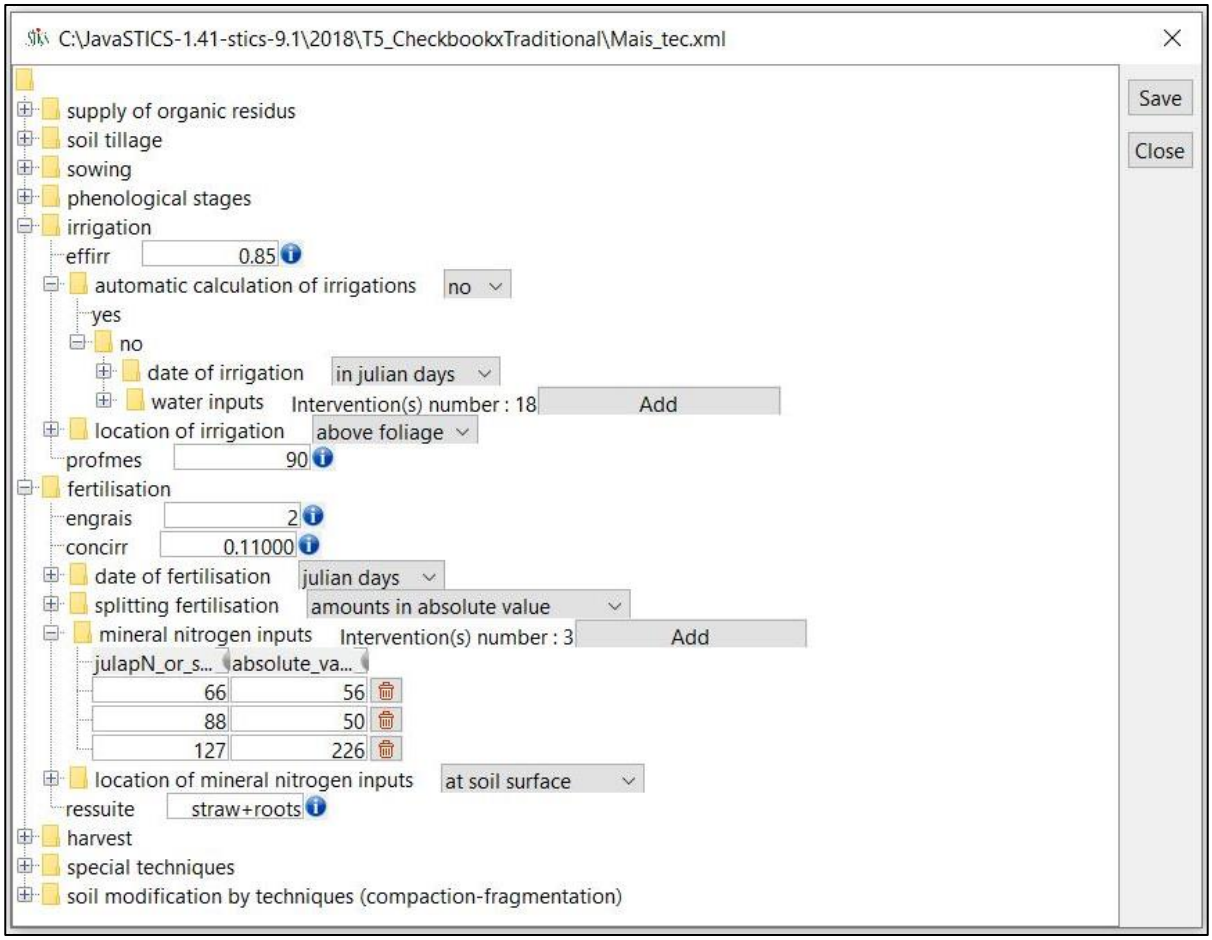

Figure 2.4 Screenshot of the STICS model showing the parameterization / input of crop management information. Each folder contains a set of default parameters that can be edited by the user

% of carbon on the dry matter and a C:N ratio of 27:5. STICS does not include a strip tillage practice option so tillage was parameterized as no tillage.

Seeding is defined by the date, sowing depth set at 50 mm, seeding density corresponding to about 8 plants per m^2 (≈ 80300 seeds ha^{-1}) and the variety sown (P1870). Irrigation efficiency is set to 85 % taking place above the canopy and all the irrigation events were recorded as Julian Day of

application and amount in mm. STICS allows the simulation of just one type of fertilizer during the growing season. Urea ammonium nitrate (UAN) solution was selected as the source of N applied at the soil surface. Fertilization events were characterized by the date of application expressed in Julian Day of the year and the amount of N applied in kg ha^{-1} (Figure 2.4).

Simulations were performed from the date of first soil sampling to harvest (Figure 2.5). Initialization values of soil water content and nitrate and ammonium content were derived from the first soil samples.

Model calibration and validation

Successful simulation of soil N content relies on successful simulation of soil water content. This is because, especially in coarse soils, the major losses of N from the root zone occurs by leaching of nitrate with water through the soil profile. For this reason, the model was calibrated for soil water content first. The model was calibrated for soil N and aboveground biomass in subsequent stages. STICS simulates volumetric soil water content (SWC) in terms of mm^3 mm^{-3} of three

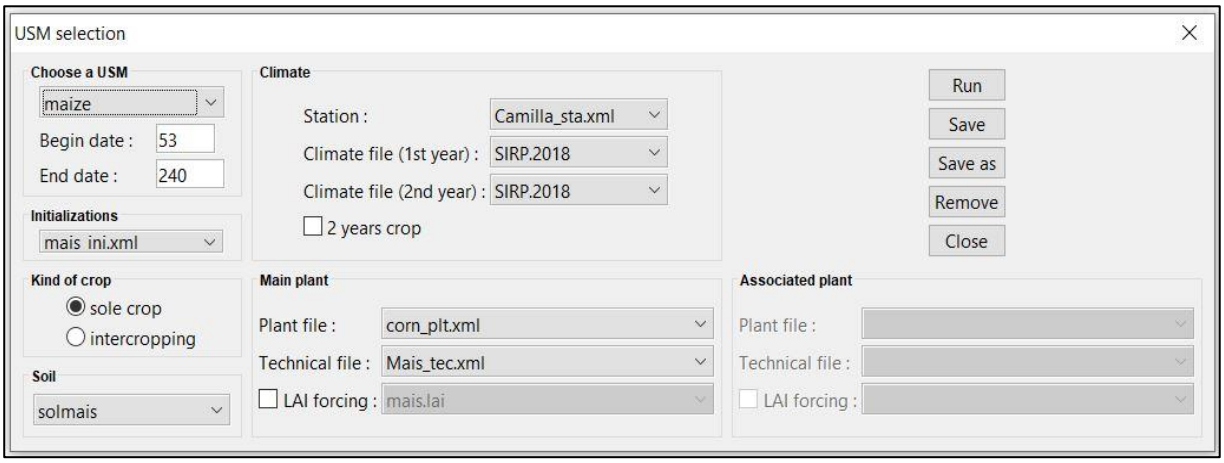

Figure 2.5 Screenshot of STICS running function, where USM is unit of simulation

selected layers of 0-0.30 m, 0.31-0.60 m and 0.61-0.90 m. The water balance used by STICS to calculate the water status of the soil and the plant is based on estimating the water requirements of the soil/leaf system on the one hand and on the water supply to the soil/root system on the other (Brisson, et al., 2003). The observed values of SWT (kPa) obtained from the UGA SSA system were used to calibrate the SWC simulation. SWT data were converted into SWC through the water retention curves. These curves are difficult and time consuming to create, so the Retention Curve (RETC) computer program (RETC, 2009) was used to perform a neural network prediction of the Van Genuchten model's parameters given texture and bulk density. The values obtained were in accordance with the values obtained by Liang et al. (2015) for the same type of soil (Liang, et al., 2016). The three Watermarks® sensors reading the SWT were located at 0.20 m, 0.40 m and 0.60 m depth, so in order to compare the recoded values with the model's output of SWC at 30 cm and 60 cm the two deeper values were combined into a weighted average. A weighted average rather than a simple average was used because we assumed that more soil water extraction took place in the shallower portions of the soil profile. To the sensor at 0.20 m was assigned a weighting factor of 0.7 while the sensor at 0.40 m was assigned a weighting factor of 0.3. After the SWC calibration was completed, the observed values of NO_3^- and NH_4^+ in the soil and in the aboveground biomass (kg ha^{-1}) were used to calibrate the soil and plant N content. Data from treatments 1 and 5 of 2018 (Table 2.2) were used for model calibration. Treatment five received the higher amount of irrigation water (checkbook method) and N (traditional method). Treatment one received a smaller input of irrigation water (app method) and the same amount of N as treatment one except that the side-dress N was applied in four events using fertigation.

The calibration was conducted using the optimization algorithm included in the STICS software. This option gives the possibility to optimize most of the model parameters according to the

observed data. This is a minimization procedure based on the simplex method using the least square criterion. The optimization stops when the spread between the criterion of each iteration has reached a minimum of 10^{-4} or after 1000 iterations (Brisson, et al., 2003).

A first step to conduct parameter optimization is to choose which parameters to optimize. These should be the parameters that most influence the accuracy of the output. The optimization process 00relied on the STICS manual and the work of Ruget et al. (2002) who run an intramodule analysis to assess the level of significance of parameters of each module (Beaudoin, et al., 2009) (Ruget, et al., 2002).

The most influential parameters for simulating maize development are the GDD of the filling stage, and the sowing depth. For simulation of LAI development, the most influential parameters are plant density and the duration of the stage between emergence and maximum acceleration of leaf growth.

For root growth, the most influential parameters are the depth at which root density is half the density at the surface (cm), that is strictly correlated to water uptake, and the growth rate in the soil profile (cm degree day^{-1}). In the soil module, there are several influential parameters that are related to water and N balance. They are field capacity of the layer (% of dry soil), bulk density of the layer (g cm^{-3}), soil organic N content of the upper layer (%), depth at which the maximum evaporation ends (mm) and infiltration capacity of the soil (mm d^{-1}). In addition to these, the maximum crop coefficient is another important parameter affecting water balance. The thickness of the active layer for mineralization (cm) and the maximal nitrate uptake rate by the low affinity uptake system of roots (μmole cm^{-1} h^{-1}) are additional important parameters for the N balance. The yield module is mainly influenced by the rate of increase of the carbon harvest index (g grain (g $plant)^{-1}$ day^{-1}) and the duration of grain filling.

After calibration, the model was validated in two steps: (i) using the 2018 data from the remaining seven treatments and (ii) in real-time between planting and harvest in 2019.

Fertigation scheduling from model prediction

In 2019, for treatments 3, 4 and 7 (Table 2.2), side-dress N was scheduled based on soil N predictions by STICS. A minimum rate of 280 kg N ha^{-1} was set as the fertilization baseline. About half of this amount (131 kg N ha^{-1}) was applied as pre-plant, at planting, and one liquid side-dress application. The remaining was applied via fertigation when a decrease in soil N was predicted by the model. The amount applied at each fertigation event was held constant at 34 kg N ha^{-1}. The entire soil profile (0-0.9 m) was considered when monitoring soil N. No distinction was made for the early stages because the initial N content of the third layer (0.60-0.90 m) was low, and because roots were assumed to reach the third layer around V8, stage of starting of the fast vegetative growth (Archontoulis S., 2017). In total, fertilizer was applied with five fertigation events for a total of 315 kg N ha^{-1}. The fourth and fifth events occurred at 70 and 78 DAP (after tasseling) which is later than originally planned but it was driven by the model predicting very low soil N at that time.

Model evaluation

The simulations were compared with measured values. Evaluation was performed using the hydroGOF package in the R environment. The indices used to assess the performance of the model are the mean absolute error (MAE) (Eq. 2.3), the normalized root mean squared error (NRMSE) normalized to the range of observed data (Eq. 2.4), the coefficient of determination (R^2) (Eq. 2.5), and the index of agreement (d) (Eq. 2.6):

$$MAE = \frac{1}{N}\sum_{i=1}^{N}|P_i - M_i| \quad [2.3]$$

$$NRMSE = 100\left(\frac{\frac{1}{N}\sum_{i=1}^{N}(P_i - M_i)^2}{M_{max} - M_{min}}\right) \quad [2.4]$$

$$R^2 = \left(\frac{\sum_{i=1}^{N}(M_i - M_{ave})(P_i - P_{ave})}{\left(\sqrt{\sum_{i=1}^{N}(M_i - M_{ave})^2}\right)\left(\sqrt{\sum_{i=1}^{N}(P_i - P_{ave})^2}\right)}\right)^2 \quad [2.5]$$

$$d = 1 - \left(\frac{\sum_{i=1}^{N}(P_i - M_i)^2}{\sum_{i=1}^{N}(|P_i - M_{ave}| + |M_i - M_{ave}|)^2}\right) \quad [2.6]$$

Where N is the total number of data, Mi and Pi are the measured and predicted values, respectively, Mave and Pave are the average of the measured and predicted values, respectively. MAE and NMSE ranges from 0 to +∞, where 0 is a perfect fit. R^2 and d ranges from 0 to 1, where 1 indicates a perfect fit. MAE measures the average difference between prediction and observations in absolute value, and all individual differences have equal weight. RMSE, and consequently NRMSE, gives a relatively high weight to large errors. MAE and NRMSE quantify the departure of the model outputs from the measurements adding up the errors. R^2 and d instead, focus on the correlation between model predictions and measurements, in other word they compare the trends. The index d was developed by Willmott (1981) and is sensitive to extreme values due to the squared differences but more consistent than R^2 (Willmott, 1981). Legates D.R. (1999) stated that d represented a remarkable improvement in respect to the coefficient of determination.

Additional assessment of the model performances was conducted using the lack of fit method developed by Whitmore (1991). The variance ratio (F) is calculated as shown in equation 2.7 where N in the number of points at which there are observations, n is the number of replicates at each point, O_{ij} is the observed value at point j, replication i, O_j is the average observation at point j, S_j is the simulated value at point j and df are the degrees of freedom. SSE is the sum of squares due to pure error.

To interpret the calculated F, it is necessary to have the F-table for the desired level of significance. The significance (α) level used was 0.05. If $F < F_{\alpha}$ the lack of fit error is small and the simulation is accurate; if $F > F_{\alpha}$, and the lack of fit is significantly greater than error, the model could almost certainly be improved (Yang, et al., 1999). This method is particularly valuable in respect to the abovementioned indices because it takes into consideration the natural variability of the observed data. Data were evaluated per variable within treatments.

$$F = \frac{\frac{\sum_{J=1}^{N} n_j (o_j - s_j)^2}{df}}{\frac{\sum_{J=1}^{N} \sum_{I=1}^{n_j} n_j (o_j - s_j)^2}{df}} \qquad [2.7]$$

CHAPTER 3

RESULTS AND DISCUSSION

Experimental results

Weather data and water use

Crop development is a function of accumulated growing degree days (GDDs) which are calculated using eq 2.1. Accumulated GDDs and rainfall amounts for the 2018 and 2019 growing seasons,

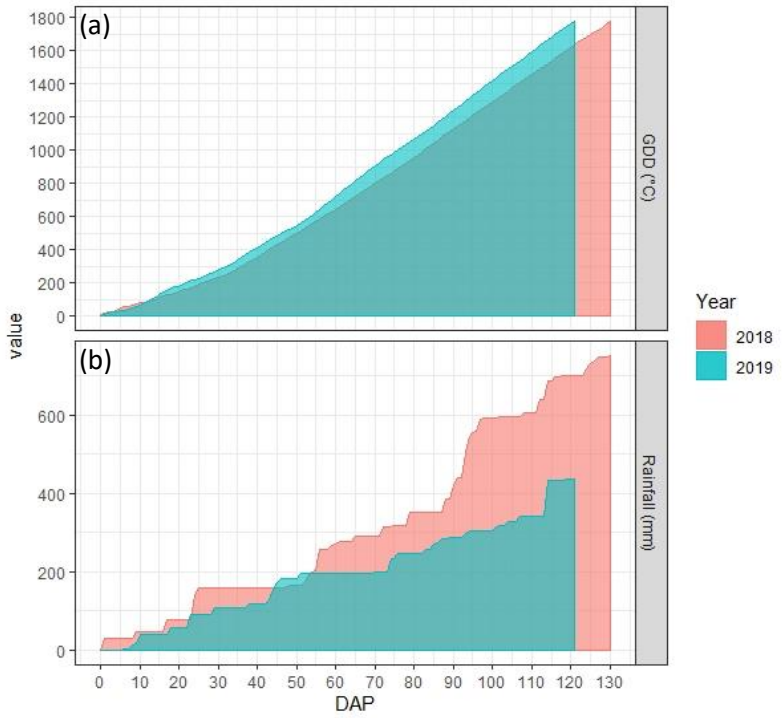

Figure 3.1 (a) Accumulated growing degree days (GDDs) (°C) and (b) cumulative precipitation (mm) for the 2018 and 2019 maize growing season expressed in days after planting (DAP)

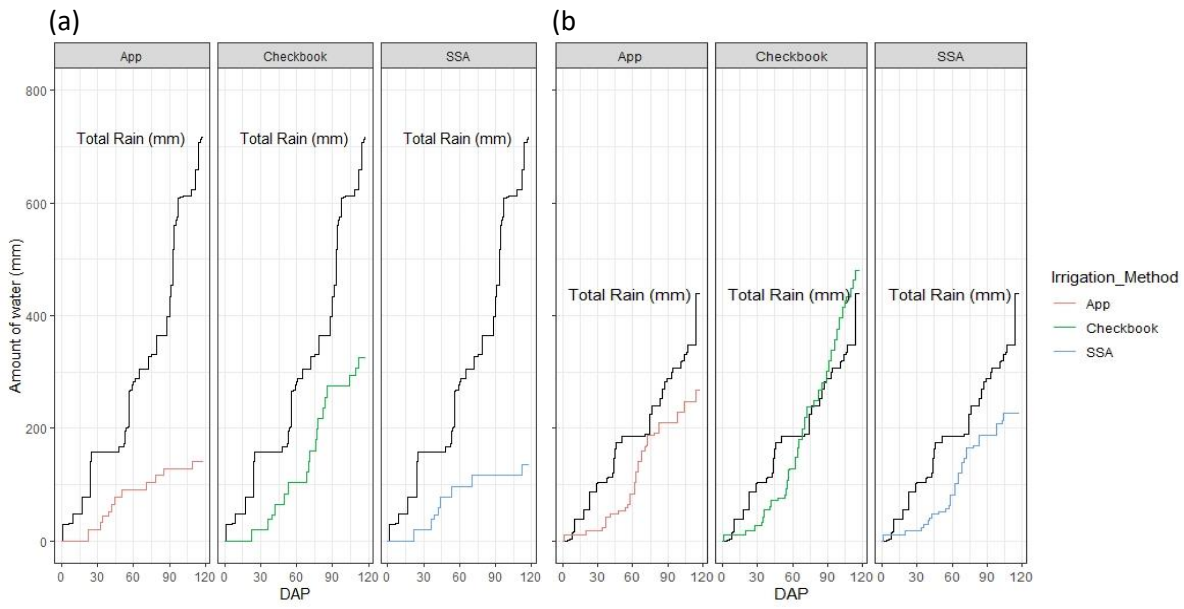

Figure 3.2 Cumulative amount of water applied per irrigation treatment (mm) of maize compared to cumulative rainfall in (a) 2018 and (b) 2019. App is the SmartIrrigation Corn App, Checkbook is the traditional irrigation method based on historical ET data, UGA SSA is a sensor-based irrigation strategy.

from planting to maturity, are shown in Figure 3.1. Maturity was set to 1800 °C GDDs. Temperatures were generally higher in 2019, which resulted in maturing occuring10 days earlier than 2018. The lower temperatures of 2018 may be a function of the higher precipitation rate that is associated with less solar radiation entering the atmosphere. During 2018 total rainfall from planting to maturity was 750 mm, while in 2019 it was 434 mm. Although the 2018 precipitation was over half on the annual average rainfall of 1300 mm, maize requires approximately 960 mm of water from planting to maturity (Noland, 2018). For this reason and because precipitation was not evenly distributed during the growing season, regular irrigation applications were needed.

Figure 3.2 shows the water uses by the three different irrigation treatment during 2018 and 2019. The Checkbook irrigation scheduling tool was considered the traditional / standard treatment in this experiment. Irrigation water savings were calculated using the irrigation water used by the Checkbook method as the baseline. The Checkbook method required 325 mm of irrigation in 2018 and 477 mm in 2019. In 2018, scheduling with the SmartIrrigation Corn App (hereafter referred to as the App) required 140 mm of irrigation and resulted in 57 % less water used compared to the Checkbook method. Scheduling with the UGA SSA wireless sensor system required 135 mm of irrigation and resulted in 59 % less water used. In 2019, scheduling with the App required 282 mm and resulted in 40 % less water than the Checkbook strategy. Scheduling with the UGA SSA required 257 mm and resulted in 53 % less water.

Biomass

A two-way ANOVA was used to evaluate the effect of irrigation and fertilization treatments on aboveground biomass and N content in the plant during the 2018 growing season. The analyses showed no significant effects of irrigation and fertilization on all the dates of sampling except for the 13 June 2018 that had a *p*-value of 0.03 for biomass and 0.053 for N in the plant due to the irrigation treatment. Tables 3.1 and 3.2 show mean values of biomass and N in the plant and their significance.

Partial nutrient balance

Despite the lack of significance of the treatments on N uptake, PNB values close to 1 (Eq. 2.1) show that the amount of N taken up by the crop is generally close to the amount applied. This index roughly indicates that the soil fertility will be sustained at a steady state (Fixen, et al., 2015).

Table 3.1 Results of ANOVA of the effects of irrigation and fertilization treatments on the average aboveground biomass accumulation in kg ha^{-1} among the growing seasons in 2018 and 2019. Different letters indicate statistical differences between the values of the same date

			Biomass (kg ha^{-1})				
Year	Treatment		27-Apr	31-May	13-Jun	26-Jul	16-Aug
2018	Irrigation	Checkbook[1]	258 a	6268 a	9498 a	22704 a	24021 a
		UGA SSA[2]	260 a	6496 a	7957 b	21573 a	22007 a
		App[3]	235 a	6376 a	9306 ab	23787 a	24291 a
	Fertilization	Traditional[4]	242 a	6426 a	9377 a	23395 a	25435 a
		F.[5] High[6]	241 a	6490 a	9120 a	21866 a	22388 a
		F. Low[7]	269 a	6224 a	8264 a	22803 a	22495 a
			29-Apr	29-May	14-Jun	31-Jul	14-Aug
2019	Irrigation	Checkbook	632 a	22678 a	35178 a	34361 a	29188 a
		UGA SSA	556 a	18885 a	30491 b	35700 a	29474 a
		App	539 a	22539 a	30615 b	28899 a	29932 a
	Fertilization	Traditional[8]	632 a	22678 a	35178 a	34361 a	29188 a
		F. Scheduled[9]	556 a	18885 a	30491 b	35700 a	29474 a
		F. Model[10]	539 a	22539 a	30615 b	28899 a	29932 a

[1] Traditional irrigation method based on historical ET data
[2] Sensor-based irrigation strategy based on soil water tension (kPa) thresholds
[3] SmartIrrigation Corn App estimates daily plant available soil water deficit and recommends irrigation accordingly
[4] 336 kg N ha^{-1} applied as preplant (56), planting (50) and one side-dress application (226)
[5] F is the abbreviation for fertigation or the application of fertilizer through the irrigation system
[6] 336 kg N ha^{-1} applied as preplant (56), planting (50), and four scheduled fertigation events (57 kg N ha^{-1} each)
[7] 280 kg N ha^{-1} applied as preplant (56), planting (50), and four scheduled fertigation events (43 kg N ha^{-1} each)
[8] 336 kg N ha^{-1} applied as preplant (57), planting (34) and as one common side-dress application (56) and two customized side-applications (95)
[9] 280 kg N ha^{-1} applied as preplant (57), planting (34), one common side-dress application (56) and five scheduled fertigation events (27 kg N ha^{-1} each)
[10] 315 kg N ha^{-1} applied as preplant (57), planting (34), one common side-dress (56) and five customized fertigation events (34 kg N ha^{-1} each)

However, this calculation doesn't take into consideration the amount of N that will return to the

Table 3.2 Results of ANOVA of the effects of irrigation and fertilization treatments on the average N content of the aboveground biomass in kg ha^{-1} among the growing seasons in 2018 and 2019. Different letters indicate statistical differences between the values of the same date

			N in plant (kg ha^{-1})				
Year	Treatment		27-Apr	31-May	14-Jun	26-Jul	16-Aug
2018	Irrigation	Checkbook[1]	9 a	134 a	201 a	279 a	310 a
		UGA SSA[2]	9 a	128 a	155 b	273 a	284 a
		App[3]	8 a	137 a	190 ab	312 a	323 a
	Fertilization	Traditional[4]	9 a	140 a	185 a	292 a	336 a
		F.[5] high[6]	8 a	132 a	192 a	286 a	291 a
		F. lower[7]	9 a	127 a	169 a	285 a	290 a
			29-Apr	29-May	26-Jun	31-Jul	14-Aug
2019	Irrigation	Checkbook	29 a	419 a	539 a	388 a	349 a
		UGA SSA	26 a	453 a	484 a	413 a	324 a
		App	25 a	355 a	504 a	337 a	392 a
	Fertilization	Traditional[8]	29 a	419 a	539 a	388 a	349 a
		F. Scheduled[9]	26 a	453 a	484 a	413 a	324 a
		F. Model[10]	25 a	355 a	504 a	337 a	392 a

[1] Traditional irrigation method based on historical ET data
[2] Sensor-based irrigation strategy based on soil water tension (kPa) thresholds
[3] SmartIrrigation Corn App estimates daily plant available soil water deficit and recommends irrigation accordingly
[4] 336 kg N ha^{-1} applied as preplant (56), planting (50) and one side-dress application (226)
[5] F is the abbreviation for fertigation or the application of fertilizer through the irrigation system
[6] 336 kg N ha^{-1} applied as preplant (56), planting (50), and four scheduled fertigation events (57 kg N ha^{-1} each)
[7] 280 kg N ha^{-1} applied as preplant (56), planting (50), and four scheduled fertigation events (43 kg N ha^{-1} each)
[8] 336 kg N ha^{-1} applied as preplant (57), planting (34) and as one common side-dress application (56) and two customized side-applications (95)
[9] 280 kg N ha^{-1} applied as preplant (57), planting (34), one common side-dress application (56) and five scheduled fertigation events (27 kg N ha^{-1} each)
[10] 315 kg N ha^{-1} applied as preplant (57), planting (34), one common side-dress (56) and five customized fertigation events (34 kg N ha^{-1} each)

soil with stovers, nor N from mineralization of the soil organic matter or N inputs from rain and irrigation water. Although mineralization of soil N was not measured, studies indicate that even in

Table 3.3 PNB of all the treatments of 2018 and treatments 3, 6 and 9 of 2019

	Fertilization treatment	N rate applied	N plant	PNB
2018	Traditional[1]	336	331	1.01
		336	376	0.89
		336	299	1.13
	F.[2] high[3]	336	298	1.13
		336	285	1.18
		336	290	1.16
	F. lower[4]	280	336	0.83
		280	268	1.04
		280	263	1.07
2019	Traditional[5]	337	349	0.97
	F. Scheduled[6]	280	349	0.80
	F. Model[7]	315	389	0.81

[1] 336 kg N ha^{-1} applied as preplant (56), planting (50) and one side-dress application (226)
[2] F is the abbreviation for fertigation or the application of fertilizer through the irrigation system
[3] 336 kg N ha^{-1} applied as preplant (56), planting (50), and four scheduled fertigation events (57 kg N ha^{-1} each)
[4] 280 kg N ha^{-1} applied as preplant (56), planting (50), and four scheduled fertigation events (43 kg N ha^{-1} each)
[5] 336 kg N ha^{-1} applied as preplant (57), planting (34) and as one common side-dress application (56) and two customized side-applications (95)
[6] 280 kg N ha^{-1} applied as preplant (57), planting (34), one common side-dress application (56) and five scheduled fertigation events (27 kg N ha^{-1} each)
[7] 315 kg N ha^{-1} applied as preplant (57), planting (34), one common side-dress (56) and five customized fertigation events (34 kg N ha^{-1} each)

similar soils, mineralization rates can be as high as 75 kg ha^{-1} yr^{-1} (Egelkraut, et al., 2003). PNB results are shown in Table 3.3.

Yield

Figure 3.3 shows maize yield (t ha^{-1}) results for each of the nine treatments during 2018 and 2019. A two-way ANOVA was conducted to compare the effects of irrigation, fertilization treatments and their interaction on yield in each year. There was not a significant effect of irrigation and fertilization treatments on yield at the $p < 0.05$ level. Yield was consistent throughout the

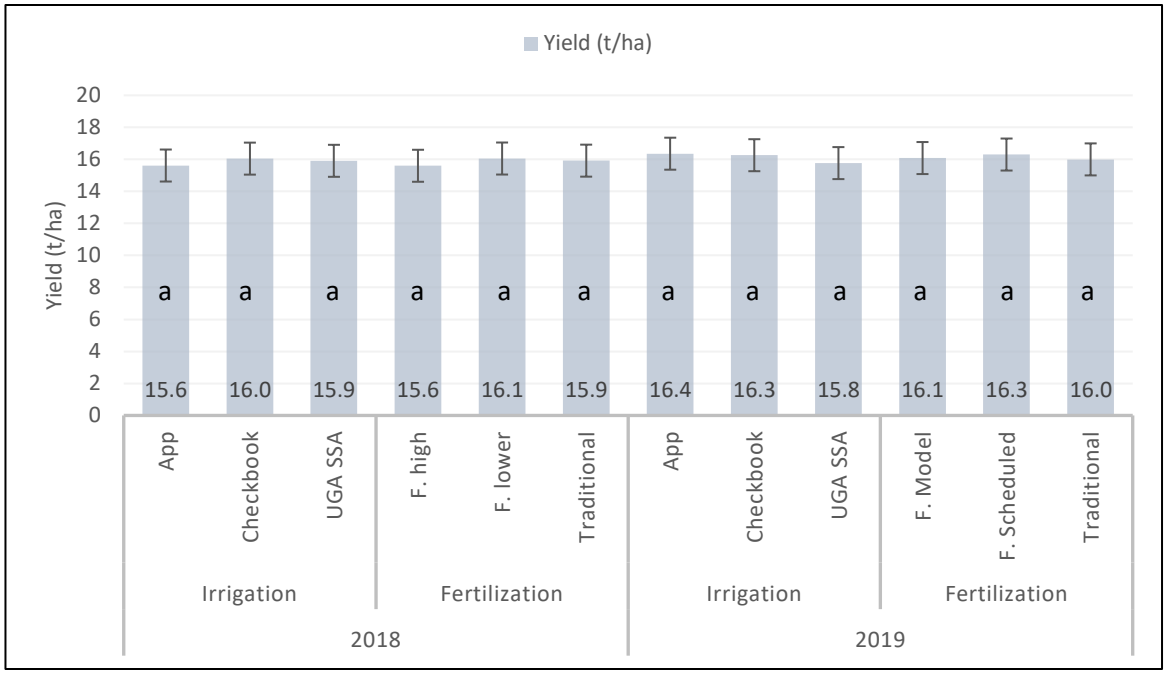

Figure 3.3 Average yield (t ha^{-1}) for each irrigation and fertilization treatment in 2018 and 2019. Two-way ANOVA run separately for 2018 and 2019 showed no differences in treatments effect. App is the SmartIrrigation Corn App, Checkbook is the traditional irrigation method based on historical ET data, UGA SSA is a sensor-based irrigation strategy. F is the abbreviation for fertigation, or the application of fertilizer through the irrigation system. F. high treatment applied 336 kg N ha^{-1} splitting the side-dress among four events; F. lower used the same fertilization strategy with a lower total rate (280 kg ha^{-1}); Traditional applied 336 kg N ha^{-1} recurring to only one side-dress application. F. Model is the strategy of application of side-dress according to the STICS model where the total rate was 315 kg N ha^{-1}; F. Scheduled was 280 kg N ha^{-1}.

treatments and the year of production with an overall average of 15.4 and 16 tons of grain per hectare in 2018 and 2019, respectively. The lack of significant differences between irrigation

treatments is in accordance with Orfanou (2019), that in the same geographic area of the Coastal Plain tested the Checkbook irrigation method and the sensor-based UGA SSA reporting no significant effect of amount of applied irrigation on final maize yield (Orfanou A., 2019). The absence of impact of the fertilization strategies on yield is an unexpected result, especially in the highly rainy season of 2018.

According to Bundy (2006), side-dress N applications were likely to produce benefits in yield by avoiding N loss compared to preplant-applied N in conditions where the risk of leaching is high, such as in coarse-textured sandy soils (Bundy, 2006). The disagreement could be explained by the fact that the traditional strategy tested was not just a preplant-application. The total N rate was divided between pre-planting, planting and one side-dress at 40 DAP, while the split fertigation strategies had the side-dress amount divided into four events later in the season. It is also possible that yield differences were not observed because even the lowest N treatment (280 kg N ha^{-1}) provided more than enough N for the growing conditions at this site. It is also likely that additional N was made available via the mineralization of organic matter that was available in the soil profile.

NUE and WUE

Uniformity of yield among treatments beside the differences in rates of water and N applied suggests a difference in efficiency of the treatments. Two-way ANOVA was used to investigate the effects of irrigation and fertilization factors on NUE and WUE in 2018 and 2019. NUE showed a significant effect of factors at $p < 0.05$ level. In 2018 the *p*-value was 0.0018 and the significance was very close to 0.05 in 2019 (*p*-value = 0.0752). Further statistical evaluation using the Tukey HSD test indicated the fertilization method to be the source of significance. In 2018 the mean score

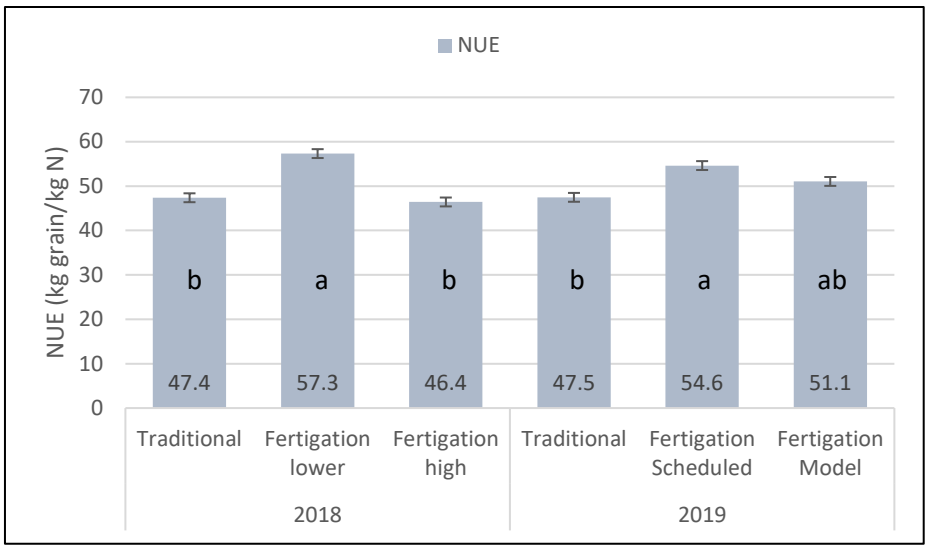

Figure 3.4 Results of the Tukey HSD test to compare means of NUE (kg grain (kg N)$^{-1}$) for different fertilization treatments in 2018 and 2019. Fertigation is the application of fertilizer through the irrigation system. Traditional applied 336 kg N ha^{-1} recurring to preplant, planting, and one side-dress application; Fertigation lower used a rate of 280 kg N ha^{-1} by splitting the side-dress application among four events; Fertigation high applied 336 kg N ha^{-1} using the same strategy of fertigation lower. For 2019, Fertigation Scheduled had a rate of 280 kg N ha^{-1} applied at pre-planting, planting, one side-dress common between treatments and five other side-dress; Fertigation Model is the strategy of application of side-dress according to the STICS model where the total rate was 315 kg N ha^{-1}.

for the lower fertigation method (M = 57.3, SD = 1.3) was significantly different than the traditional and high fertigation conditions (M = 47.4 and 46.4, SD = 1.3). Also, in 2019 the fertigation scheduled method which was the same as the lower fertigation treatment of 2018, (M = 54.6, SD = 1.4) was significantly different from the traditional fertilization method (M = 47.5, SD = 1.4). However, the fertigation model treatment (M = 51.1, SD = 1.4) did not significantly

differ from the other two fertilization treatments tested in 2019. Figure 3.4 shows the results of the Tukey HSD test by analyzing each year separately. Bars with different letters within the same year are significantly different. A significant effect of the factors was seen also on WUE with *p*-values < 0.0001 in both years due to the effect of the irrigation factor. Further statistical evaluation using the Tukey HSD test indicated that the mean score of 1099.6 and 1178.5 kg grain ha^{-1} mm^{-1} of irrigation water of the App and UGA SSA methods were significantly different than the traditional Checkbook of 493.7 kg grain ha^{-1} mm^{-1}. This gap occurs because App and Sensors are responding to actual environmental conditions by getting daily updates during the season, while the Checkbook method schedules according to historical average water demand that do not account for changes in ET rates. For the same reason, the difference is made bigger in years with abundant rain.

The 2019 growing season was drier and required higher irrigation water application (257 to 477 mm). Although WUE was lower compared to 2018 (more irrigation water was needed to grow the crop), significantly lower WUE was recorded for the Checkbook method for which the mean was 33.9 kg grain ha^{-1} mm^{-1}. In 2019 there was also a significant difference between the WUE of the App (61.3 kg grain ha^{-1} mm^{-1}) and the UGA SSA (69.8 kg grain ha^{-1} mm^{-1}) scheduling methods (Figure 3.5). This is likely explained because during 2019 temperatures were unusually high and relative humidity unusually low for extended periods during the growing season. This resulted in higher than normal reference (Penman-Monteith) ET rates which directly affected daily crop water use calculations (ETc) in the App. We hypothesize that estimated ETc rates were greater than actual ETc rates and this resulted in the App overestimating the need for irrigation.

Table 3.4 Average mineral N (NO_3^- and NH_4^+) in the soil profile among three depths (0-0.3 m, 0.31-0.6 m and 0.61-0.9 m) in the five sampling dates among the growing seasons. Different letters indicate statistical differences between the values of the same date

		N in the soil (kg/ha)				
Year	Soil depth	11-Apr	25-May	27-Jun	25-Jul	10-Sep
2018	0-0.30 cm	56 a	32 a	33 a	22 a	5 a
	0.31-0.60 cm	25 b	11 b	18 ab	9 b	4 a
	0.61-0.90 cm	28 b	15 b	27 b	14 b	4 a
		29-Apr	29-May	26-Jun	31-Jul	14-Aug
2019	0-0.30 cm	106 a	57 a	61 a	19 a	32 a
	0.31-0.60 cm	11 b	12 b	55 ab	19 a	29 a
	0.61-0.90 cm	10 b	6 b	26 b	18 a	20 a

Soil

A three-way ANOVA was conducted to evaluate the effect of treatments and soil layers on the soil N content. The analysis was conducted by soil layer 1 (0-0.30 m), layer 2 (0.31-0.60 m) and layer 3 (0.61-0.90 m) for the each of soil sampling dates of the season. The shallowest layer that consists mostly of topsoil (layer 1) consistently had higher N content than the subsoil layers (layer 2 and layer 3) throughout the growing season. Irrigation and fertilization treatments did not appear to have an effect on soil N, so only the effect of depth was further investigated and is reported in Table 3.4. As described earlier, in 2019 soil samples were collected in only nine of the 27 plots and this more limited number of samples did not support the use of ANOVA analyses. Based on the 2018 results, we hypothesized that depth was the only factor having effect on soil N content and the Tukey HSD test was used to compare the means of each layer. Results of the 2019 analyses are reported in Table 3.1 and are similar to results from 2018 with one exception. The data from the 31 July 2019 sampling showed no significant difference between layers.

Model results

The primary goal of this work was to evaluate the STICS model's suitability to predict soil N content available for maize uptake under southeastern growing conditions. Differentiating between the vegetative and reproductive stages of maize development is important in understanding soil N uptake by the plant and for interpreting the results of model simulations as most soil N uptake takes place during the vegetative stage. Consequently, the vegetative stage is the period of greatest

Table 3.5 Evaluation indices of the simulations of the calibration treatments 1 (Corn App × Fertigation High) and 5 (Checkbook × Traditional) from 2018

	SWC[1] layer 1[2] (mm^3/mm^3)				Soil N layer 1 (kg/ha)			
Treatment	MAE	D	NMRSE	R2	MAE	d	NMRSE	R2
1	0.04	0.62	28.10	0.28	21.72	0.65	77.90	0.45
5	0.04	0.73	23.90	0.38	14.76	0.85	33.50	0.71
	SWC layer 2[2] (mm^3/mm^3)				Soil N layer 2 (kg/ha)			
Treatment	MAE	d	NMRSE	R2	MAE	d	NMRSE	R2
1	0.05	0.60	35.70	0.32	15.55	0.11	151.10	0.01
5	0.02	0.64	20.90	0.29	20.86	0.18	151.00	0.00
					Soil N layer 3[4] (kg/ha)			
Treatment					MAE	d	NMRSE	R2
1					9.36	0.82	28.40	0.58
5					10.28	0.36	166.60	0.26
	Biomass Dry Weight (kg/ha)				N in plant (kg/ha)			
Treatment	MAE	d	NMRSE	R2	MAE	d	NMRSE	R2
1	1693.51	0.98	10.70	0.99	17.44	0.99	7.50	0.99
5	897.92	1.00	4.30	0.99	24.37	0.97	10.40	0.93

[1] Soil Water Content
[2] Soil depth 0-0.30 m
[3] Soil depth 0.31-0.60 m
[4] Soil depth 0.61-0.90 m

interest for this study. Tasseling (flowering) is a key stage because it is the transition between the

Table 3.6 Evaluation indices of simulations from 2018 organized by variable

	SWC[1] layer 1[2] (mm^3/mm^3)				Soil N layer 1 (kg/ha)			
Treatment	MAE	d	NMRSE	R2	MAE	d	NMRSE	R2
2	0.04	0.66	27.80	0.38	19.47	0.60	60.90	0.33
3	0.04	0.61	23.30	0.23	21.44	0.70	48.00	0.35
4	0.05	0.55	38.20	0.27	21.44	0.70	48.00	0.35
6	0.06	0.65	27.20	0.48	14.85	0.84	35.50	0.68
7	0.05	0.63	24.50	0.33	24.45	0.55	69.90	0.08
8	0.05	0.65	38.30	0.47	14.71	0.83	38.70	0.72
9	0.05	0.66	29.60	0.38	18.89	0.80	51.10	0.74
	SWC layer 2[3] (mm^3/mm^3)				Soil N layer 2 (kg/ha)			
Treatment	MAE	d	NMRSE	R2	MAE	d	NMRSE	R2
2	0.04	0.56	47.30	0.26	21.16	0.21	106.20	0.03
3	0.03	0.66	28.90	0.27	17.29	0.15	108.10	0.03
4	0.04	0.41	74.50	0.22	17.54	0.06	182.30	0.02
6	0.05	0.34	79.10	0.15	17.58	0.08	143.10	0.09
7	0.04	0.61	29.60	0.23	20.13	0.13	126.60	0.02
8	0.06	0.47	56.00	0.32	16.33	0.45	144.30	0.41
9	0.05	0.50	44.00	0.15	25.80	0.38	67.20	0.00
					Soil N layer 3[4] (kg/ha)			
Treatment					MAE	d	NMRSE	R2
2					14.66	0.65	37.90	0.19
3					15.63	0.39	57.90	0.02
4					15.84	0.10	79.60	0.08
6					8.53	0.48	85.40	0.11
7					12.15	0.61	53.10	0.13
8					11.74	0.56	75.80	0.25
9					18.29	0.18	70.50	0.21
	Biomass Dry Weight (kg/ha)				N in plant (kg/ha)			
Treatment	MAE	d	NMRSE	R2	MAE	d	NMRSE	R2
2	1292.83	0.99	7.10	0.98	15.29	0.99	7.60	0.97
3	965.31	1.00	4.40	0.99	26.72	0.98	10.60	0.96
4	1617.12	0.99	9.40	0.99	22.65	0.98	10.20	0.98
6	1223.53	0.99	7.70	0.98	9.96	1.00	4.50	0.99
7	2632.46	0.97	14.80	0.98	35.06	0.96	15.50	0.94
8	2184.28	0.98	11.50	1.00	25.16	0.98	10.30	0.99
9	1877.12	0.98	11.30	0.97	28.63	0.97	13.50	0.94

[1] Soil Water Content
[2] Soil depth 0-0.30 m
[3] Soil depth 0.31-0.60 m
[4] Soil depth 0.61-0.90 m

vegetative and reproductive stages of maize development. The vegetative stage corresponds to approximately the first 60 days after planting (DAP). In this study, tasseling began at about 65 DAP in 2018 and 60 DAP in 2019.

Table 3.7 Evaluation indices of simulations from 2019 organized by variable

	SWC[1] layer 1[2] (mm^3/mm^3)					Soil N layer 1 (kg/ha)			
Treatment	MAE	d	NMRSE	R2	Treatment	MAE	d	NMRSE	R2
1	0.06	0.50	24.10	0.12	3	19.06	0.90	28.10	0.88
2	0.04	0.56	19.10	0.13	6	23.80	0.83	36.50	0.68
3	0.06	0.48	26.90	0.09	9	13.05	0.95	15.00	0.91
4	0.05	0.57	23.00	0.16					
5	0.04	0.61	20.20	0.16		Soil N layer 2 (kg/ha)			
6	0.04	0.55	23.30	0.09	Treatment	MAE	d	NMRSE	R2
7	0.04	0.65	26.50	0.22	3	18.66	0.10	71.70	0.16
8	0.04	0.61	19.20	0.20	6	26.51	0.19	63.00	0.23
9	0.05	0.48	23.50	0.10	9	21.09	0.15	83.00	0.00
	SWC layer 2[3] (mm^3/mm^3)					Soil N layer 3[4] (kg/ha)			
Treatment	MAE	d	NMRSE	R2	Treatment	MAE	d	NMRSE	R2
1	0.05	0.49	28.60	0.23	3	8.66	0.45	35.70	0.22
2	0.03	0.55	31.60	0.29	6	11.78	0.41	38.30	0.02
3	0.03	0.60	24.30	0.26	9	6.85	0.54	50.70	0.02
4	0.04	0.45	37.60	0.16					
5	0.07	0.43	41.50	0.13					
6	0.02	0.56	21.40	0.28					
7	0.04	0.67	33.00	0.43					
8	0.04	0.52	32.60	0.43					
9	0.03	0.49	20.80	0.12					
	Biomass Dry Weight (kg/ha)					N in plant (kg/ha)			
Treatment	MAE	d	NMRSE	R2	Treatment	MAE	d	NMRSE	R2
3	7280.08	0.80	34.20	0.60	3	125.00	0.72	38.00	0.34
6	7937.43	0.84	28.10	0.76	6	104.35	0.79	31.10	0.62
9	8226.03	0.80	32.60	0.62	9	111.59	0.76	31.40	0.49

[1] Soil Water Content
[2] Soil depth 0-0.30 m
[3] Soil depth 0.31-0.60 m
[4] Soil depth 0.61-0.90 m

Table 3.8 Evaluation of model performances according to the observed values using lack of fit method organized by variable. $F < F_{0.05}$ represent a good simulation; $F > F_{0.05}$ mean that the model can be improved

Variable	Calibration		Validation 2018		Validation 2019	
	F	$F_{0.05}$	F	$F_{0.05}$	F	$F_{0.05}$
Soil N layer 1[1]	5.98	2.35	3.63	1.60	3.65	1.90
Soil N layer 2[2]	53.57	2.35	11.33	1.60	9.41	1.90
Soil N layer 3[3]	7.72	2.35	4.03	1.60	2.62	1.90
Biomass DW[4]	4.29	2.35	3.36	1.60	42.54	1.72
N in plant	3.64	2.35	2.42	1.60	52.06	1.72
Yield DW	3.23	6.94	8.97	2.76	3.78	2.46
N in grain					5.13	2.46

[1] Soil depth 0-0.30 m
[2] Soil depth 0.31-0.60 m
[3] Soil depth 0.61-0.90 m
[4] Dry weight is abbreviated by DW

Two treatments (Checkbook × Traditional, App × Fertigation high) from 2018 were used for calibrating the model. The seven remaining 2018 treatments and all 2019 nine treatments were used to validate the model's performances. Four evaluation indices were used to assess the performance of the model. The results of the evaluation indices are reported in Table 3.5 for the calibration, in Table 3.6 for the validation of 2018 and in Table 3.7 for the validation of 2019. As described in the previous chapter, MAE and NRMSE quantify the departure of the model outputs from the measurements adding up the errors. As a result, predictions that follow the trend with a consistent under-prediction or over-prediction do not appear to be useful. In this study, the ability of the model to match the observed trends in the data is more important. Because of this d and R^2 were primarily used to assess performance as they measure the correlation between model predictions and observations; in other word they compare the trends. Table 3.8 illustrates the

results of the lack of fit test showing the F calculated and the respective F_{α} from the F-table. Good simulations have $F < F_{\alpha}$.

Soil water content - calibration

Simulation of soil water content (SWC) is important not only to estimate plant water uptake, but also to calculate N mineralization and nitrification that are strongly dependent upon soil moisture. For this reason, SWC was the first variable to be calibrated. As mentioned in the previous chapter,

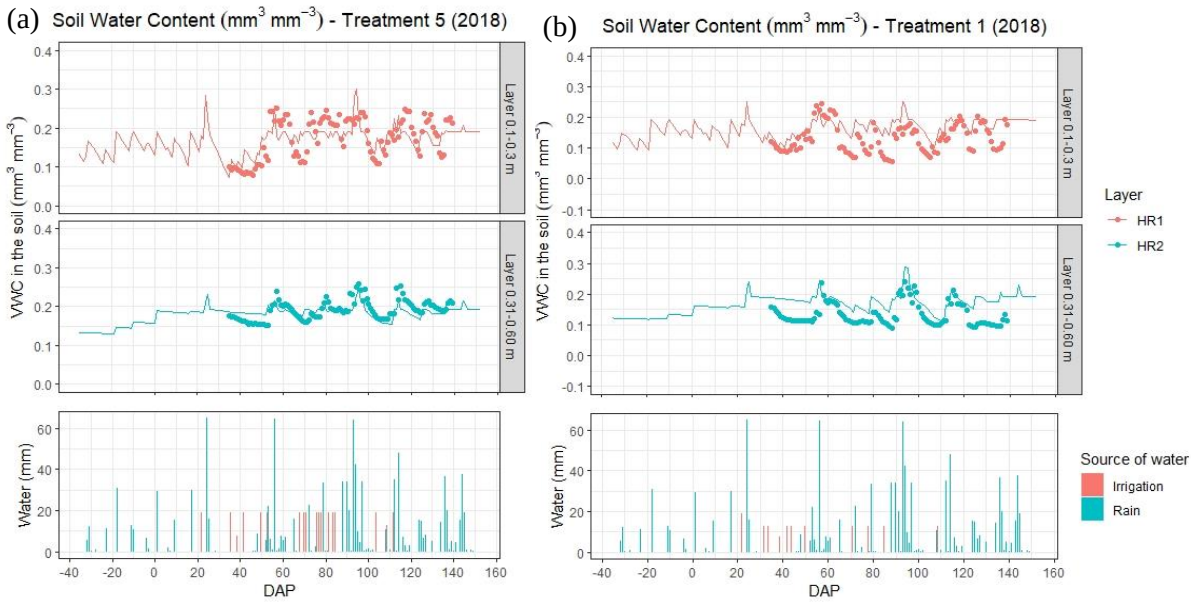

Figure 3.6 Dynamics of measured (dots) and simulated (lines) SWC in successive soil layers over time expressed as DAP for calibration treatment 5 (Checkbook × Traditional) (a) and treatment 1 (App × Fertigation high) (b) of 2018. The bar graphs show irrigation (red) and rainfall (blue) expressed in mm over the same x axes

data from the soil moisture probes were collected up to a depth of 0.60 m. SWC simulations to the top two layers of the soil profile from which field observations were available.

Among the four indices used for the model evaluation, the index of agreement (d) consistently resulted in higher values compared to the R^2, in agreement with Valbuena, et al. (2019). This index ranges from 0 to 1 with results closer to 1 indicating good model performances.

In the treatments used for calibration, d for SWC of layer 1 is respectively 0.73 in treatment 5 (Checkbook × Traditional) and 0.62 in treatment 1 (App × Fertigation high), while in layer 2 is 0.64 and 0.60 (Table 3.5). In treatment 5 and especially in the second soil layer, observed water content was mostly higher than the simulated values (Figure 3.6).

One explanation for this trend is that gravimetric water content at FC of the layer was set to 12 % of dry soil and multiplied by bulk density (1.6 g cm^{-3}) to obtain volumetric water content (VWC) at FC, which was estimated at 19.2 mm^3 mm^{-3} (Liang, et al., 2016). Simulations do not match the higher observed values because FC is set as the upper threshold, with exception of four peaks during the season in which the very high rainfall resulted in simulations over FC. However, the general trend of the simulation of SWC of both treatments used for the calibration is in agreement with the observed values.

It is important to point out that the observed values of SWC carry some errors. First, the values of the second layer result from the weighted average of two sensors located at 0.4 m and 0.6 m, respectively. Also, SWT values are the average of the readings at 7:00 am of the three replicates and therefore may be not representative of the average daily condition calculated by the model. For the same reason, errors can also result from rainfall events or high ET rates that occurred during the day that are not captured by the sensor data used for the observed values.

The conversion of SWT to VWC through predicted water retention curves is a further possible source of error. Ultimately, the plant canopy can influence the moisture condition around the probe by either deflecting irrigation water away from the sensor or channeling it towards the sensor probes.

Soil water content – validation 2018

The remaining treatments of 2018 all of which had different irrigation and fertilization strategies than the ones used for calibration where used to validate the calibrated model. Validation results

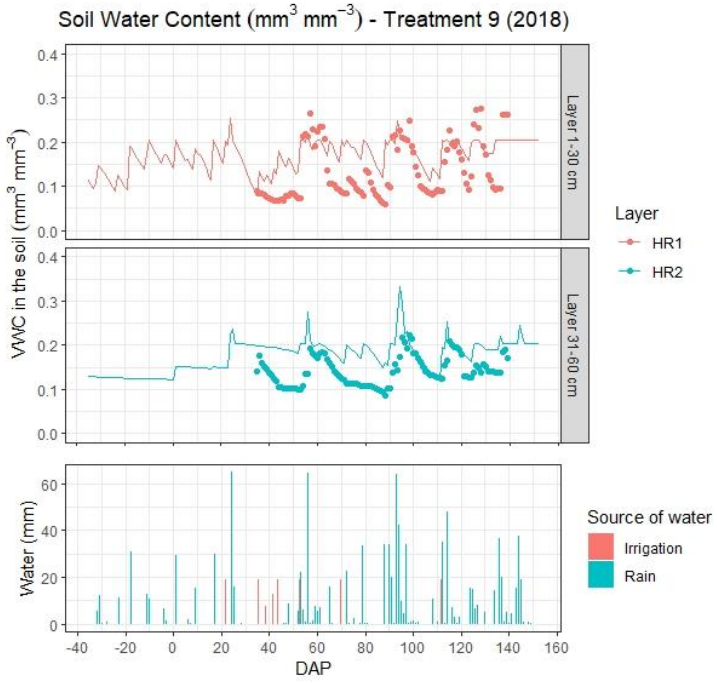

Figure 3.7 Dynamics of measured (dots) and simulated (lines) SWC in the soil during the growing season expressed in DAP for treatment 9 (UGA SSA × Fertigation lower) in 2018. The bar graphs show irrigation (red) and rainfall (blue) expressed in mm over the same x axes

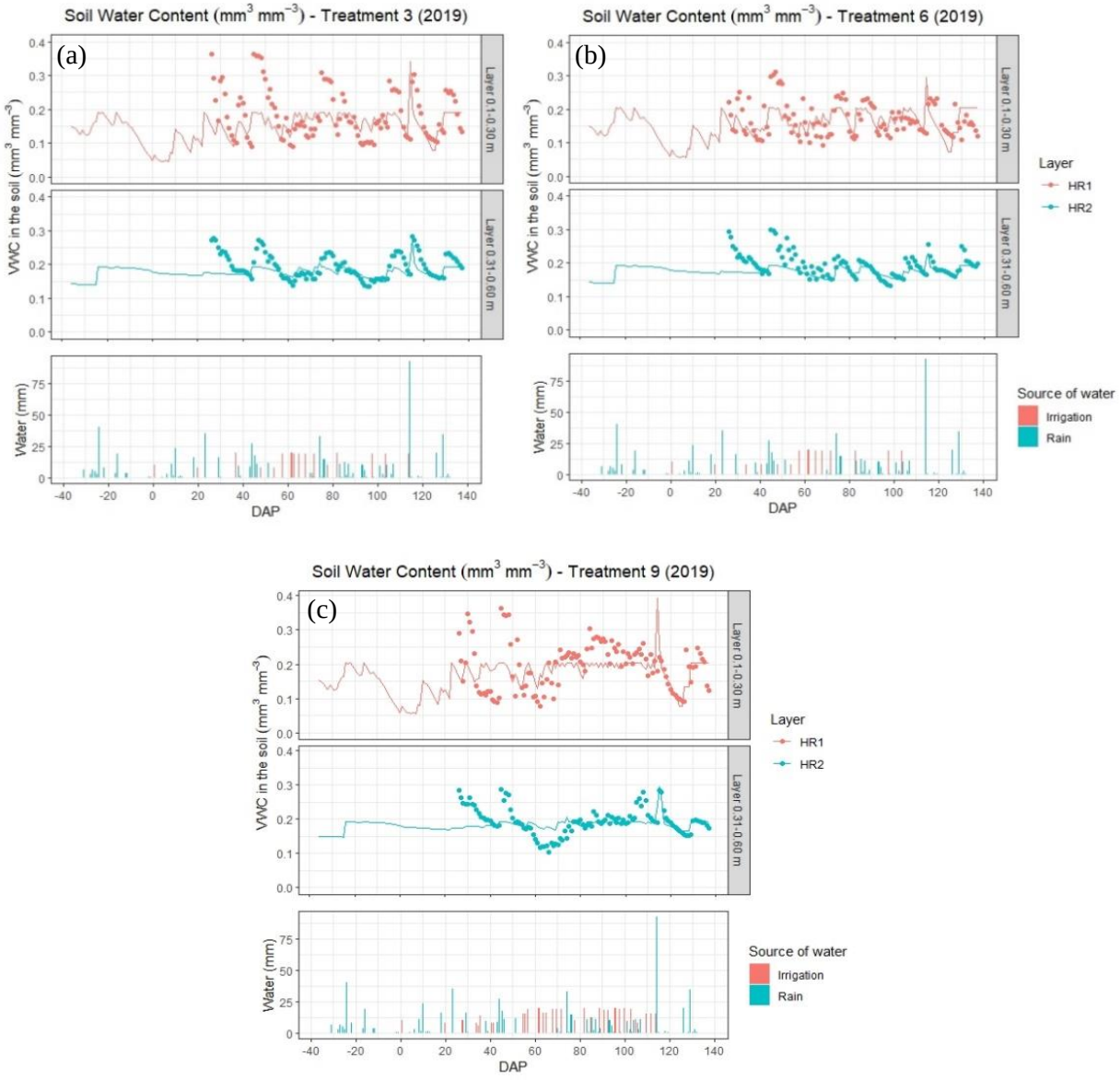

Figure 3.8 Dynamics of measured (dots) and simulated (lines) SWC in the soil during the growing season expressed in DAP for treatment 3 (a), 6 (b) and 9 (c) of 2019 (App × Fertigation Model, UGA SSA × Fertigation scheduled and Checkbook × Traditional). The bar graphs show irrigation (red) and rainfall (blue) expressed in mm over the same x axes

of SWC from treatment 9 (UGA SSA × Fertigation lower) are shown in Figure 3.7. Results from

the other six treatments are reported in Figure A.1 in Appendix A. For treatment 9, as well as for the other validated treatments of 2018, the model described the changes in water content well. The average index of agreement of SWC was 0.63 in layer 1 and 0.51 in layer 2. R^2 was 0.36 and 0.24, respectively, all acceptable values for simulations of field studies.

Soil water content – validation 2019

In 2019, the model was validated for all nine treatments. There are similar soil texture conditions between the two fields where maize was cultivated in 2018 and 2019. Both have a loamy fine sand topsoil and a sandy loam subsoil, with the difference that in 2018 layer 2 is classified as loamy fine sand, while in 2019 layer 2 is classified as a sandy loam.

Validation results of SWC for treatments 3 (App × Fertigation Model), 6 (UGA SSA × Fertigation Scheduled) and 9 (Checkbook × Traditional) are reported in Figure 3.8. Validation of the-remaining treatments are shown in Appendix A, Figure A.4.Values of the evaluation indices for SWC of 2019 were lower than those of 2018 which was expected as growing conditions were different from the 2018 conditions used to calibrate the model. The average d was 0.56 for layer 1 and 0.53 for layer 2. Average R^2 was 0.14 and 0.26 in layer 1 and 2, respectively. SWC values in 2019 had a wider range than in 2018 due to the frequent, but not substantial, rainfall that caused notable fluctuations in the dynamics, especially in the stages of fast vegetative growth (before 60 DAP). There was considerable rainfall on DAP 114, amounting to a total of 92 mm. This rainfall caused a large peak in simulated soil moisture, especially in layer 1, exceeding the measured values in treatments 6 and 9 but especially treatment 9. It is not clear why the shallow sensors in this treatment did not respond especially since the sensors located in layer 2 responded and matched the simulated SWC.

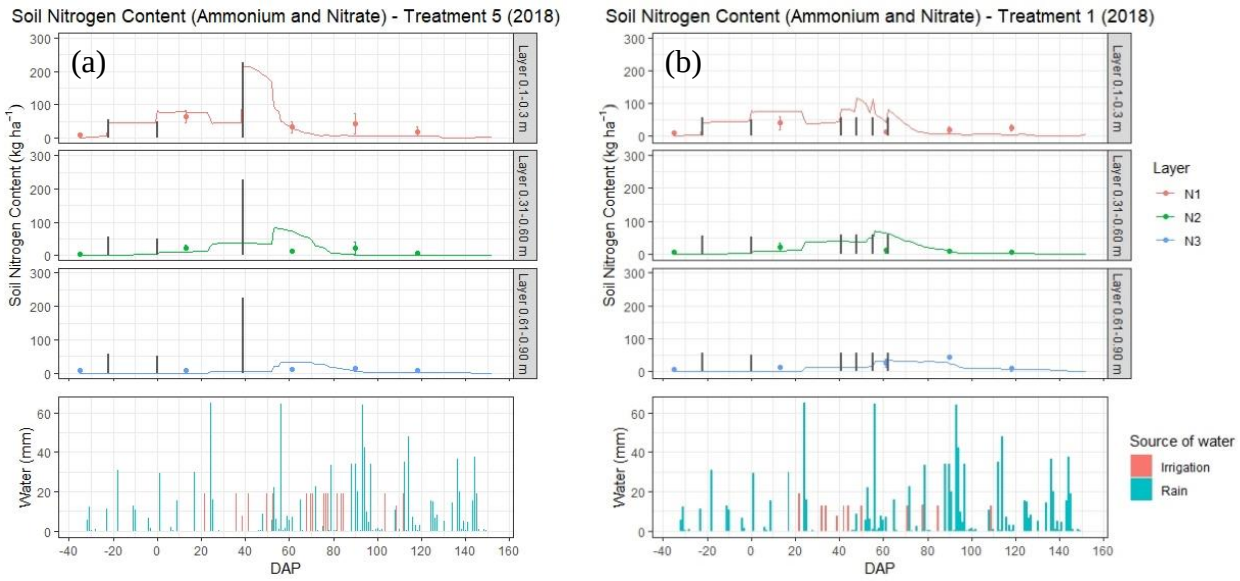

Figure 3.9 Dynamics of measured (dots) and simulated (lines) N in the soil in successive soil layers over time expressed as DAP for calibration treatments 5 (a) and 1 (b) of 2018 (Checkbook × Traditional and App × High nitrogen). Black bars represent fertilizer applications in kg N ha^{-1}. The bar graphs show irrigation in red and rain in blue expressed in mm over the same x axes

Soil nitrogen content - calibration

Figure 3.9 shows the simulated response and observations of soil mineral N content in three successive layers of 2018 treatments 5 and 1 used for calibration. The simulation trends responded to fertilization events with a rapid increase of the amount of layer 1 that later on was absorbed by the plant or leached to the lower layer after rainfall events. N in layer 1 is simulated accurately. In treatment 5, d = 0.85, R^2 = 0.71 and in treatment 1, d = 0.65, R^2 = 0.45. Similarly, predictions of layer 3 reported good indices values (d = 0.36 and 0.82 in treatments 5 and 1, respectively). On the contrary, N content in layer 2 is not well simulated. The same discrepancies between the simulation of the different layers is shown by the F values (Table 3.7). All the F values calculated were higher than the threshold ($F_{0.05}$) suggesting that the overall N simulation can be improved,

but the magnitude of the divergence for layer 2 is much more relevant than layer 1. Compared to observed N, STICS over-predicted total mineral N at the third sampling date that took place at tasseling (DAP 63). Because the simulated peak in N that occurs prior to the sampling date matches the trend that is simulated in layers 1 and 3, one possible explanation is that the laboratory analysis did not accurately capture the N in the soil sample or that depths were inaccurately sampled during sample collection. This explanation is supported by good predictions of aboveground biomass and N in the plant at the same sampling date (Figure 3.12) which indicate that the model was performing well. Another possible explanation is that the model may have under-predicted leaching of N from layer 2. This explanation can not be confirmed due to the absence of leaching

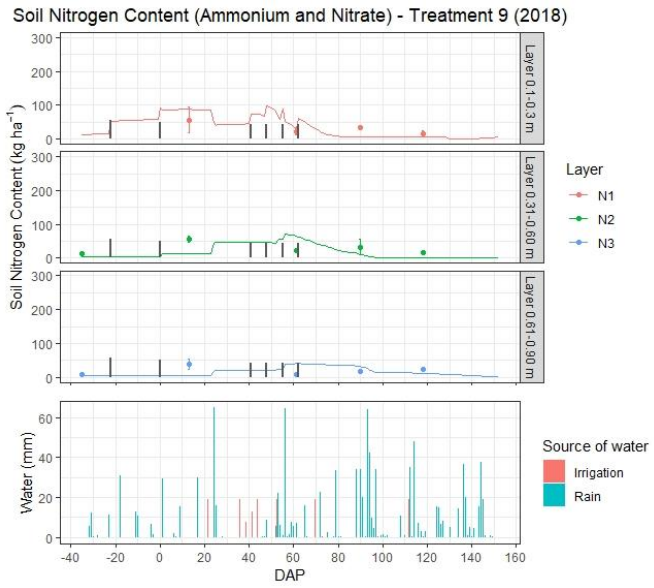

Figure 3.10 Dynamics of measured (dots) and simulated (lines) SWC and N in the soil during the growing season expressed in DAP for treatment 9 (UGA SSA × Fertigation lower) in 2018. Black bars in (b) represent fertilizer applications in kg N ha^{-1}. The bar graphs show irrigation in red and rain in blue expressed in mm over the same x axes

observations or of measured mineralization values that could be used to compute a simplified N mass balance.

Soil nitrogen content – validation 2018

Treatment 9 (Figure 3.10) as well as the other validated treatments of 2018 (Figure A.2) had similar trends and evaluation indices as the calibration treatments. The over-prediction of the third observed point is consistent throughout the simulations. Average d values were 0.70 for layer 1, 0.18 and 0.10 for layer 2 and 0.46 for layer 3. Layer 3 actually reported poor predictions in two treatments out of seven (Treatments 4 and 9) with d values of 0.10 and 0.18; the reason is the considerable under-prediction of the second observed point that could result from the same above-mentioned problem of N percolation through the profile.

Soil nitrogen content – validation 2019

In 2019, the model provided a more accurate estimate of soil N content than the calibration (Figure 3.11). Observed values of N in the soil were collected only in treatments 3, 6 and 9. The simulation of the first 0.3 m of the soil profile was excellent (d = 0.90, 0.83, 0.95; R^2 = 0.88, 0.68, 0.91). Simulation of layer 2 was poor for all treatments (d = 0.10, 0.19, 0.15) and layer 3 was good with average d of 0.47, very close to the accuracy observed in the validation in 2018.

Aboveground biomass, nitrogen in the plant and grain - calibration

As already mentioned earlier, aboveground biomass and biomass N content are simulated well by the model (Figure 3.12 a, b, d, e). The evaluation indices d and R^2 have values close to the best fit: d values for biomass simulation are 1.00 for treatment 5 and 0.98 for treatment 1, while for N in

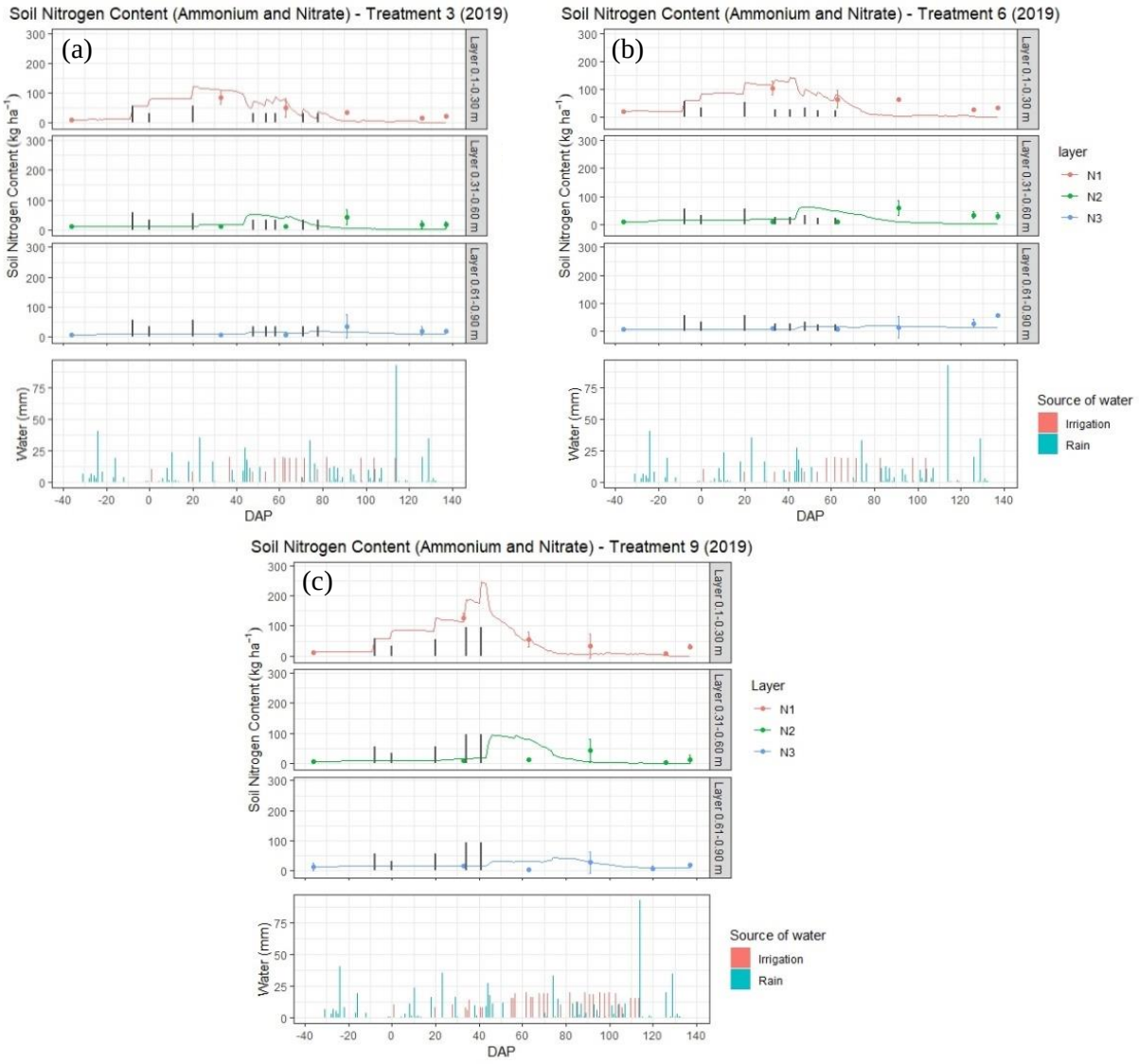

Figure 3.11 Dynamics of measured (dots) and simulated (lines) soil mineral N during the growing season expressed in DAP for treatment 3 (a), 6 (b) and 9 (c) of 2019 (App × Fertigation Model, UGA SSA × Fertigation scheduled and Checkbook × Traditional). Black bars represent fertilizer applications in kg N ha^{-1}. The bar graphs show irrigation (red) and rainfall (blue) expressed in mm over the same x axes

the aboveground biomass d is respectively 0.97 and 0.99; R^2 values are between 0.93 and 0.99.

These variables allow to clearly notice the difference in the method of evaluation of the different indices. Despite the very good results of d and R^2, F values are slightly higher than F0.05 suggesting further improvement of the model.

Leaf are index (LAI) data were collected in 2019. However, simulations of LAI returned unreasonably high values. This parameter of the model requires additional calibration but because its poor simulation does not appear to affect other biomass-related simulations, simulation results were not reported here.

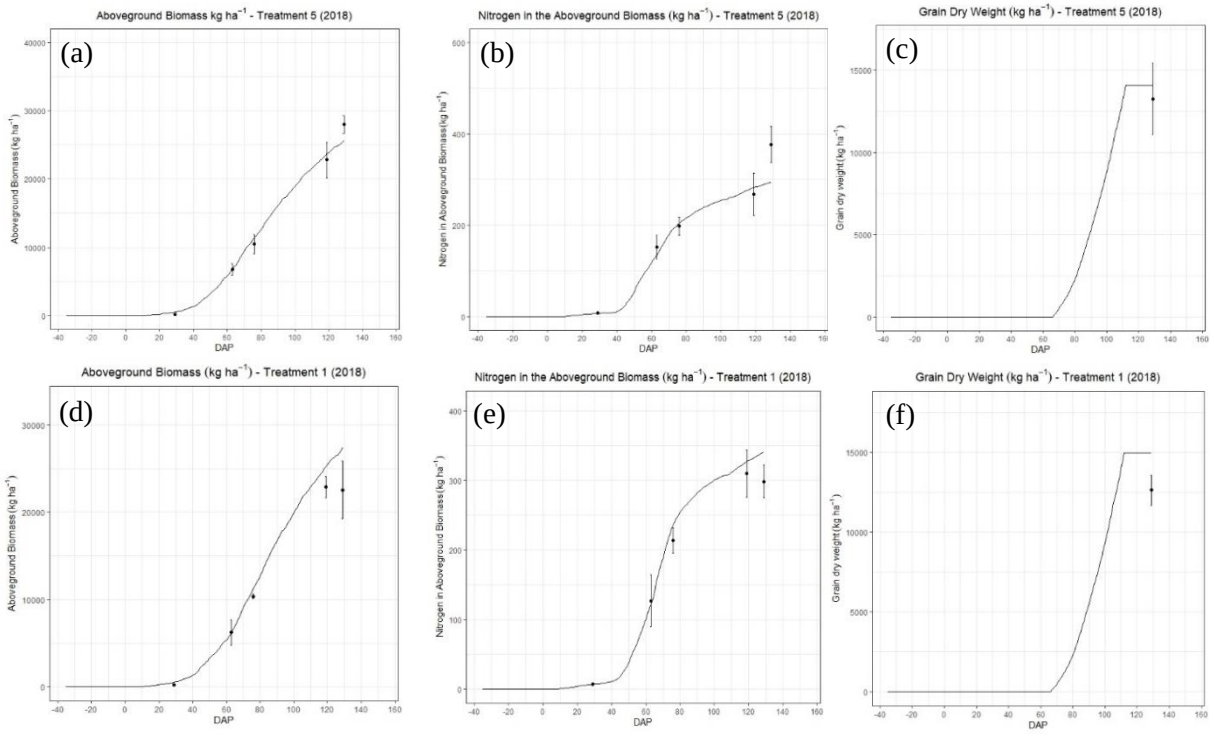

Figure 3.12 Results of calibration treatments 5 (Checkbook × Traditional) and treatments 1 (App × High nitrogen) of 2018 for aboveground biomass dry weight (a, d), plant N content (b, e) and grain dry weight (c, f). Lines represent the model simulations and dots the observed values over time expressed as days after planting (DAP)

After the model was calibrated, the simulated grain filling period began at 67 DAP, which was between the range observed in the field study. The predicted duration of grain filling was 62 days. The simulation ended about 20 days before the actual harvest date because the model predicted that the grain was ready to harvest. This coincided well with observed maturity. Harvest was delayed by a few days to allow for the moisture content of the grain to decrease naturally. Additional delays were caused by scheduling of the grain plot harvester.

The simulation of grain dry weight corresponded well to the observed value in treatment 5 (Figure 3.12 c), while treatment 1 was slightly over-predicted (Figure 3.12 f). F value from the calibration was lower than the respective $F_{0.05}$ showing reliable model simulation. Performance indices were not used for this variable because there was only on observed value per simulation.

Aboveground biomass, nitrogen in the plant and grain – validation 2018

Results from the validation simulation of the 2018 treatment 9 are shown in figure 3.13. The simulation results for all the other treatments are shown in figure A.3 in Appendix A. Among all

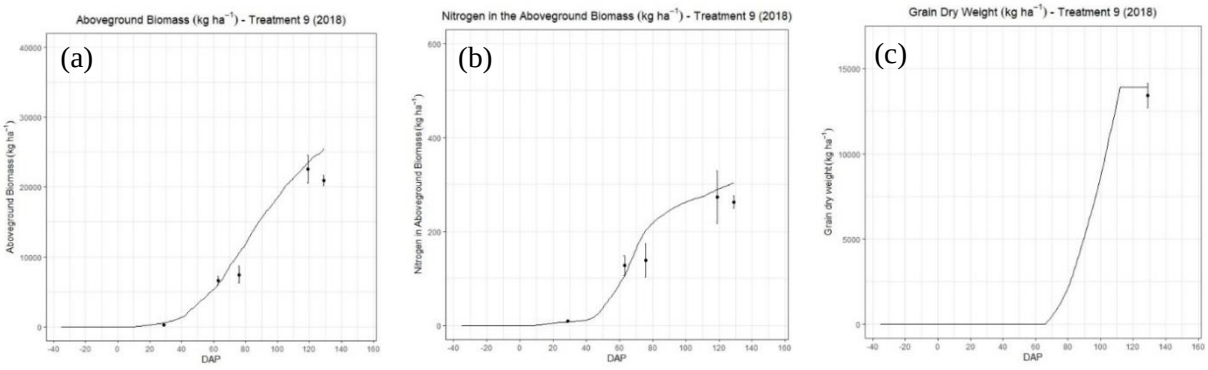

Figure 3.13 Dynamics of measured (dots) and simulated (lines) aboveground biomass (a), N in the plant (b) and grain dry weight (c) of treatment 9 (UGA SSA × Fertigation lower) in 2018

treatments, the average predicted N in aboveground biomass (316 kg ha^{-1}) was slightly higher than the observed (305 kg ha^{-1}). The average observed N uptake was also greater than the average simulated uptake. The observed and simulated N uptake was greater than that of published uptake estimates (287 kg ha^{-1}) of hybrids cultivated in the Corn Belt for similar yields (Bender, et al., 2013). However, for the vegetative stage prior to tasseling which is of greatest interest to this study because it is when side-dress N is applied, the average simulated amount of N in the plant (144 kg ha^{-1}) was lower than estimated by Bender et al. (180 kg ha^{-1}). This might suggest an under-prediction in the uptake before tasseling and over-prediction in N uptake after tasseling that would also explain the excess N in the soil predicted at DAP 63 and the under-prediction of soil N during the reproductive stage of maize. However, it is difficult to identify and quantify possible errors because of the lack of samples between V6 and VT. In addition, studies like the one conducted by Bender et al. (2013) are not available for the environmental conditions and varieties of the southeastern Coastal Plain. Simulation of yield was not as good as the calibration treatments according to the lack of fit evaluation method.

Aboveground biomass, nitrogen in the plant and grain – validation 2019

The simulations results of the 2019 treatments for aboveground biomass and N content matched the first and the last observed points, while intermediate observations were under-predicted by the model (Figure 3.14). The weather during the 2019 growing season may be the cause of the difference in biomass accumulation and N content. Index of agreement (d) for biomass was 0.80, 0.84 and 0.80 in treatments 3, 6 and 9, respectively, which are lower than 2018, but nevertheless indicate good performance. The d values for biomass N content were 0.72, 0.79 and 0.76 in treatments 3, 6 and 9 respectively. F values were substantially higher than the threshold of

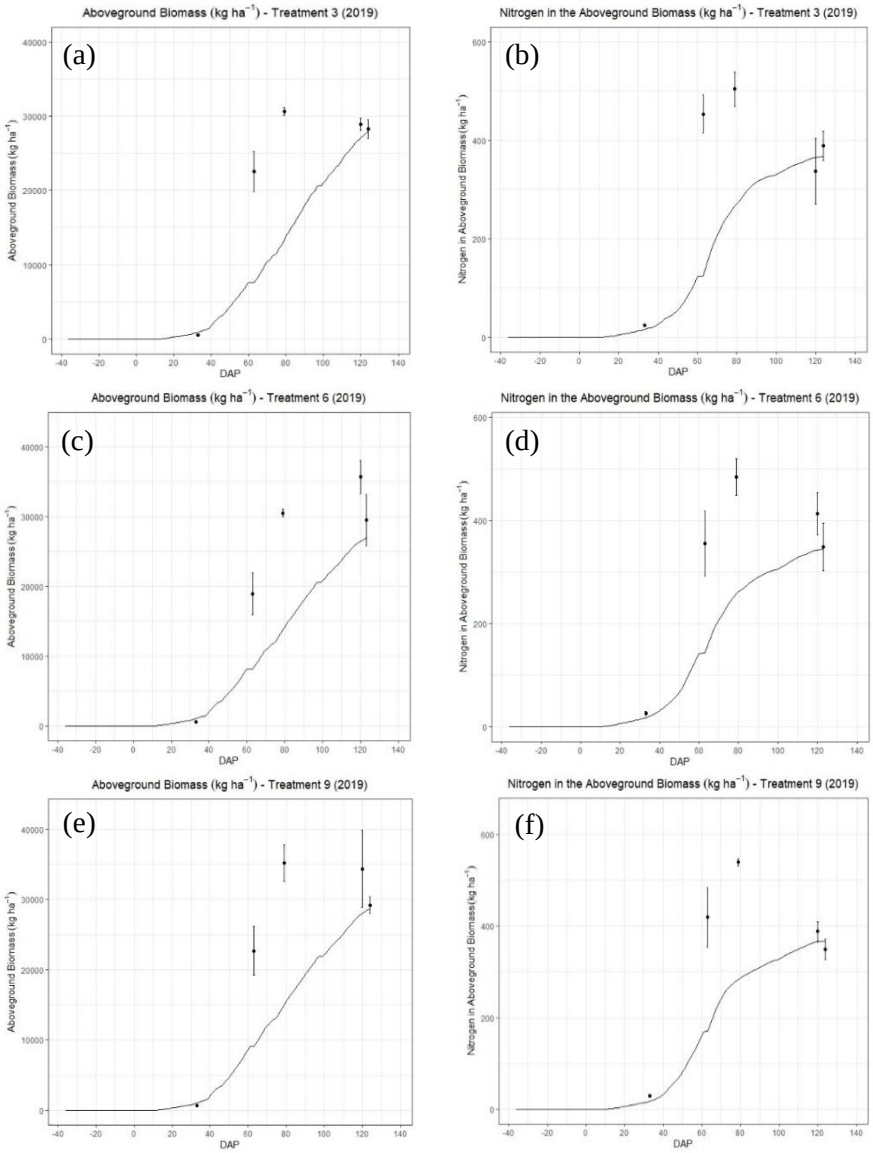

Figure 3.14 Dynamics of measured (dots) and simulated (lines) aboveground biomass (a, c, e) and N in the plant (b, d, f) during the growing season expressed in DAP for treatment 3 (a, b), 6 (c, d) and 9 (e, f) of 2019 (App × Fertigation Model, UGA SSA × Fertigation scheduled and Checkbook × Traditional)

significance. High values of biomass N content compared to 2018 were observed at 63 and 79

DAP. Between middle June (79 DAP) and the end of July (126 DAP) a sharp decrease of biomass

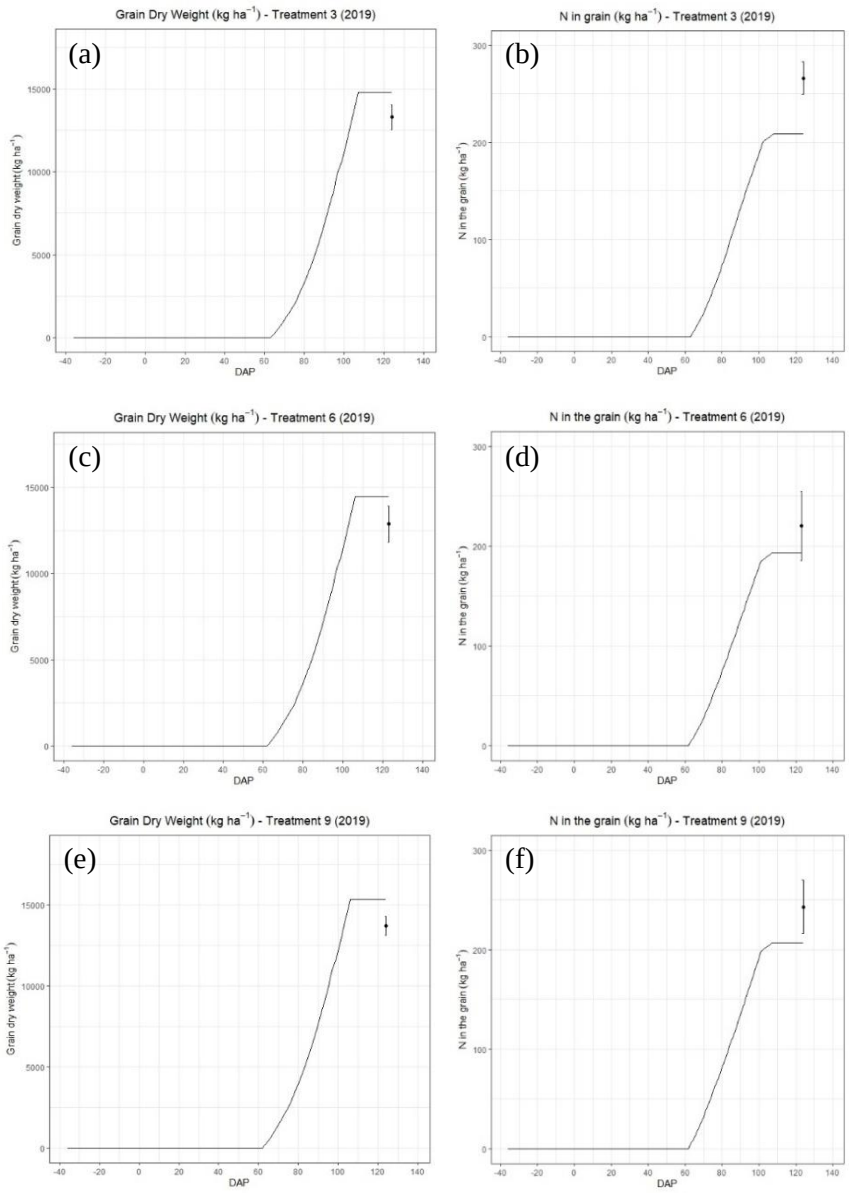

Figure 3.15 Dynamics of measured (dots) and simulated (lines) grain dry weight (a, c, e) and N in the grain (b, d, f) during the growing season expressed in DAP for treatment 3 (a, b), 6 (c, d) and 9 (e, f) of 2019 (App × Fertigation Model, UGA SSA × Fertigation scheduled and Checkbook × Traditional).

N content was observed that approached 200 kg N ha^{-1} in treatment 3, 70 kg ha^{-1} in treatment 6 and 150 kg ha^{-1} in treatment 9. The abrupt decrease which was not observed in 2018 and is not an expected trend (DeBruin, et al., 2013), was most likely the result sampling one or small ears per plant at 63 and 79 DAP that did not reach maturity and were aborted by the plant. Most mature plants had only one full ear. Field observations show that the average number of ears per linear yard (0.914 m) of maize were 13 and 11 respectively at 63 and 79 DAP, and 8 at 126 DAP close to maturity. The small plateau in the simulation curves around 60 DAP corresponds to the tasseling stage during which plant biomass and N uptake slow down (Bender, et al., 2013).

Despite the difference in weather pattern and biomass accumulation, grain yield was accurately predicted (Figure 3.15 a, c, e). In 2019, the grain was analyzed for TKN and the model simulated this variable relatively well without calibration (Figure 3.15 b, d, f).

This is because the simulation of N in the grain is directly related to the amount of N in the biomass and the harvest index calculated to simulate yield. Good simulation of biomass and grain yield is reflected in good simulation of N in the grain. Similarly, to dry weight of grain, no statistical evaluation was conducted on this variable due to the insufficient number of observed values.

The biggest difference between observed and simulated N in the grain was in treatment 3 in which the observed N was slightly higher than that observed in treatments 6 and 9. This result may be because the treatment received a fertigation application after tasseling. Mueller, et al. (2017) also observed higher N content in grain when N fertilizer was applied after tasseling. However, there is no evidence of this difference in treatments 4 and 7 that also received N via fertigation after tasseling (Figure A.5, Appendix A).

Summary

Overall, model validation was determined to be good as the evaluation indices from validation were similar to those from calibration. The best-simulated variables were aboveground biomass and biomass N content.

SWC of layer 2 was worse simulated compared to layer 1. This is in contrast to the relatively good simulation of SWC in layer 1. Saglam M. (2017) also observed lower accuracy in the prediction of subsoil water content and attributed it to uncertainties in root water uptake parameterization and spatial differences in root distribution.

Simulations performance of soil N for layers 1, soil N for layer 3, SWC of layer 1 and SWC of layer 2 were similar. As with SWC, the worst agreement with observed data occurred for layer 2.

Overall, the evaluation of the lack of fit showed poor predictions for all the variables (yield dry weight was the only not significant variable at the 0.05 level). Significance of all the variables indicate a lack of fit error which is significantly different from experimental error. The discrepancies were higher for N in the soil of layer 2 among all the simulations, and for biomass and N in the plant in 2019. However, the uniformity of the results between calibration and validation is meaningful. It suggests that the performance of the model was consistent between treatments.

Fertigation Model treatment

Side-dress fertilizer was applied to 2019 treatments 3, 4 and 7 by scheduling fertigation with the STICS model. For these treatments, daily simulations were run during the growing season to monitor the evolution of N content in the soil profile. Fertigation was scheduled when simulated soil N began to decrease sharply. Figure 3.16 shows the final trend of N from the first date of soil

sampling to harvest. As described earlier, during 2019, soil samples were collected in nine of the 27 plots and so soil N content data were available only for only one of the model fertigation treatments (Treatment 3 – App × Fertigation Model).

Because roots are likely to reach a depth of 0.60 m by the V7 stage (Archontoulis S., 2017), which in this study corresponded to about 40 DAP and extend beyond that as the plant grows, all three soil layers were considered in the model. The minimum N application rate set for this model fertigation treatment was 280 kg ha^{-1} of which 135 kg ha^{-1} was to be applied through fertigation in 34 kg ha^{-1} increments. This was the minimum rate that could be reliably replicated by the fertilizer injection system used in the study. As shown in Figure 3.16, the similar trends between treatments

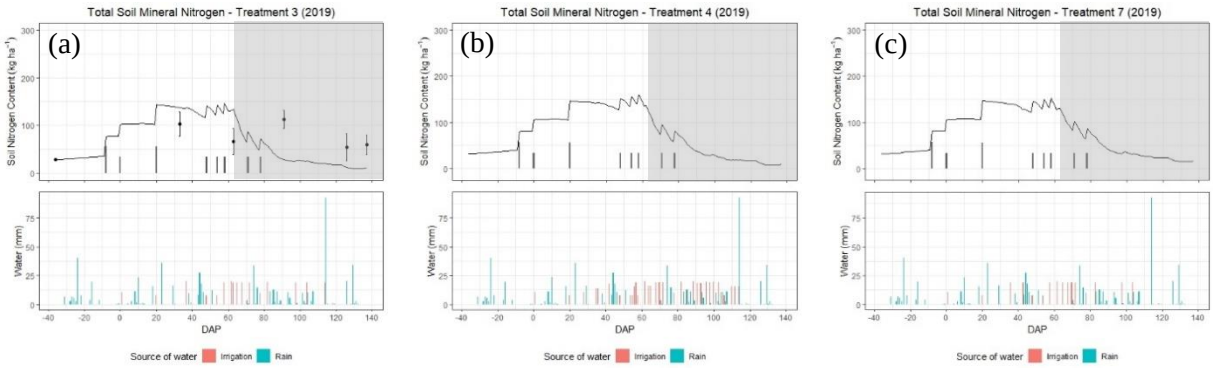

Figure 3.16 Dynamics of measured (dots) and simulated (lines) total N in the soil profile during the growing season expressed as DAP for treatment 3 (a), 4 (b) and 7 (c) of 2019 (App × Fertigation Model, Checkbook × Fertigation Model and UGA SSA × Fertigation Model). Black bars represent fertilizer applications in kg N ha^{-1}. The bar graphs show irrigation (red) and rainfall (blue) expressed in mm over the same x axes. Grey background identifies post-flowering stages

justified the uniformity in dates of fertigation. Fertilization was triggered whenever a drop in total soil nitrogen content was detected by the model. Three events took place before tasseling: 48 DAP, 54 DAP and 58 DAP. During tasseling, the model showed a sharp decrease in soil N but fertigation was postponed until after tasseling to avoid interference during the critical pollination stage. The next fertigation event was applied at 71 DAP. A week later, the model showed that soil N had decreased to 65 kg ha^{-1} and the decision was made to apply another dose of 34 kg ha^{-1} at 78 DAP. This decision was made because the scientific literature reports that modern maize hybrids uptake significant amounts of after tasseling. (DeBruin, et al., 2013) reported that 37 % of the total uptake occurs post-flowering. Distribution of N uptake during the crop life cycle is shown in (Figure 1.1). The first fertigation driven by the model occurred 14 days after the first event of the scheduled treatment, at stage V9/V10. This delay did not affect yield indicating that there was adequate soil N from the earlier applications to support vigorous growth during V9/V10.

Comparison of the simulation with the observed values of treatment 3 (Figure 3.16 a) shows that soil N after tasseling was under-predicted by the model. This suggests that the last fertigation event might have been avoided resulting in increased NUE without causing a decrease in yield. This conclusion is supported by the similar yield results of the scheduled fertigation treatments that did not receive the fifth fertigation application. Further analysis of the model is needed to determine why it under-predicted soil N after tasseling.

The method currently used to trigger fertigation has important limitations. It does not include an estimate of future plant nitrogen requirements and as such, it is not able to estimate how much more N should be applied to meet plant needs. Furthermore, the scientific literature does not provide soil N value below which additional N should be applied as a function of crop phenological stage. As a result, fertigation was triggered when a sharp decline in soil N was predicted by the

model. Another obstacle that was encountered during the study was that due to time constraints, the model was not fully calibrated at the time that side-dress N was needed during the 2019 growing season. As a result, the model simulations used to apply fertigation were likely not optimal. the fertigation model treatment was applied according to a primitive model adjustment. Additional research is needed to determine how and when to trigger fertigation with a simulation model.

CHAPTER 4

CONCLUSIONS

Field experiment

Efficient use of irrigation water and N management is important to minimize agricultural contributions to nitrate pollution of groundwater and optimize profits for maize producers. Results from this study suggest that both water and nitrogen recommendations currently used in Georgia overestimate maize requirements. The methods recommended by the University of Georgia Extension Service and which were used as the baseline "traditional" methods in this study are the Checkbook method for irrigation and a 1.2 multiplier to determine N application rates based on yield goals in bu ac^{-1}, respectively. In this study, these traditional methods were compared to irrigation and fertilization management strategies with potential to improve WUE and NUE.

For both years of the study, WUE for the UGA SSA and SmartIrrigation Corn App irrigation scheduling strategies were statistically significantly better the than the Checkbook strategy (Figure 3.5). Although these two strategies had similar performance, the Corn App does not require soil moisture sensor installation after planting and removal prior to harvest. However, the Corn App does require accurate precipitation data and if a weather station is not close by, an automated rain gage is needed in or near the field for peak performance.

Average grain yield achieved at the study site ranged from 13.5 to 18.5 tons ha^{-1} with no statistically significant differences between treatments (Figure 3.3). However, the fertigation strategy that used a 1.0 multiplier to determine N application rates based on yield goals in bu ac^{-1}

used considerably less N than the traditional method. Consequently, NUE for this strategy was statistically significantly higher (Figure 3.4). The hypothesis that side-dress N applied via fertigation would result in higher yields was rejected. This is likely because even the lowest fertilizer treatment (280 kg ha^{-1} or 250 bu ac^{-1}) provided more than enough N to meet the fields' yield potential under the environmental conditions encountered in 2018 and 2019. Additional research is needed to determine this threshold.

STICS

The principal objective of this study was to adapt, calibrate, and validate the STICS model for maize production under the growing conditions of the southeastern Coastal Plain and specifically the Lower Flint River basin. The model was adapted to local conditions using observed data, values from the literature and the STICS's optimization function. Calibration was conducted using data from relatively uniform environmental conditions from two treatments of a one-year dataset, similarly to the strategy used by Jégo, et al. (2011), that led to good evaluation results. Validation was conducted using different irrigation and fertilization strategies from 2018 and 2019. Validation showed that the calibrated cultivar P1870 provided good predictions of aboveground biomass, nitrogen uptake, yield, and nitrogen in the grain. STICS gave good predictions for 2019 despite that growing season being hotter and shorter than the 2018 season used for calibration. Observed crop growth stages were consistent with the simulated phenology. Simulations of soil water and nitrogen content were not as good as the simulation of crop variables. Soil water content simulation could be improved by using actual soil water retention curves of the soils used in the study rather than curves developed using the van Genuchten method. Soil moisture sensors that measure

volumetric water content would also likely improve the simulation results by providing directly comparable observations.

Most of the discrepancies between the simulated and the measured soil N content values were observed as over-predictions during the period of rapid maize growth. This was probably due to underprediction of nitrogen percolation through the soil profile, or to a mistake in the simulation of nitrogen uptake that in reality could be higher in the vegetative phase of development and lower afterwards. The under-prediction of observed values after tasseling would confirm the second assumption. To overcome this problem and assess the actual uptake pattern, more observation points should be collected during the critical phase of rapid vegetative growth between V8 and VT (30 to 60 DAP). Four or five points during the growing season may be enough to catch the general trend, but not to properly define it.

In this study, three different fertilizer types were used prior to planting, at planting and for the side-dress applications. The model does not allow the user to differentiate between the fertilizer type used in the fertilization events. This likely reduces the model's ability to accurately estimate soil N content. Another simulation variable which requires improvement is LAI. That being said, the accuracy obtained in this context is still useful to reproduce main trends in the response of output variables associated to seasonal weather conditions, soil and management practices.

Overall, the hypothesis that STICS predictions are representative of observed conditions in the southeastern Coastal Plain can be accepted, but there is still room for improvement of the model. The last hypothesis of consistent predictions through spatial and temporal variability is proved by the homogeneity of evaluation indices among different treatments and years. However, the model should be further evaluated in different experimental conditions in terms of weather patterns and soil conditions. Indeed, is important to take into consideration that the calibration was performed

using data from a wet year that do not ensure that the simulations would be acceptable in very dry conditions (Gao X., 2018). Exhaustive evaluation would reinforce the assessment that model simulations can accurately capture the relative differences between treatments.

Model-based fertilization scheduling

A model-based methodology was presented in this thesis to identify the optimum timing of N side-dress application. The performance of the proposed methodology indicated that although promising, this approach is not yet robust enough to provide reliable recommendations. It should be noted that the identification of optimum timing of application is a complex problem (Mesbah, et al., 2017). The approached used in this study to use simulated decreases in soil N may not be the best strategy to trigger fertilization and further studies are necessary to develop an improved approach. However, the use of a process-based crop model is an important step towards development of a reliable digital decision toolkit able to make accurate predictions and to gain trust from the final user, the farmer.

References

Abendroth, L.J., R.W. Elmore, M.J. Boyer and S.K. Marlay. 2011. Corn growth and development. PMR.

Alboresi, A., C. Gestin, M.T. Leydecker, M. Bedu, C. Meyer and H.N. Truong. 2005. Nitrate, a signal relieving seed dormancy in Arabidopsis. Plant, cell & environment 28: 500-512.

Allen R.G., P.L.S., Raes D., Smith M. 1998. Crop evapotranspiration - Guidelines for computing crop water requirementsFAO, Rome.

Andraski, T.W. and L.G. Bundy. 2002. Using the presidedress soil nitrate test and organic nitrogen crediting to improve corn nitrogen recommendations. Agronomy Journal 94: 1411-1418.

Archontoulis S., L.M. 2017. How Fast and Deep do Corn Roots Grow in Iowa? ICM News.

Arnold J. G., R.S., R. S. Muttiah, J. R. Williams. 2007. Large area hydrologic modeling and assessment part I: Model Development. JAWRA Journal of the American Water Resources Association 34: 73-89.

Banger, K., M. Yuan, J. Wang, E.D. Nafziger and C.M. Pittelkow. 2017. A Vision for Incorporating environmental effects into nitrogen management decision support tools for US maize production. Frontiers in plant science 8: 1270.

Basso, B., D. Cammarano, C. Fiorentino and J.T. Ritchie. 2013. Wheat yield response to spatially variable nitrogen fertilizer in Mediterranean environment. European Journal of Agronomy 51: 65-70.

Beaudoin, N., B. Mary, M. Launay and N. Brisson. 2009. Conceptual basis, formalisations and parameterization of the STICS crop modelQuae.

Beevers, L. and R. Hageman. 1969. Nitrate reduction in higher plants. Annual Review of Plant Physiology 20: 495-522.

Below, F. 1987. Effect of mixed N nutrition on nutrient accumulation, partitioning, and productivity of corn. J. Fert. Issues 4: 79-85.

Bender, R.R., J.W. Haegele, M.L. Ruffo and F.E. Below. 2013. Nutrient uptake, partitioning, and remobilization in modern, transgenic insect-protected maize hybrids. Agronomy Journal 105: 161-170.

Binder, D.L., D.H. Sander and D.T. Walters. 2000. Maize response to time of nitrogen application as affected by level of nitrogen deficiency. Agronomy Journal 92: 1228-1236.

Bonachela, S. 1996. Root growth of triticale and barley grown for grain or for forage-plus-grain in a Mediterranean climate. Plant and Soil 183: 239-251. doi:10.1007/bf00011439.

Boote, K., J. Jones, G. Hoogenboom and N. Pickering. 1998. The CROPGRO model for grain legumes. Understanding options for agricultural production. Springer. p. 99-128.

Boote, K.J., L.H. Allen Jr, P.V. Prasad and J.W. Jones. 2010. Testing effects of climate change in crop models. Handbook of climate change and agroecosystems. Imperial College Press, London: 109-129.

Bouaziz, A. and L. Bruckler. 1989. Modeling Wheat Seedling Growth and Emergence: I. Seedling Growth Affected by Soil Water Potential. Soil Science Society of America Journal 53: 1832-1838. doi:10.2136/sssaj1989.03615995005300060036x.

Boussadia, O., K. Steppe, H. Zgallai, S.B. El Hadj, M. Braham, R. Lemeur and M.-C. Van Labeke. 2010. Effects of nitrogen deficiency on leaf photosynthesis, carbohydrate status and biomass production in two olive cultivars 'Meski'and 'Koroneiki'. Scientia Horticulturae 123: 336-342.

Brilli, L., L. Bechini, M. Bindi, M. Carozzi, D. Cavalli, R. Conant, C.D. Dorich, L. Doro, F. Ehrhardt and R. Farina. 2017. Review and analysis of strengths and weaknesses of agro-ecosystem models for simulating C and N fluxes. Sci. Total Environ. 598: 445-470.

Brilli, L., L. Bechini, M. Bindi, M. Carozzi, D. Cavalli, R. Conant, C.D. Dorich, L. Doro, F. Ehrhardt, R. Farina, R. Ferrise, N. Fitton, R. Francaviglia, P. Grace, I. Iocola, K. Klumpp, J. Leonard, R. Martin, R.S. Massad, S. Recous, G. Seddaiu, J. Sharp, P. Smith, W.N. Smith, J.F. Soussana and G. Bellocchi. 2017. Review and analysis of strengths and weaknesses of agro-ecosystem models for simulating C and N fluxes. Sci Total Environ 598: 445-470. doi:10.1016/j.scitotenv.2017.03.208.

Brisson, N., C. Gary, E. Justes, R. Roche, B. Mary, D. Ripoche, D. Zimmer, J. Sierra, P. Bertuzzi and P. Burger. 2003. An overview of the crop model STICS. European Journal of agronomy 18: 309-332.

Brisson, N., B. Mary, D. Ripoche, M.H. Jeuffroy, F. Ruget, B. Nicoullaud, P. Gate, F. Devienne-Barret, R. Antonioletti and C. Durr. 1998. STICS: a generic model for the simulation of crops and their water and nitrogen balances. I. Theory and parameterization applied to wheat and corn.

Brisson, N. and A. Perrier. 1991. A semiempirical model of bare soil evaporation for crop simulation models. Water resources research 27: 719-727.

Brutsaert, W. 1982. Evaporation into the atmosphere: Theory. History, and Applications 1.

Bundy, A.G. 2006. Sidedressing nitrogen: useful on all soils? Wisconsin Fertilizer, Aglime & Pest Management Conference.

Bundy, L. and E. Malone. 1988. Effect of residual profile nitrate on corn response to applied nitrogen. Soil Science Society of America Journal 52: 1377-1383.

Cassman, K.G., A. Dobermann and D.T. Walters. 2002. Agroecosystems, nitrogen-use efficiency, and nitrogen management. AMBIO: A Journal of the Human Environment 31: 132-141.

Christianson, L.E. and R. Harmel. 2015. 4R Water quality impacts: An assessment and synthesis of forty years of drainage nitrogen losses. Journal of environmental quality 44: 1852-1860.

Ciampitti, I.A. and T.J. Vyn. 2012. Physiological perspectives of changes over time in maize yield dependency on nitrogen uptake and associated nitrogen efficiencies: A review. Field Crops Research 133: 48-67.

Claudio O.Stockle, S.A.M., Gaylon S. Campbell. 1994. CropSyst, a cropping systems simulation model: water/nitrogen budgets and crop yield. Agricultural systems 46: 335-359.

Coleman, D.C., D.M. Swift and J.E. Mitchell. 2004. From the Frontier to the Biosphere. Rangelands 26: 8-16.

DeBruin, J., C.D. Messina, E. Munaro, K. Thompson, C. Conlon-Beckner, L. Fallis, D.M. Sevenich, R. Gupta and K.S. Dhugga. 2013. N distribution in maize plant as a marker for grain yield and limits on its remobilization after flowering. Plant breeding 132: 500-505.

Duncan, W. 1971. SIMCOT, a simulator of cotton growth and yield.

Duru, M., H. Ducrocq and V. Tirilly. 1995. Modeling growth of cocksfoot (Dactylis glomerata L.) and tall fescue (Festuca arundinacea Schreb.) at the end of spring in relation to herbage nitrogen status. Journal of plant nutrition 18: 2033-2047.

Egelkraut, T., D. Kissel, M. Cabrera and W. Adkins. 2003. Predicting N mineralized in a Georgia Coastal Plain field. Nutrient cycling in agroecosystems 66: 1-12.

Fixen, P., F. Brentrup, T. Bruulsema, F. Garcia, R. Norton and S. Zingore. 2015. Nutrient/fertilizer use efficiency: measurement, current situation and trends. p. 8-38.

Gao X., C.X., Biggs T.W., Yao H. 2018. Separating Wet and Dry Years to Improve Calibration af SWAT in Barrett Watershed, Southern California. water 10: 274.

Gerwitz, A. and E. Page. 1974. An empirical mathematical model to describe plant root systems. Journal of Applied Ecology: 773-781.

Gutiérrez, R.A., L.V. Lejay, A. Dean, F. Chiaromonte, D.E. Shasha and G.M. Coruzzi. 2007. Qualitative network models and genome-wide expression data define carbon/nitrogen-responsive molecular machines in Arabidopsis. Genome biology 8: R7.

Havlin, J.L., S.L. Tisdale, W.L. Nelson and J.D. Beaton. 2016. Soil fertility and fertilizersPearson Education India.

Heady, E.O. 1957. An econometric investigation of the technology of agricultural production functions. Econometrica: Journal of the Econometric Society: 249-268.

Heady, E.O. and L.D. John. 1960. Agricultural production funcitons. Agricultural production funcitons.

Heitholt, J., R. Johnson and D. Ferris. 1991. Stomatal limitation to carbon dioxide assimilation in nitrogen and drought-stressed wheat. Crop Science 31: 135-139.

Hénault, C., F. Bizouard, P. Laville, B. Gabrielle, B. Nicoullaud, J. Germon and P. Cellier. 2005. Predicting in situ soil N2O emission using NOE algorithm and soil database. Global Change Biology 11: 115-127.

Henry F. Perkins, J.E.H., Nancy W. Barbour. 1986. Soil Characteristics of Selected Areas of the Coastal Plain Experiment Station and ABAC Research FarmsAgricultural Experiment Stations. The University of Georgia.

Hirel, B. and A. Gallais. 2011. Nitrogen use efficiency: physiological, molecular and genetic investigations towards crop improvement. Advances in maize 3: 285-310.

Holzworth, D.P., N.I. Huth, P.G. deVoil, E.J. Zurcher, N.I. Herrmann, G. McLean, K. Chenu, E.J. van Oosterom, V. Snow and C. Murphy. 2014. APSIM–evolution towards a new generation of agricultural systems simulation. Environmental Modelling & Software 62: 327-350.

Hoogenboom, G., Jones, J.W., Wilkens, P.W., Porter, C.H., Boote, K.J., Hunt, L.A., Singh, U., Lizaso, J.L., White, J.W., Uryasev, O., Royce, F.S., Ogoshi, R., Gijsman, A.J., Tsuji, G.Y., Koo, J. 2012. Decision Support System for Agrotechnology Transfer (DSSAT) Version 4.5 University of Hawaii, Honolulu, Hawaii.

Hunt, L.A., and S. Pararajasingham. 1995. CROPSIM-WHEAT: A model describing the growth and development of wheat. Canadian J. Plant Science 75: 619-632.

Hutson, J. 20003. LEACHM - a process-based model of water and solutemovement, transformations, plant uptake and chemical reactions in theunsaturated zone.

Idso, S.B., R.D. Jackson and R.J. Reginato. 1978. Extending the" degree day" concept of plant phenological development to include water stress effects. Ecology 59: 431-433.

Jaaffar, Z. and F. Gardner. 1988. Canopy development, yield, and market quality in peanut as affected by genotype and planting pattern. Crop science 28: 299-305.

Janssen, B.H., F. Guiking, D. Van der Eijk, E. Smaling, J. Wolf and H. Van Reuler. 1990. A system for quantitative evaluation of the fertility of tropical soils (QUEFTS). Geoderma 46: 299-318.

Jégo, G., E. Pattey, G. Bourgeois, C.F. Drury and N. Tremblay. 2011. Evaluation of the STICS crop growth model with maize cultivar parameters calibrated for Eastern Canada. Agronomy for Sustainable Development 31: 557-570. doi:10.1007/s13593-011-0014-4.

Jérémie Lecoeur, T.R.S. 2001. Analysis of nitrogen partitioning in field pea resulting in linear increase in nitrogen harvest index. Field Crops Research 71: 151-158.

Jeuffroy, M.-H. and S. Recous. 1999. Azodyn: a simple model simulating the date of nitrogen deficiency for decision support in wheat fertilization. European journal of Agronomy 10: 129-144.

Jones, C. and J. Kiniry. 1986. CERES-Maize: A Simulation Model of Maize Growth and Development. Texas A&M University Press. College Station, Texas.

Jones, C.A. 1986. CERES-Maize; a simulation model of maize growth and development.

Jones, J. 1993. Decision support systems for agricultural development. Systems approaches for agricultural development. Springer. p. 459-471.

Jones, J.W., J.M. Antle, B. Basso, K.J. Boote, R.T. Conant, I. Foster, H.C.J. Godfray, M. Herrero, R.E. Howitt and S. Janssen. 2017. Brief history of agricultural systems modeling. Agricultural systems 155: 240-254.

Jones, J.W., G. Hoogenboom, C.H. Porter, K.J. Boote, W.D. Batchelor, L. Hunt, P.W. Wilkens, U. Singh, A.J. Gijsman and J.T. Ritchie. 2003. The DSSAT cropping system model. European journal of agronomy 18: 235-265.

Jung, P.E., L. Peterson and L. Schrader. 1972. Response of Irrigated Corn to Time, Rate, and Source of Applied N on Sandy Soils 1. Agronomy Journal 64: 668-670.

Keating, B.A., P.S. Carberry, G.L. Hammer, M.E. Probert, M.J. Robertson, D. Holzworth, N.I. Huth, J.N. Hargreaves, H. Meinke and Z. Hochman. 2003. An overview of APSIM, a model designed for farming systems simulation. European journal of agronomy 18: 267-288.

Kim, K.-I., D.E. Clay, C. Carlson, S. Clay and T. Trooien. 2008. Do synergistic relationships between nitrogen and water influence the ability of corn to use nitrogen derived from fertilizer and soil? Agronomy Journal 100: 551-556.

Kimball, B.A., K.J. Boote, J.L. Hatfield, L.R. Ahuja, C. Stockle, S. Archontoulis, C. Baron, B. Basso, P. Bertuzzi, J. Constantin, D. Deryng, B. Dumont, J.-L. Durand, F. Ewert, T. Gaiser, S. Gayler, M.P. Hoffmann, Q. Jiang, S.-H. Kim, J. Lizaso, S. Moulin, C. Nendel, P. Parker, T. Palosuo, E. Priesack, Z. Qi, A. Srivastava, T. Stella, F. Tao, K.R. Thorp, D. Timlin, T.E. Twine, H. Webber, M. Willaume and K. Williams. 2019. Simulation of maize evapotranspiration: An inter-comparison among 29 maize models. Agricultural and Forest Meteorology 271: 264-284. doi:10.1016/j.agrformet.2019.02.037.

Kiniry, J., C. Tischler and G. Van Esbroeck. 1999. Radiation use efficiency and leaf CO2 exchange for diverse C4 grasses. Biomass Bioenergy 17: 95-112.

Köhne, J.M., S. Köhne and J. Šimůnek. 2009. A review of model applications for structured soils: a) Water flow and tracer transport. Journal of contaminant hydrology 104: 4-35.

Krouk, G., N.M. Crawford, G.M. Coruzzi and Y.-F. Tsay. 2010. Nitrate signaling: adaptation to fluctuating environments. Current opinion in plant biology 13: 265-272.

Kucharik, C.J. and N. Ramankutty. 2005. Trends and Variability in U.S. Corn Yields Over the Twentieth Century. Earth Interactions 9: 1-29. doi:10.1175/ei098.1.

Ladha, J.K., H. Pathak, T. J. Krupnik, J. Six and C. van Kessel. 2005. Efficiency of Fertilizer Nitrogen in Cereal Production: Retrospects and Prospects. Advances in Agronomy Volume 87. p. 85-156.

Legates D.R., M.G.J. 1999. Evaluating the use of "goodness-of-fit" Measures in hydrologic and hydroclimatic model validation. Water Resources Research 35: 233-241.

Li, C., S. Frolking and T.A. Frolking. 1992. A model of nitrous oxide evolution from soil driven by rainfall events: 1. Model structure and sensitivity. Journal of Geophysical Research: Atmospheres 97: 9759-9776.

Li, C., W. Salas, R. Zhang, C. Krauter, A. Rotz and F. Mitloehner. 2012. Manure-DNDC: a biogeochemical process model for quantifying greenhouse gas and ammonia emissions from livestock manure systems. Nutrient Cycling in Agroecosystems 93: 163-200.

Liakos, V., G. Vellidis, M. Tucker, C. Lowrance and X. Liang. 2015. A decision support tool for managing precision irrigation with center pivots. Precision agriculture'15. Wageningen Academic Publishers. p. 713-720.

Liang, X., V. Liakos, O. Wendroth and G. Vellidis. 2016. Scheduling irrigation using an approach based on the van Genuchten model. Agricultural Water Management 176: 170-179.

Magdoff, F., D. Ross and J. Amadon. 1984. A Soil Test for Nitrogen Availability to Corn 1. Soil Science Society of America Journal 48: 1301-1304.

Marella, R. and M. Berndt. 2005. Water withdrawals and trends from the Floridian Aquifer System in the Southerneast Uniter States, 1950-2000.

Marschner, H. 2011. Marschner's mineral nutrition of higher plantsAcademic press.

McCann, R., M. J. McFarland and J. A. Witz. 1991. NEAR-SURFACE BARE SOIL TEMPERATURE MODEL FOR BIOPHYSICAL MODELS. Transactions of the ASAE 34: 748-0755. doi:https://doi.org/10.13031/2013.31726.

McCown, R.L., G.L. Hammer, J.N.G. Hargreaves, D.P. Holzworth and D.M. Freebairn. 1996. APSIM: a novel software system for model development, model testing and simulation in agricultural systems research. Agricultural systems 50: 255-271.

Mesbah, M., E. Pattey and G. Jégo. 2017. A model-based methodology to derive optimum nitrogen rates for rainfed crops – a case study for corn using STICS in Canada. Computers and Electronics in Agriculture 142: 572-584. doi:10.1016/j.compag.2017.11.011.

Monteith, J. 1972. Solar radiation and productivity in tropical ecosystems. J. Appl. Ecol. 9: 747-766.

Morris, T.F., T.S. Murrell, D.B. Beegle, J.J. Camberato, R.B. Ferguson, J. Grove, Q. Ketterings, P.M. Kyveryga, C.A.M. Laboski, J.M. McGrath, J.J. Meisinger, J. Melkonian, B.N. Moebius-Clune, E.D. Nafziger, D. Osmond, J.E. Sawyer, P.C. Scharf, W. Smith, J.T. Spargo, H.M. van Es and H. Yang. 2018. Strengths and Limitations of Nitrogen Rate Recommendations for Corn and Opportunities for Improvement. Agronomy Journal 110. doi:10.2134/agronj2017.02.0112.

Muchow, R. 1988. Effect of nitrogen supply on the comparative productivity of maize and sorghum in a semi-arid tropical environment I. Leaf growth and leaf nitrogen. Field Crops Research 18: 1-16.

Mueller, S.M., J.J. Camberato, C. Messina, J. Shanahan, H. Zhang and T.J. Vyn. 2017. Late-split nitrogen applications increased maize plant nitrogen recovery but not yield under moderate to high nitrogen rates. Agronomy Journal 109: 2689-2699.

Muller, B. and P. Martre. 2019. Plant and crop simulation models: powerful tools to link physiology, genetics, and phenomics. J Exp Bot 70: 2339-2344. doi:10.1093/jxb/erz175.

Nafziger, E.D., J.E. Sawyer and R.G. Hoeft. 2004. Formulating N recommendations for corn in the corn belt using recent data.

Nelson, D. and L. Sommers. 1973. Determination of Total Nitrogen in Plant Material 1. Agronomy Journal 65: 109-112.

Noland, R. 2018. A Guide to Corn Production in Georgia.

Ong, C. 1983. Response to temperature in a stand of pearl millet (Pennisetum typhoides S. & H.) 4. Extension of individual leaves. J. Exp. Bot. 34: 1731-1739.

Orfanou A., P.D., Portew W.M. 2019. Maize yield and irrigation applied in conservation and conventional tillage at various plant densities. Water 11(8).

P.H., N. 1981. Changes of pH across te rhizosphere induced by roots. Plant and Soil 61: 7-26.

Pararajasingham, S. and L. Hunt. 1991. Wheat spike temperature in relation to base temperature for grain filling duration. Canadian journal of plant science 71: 63-69.

Parent, B. and F. Tardieu. 2014. Can current crop models be used in the phenotyping era for predicting the genetic variability of yield of plants subjected to drought or high temperature? Journal of experimental botany 65: 6179-6189.

Parton, W.J., D.S. Ojima, C.V. Cole and D.S. Schimel. 1994. A general model for soil organic matter dynamics: sensitivity to litter chemistry, texture and management. Quantitative modeling of soil forming processes: 147-167.

Passioura, J.B. 1996. Simulation models: science, snake oil, education, or engineering? Agron. J. 88: 690-694.

Pinter Jr, P.J., J.C. Ritchie, J.L. Hatfield and G.F. Hart. 2003. The Agricultural Research Service's Remote Sensing Program. Photogrammetric Engineering & Remote Sensing 69: 615-618.

Plant, R.E. 1989. An integrated expert decision support system for agricultural management. Agricultural Systems 29: 49-66.

Polesskaya, O., E. Kashirina and N. Alekhina. 2004. Changes in the activity of antioxidant enzymes in wheat leaves and roots as a function of nitrogen source and supply. Russian journal of plant physiology 51: 615-620.

Priestley, C.H.B. and R. Taylor. 1972. On the assessment of surface heat flux and evaporation using large-scale parameters. Monthly weather review 100: 81-92.

Pruitt, J.D. 2016. A brief history of corn: looking back to move forward.

Qin, Z., D.B. Myers, C.J. Ransom, N.R. Kitchen, S.-Z. Liang, J.J. Camberato, P.R. Carter, R.B. Ferguson, F.G. Fernandez, D.W. Franzen, C.A.M. Laboski, B.D. Malone, E.D. Nafziger, J.E. Sawyer and J.F. Shanahan. 2018. Application of Machine Learning Methodologies for Predicting Corn Economic Optimal Nitrogen Rate. Agronomy Journal 110. doi:10.2134/agronj2018.03.0222.

Raun, W.R. and G.V. Johnson. 1999. Improving nitrogen use efficiency for cereal production. Agronomy journal 91: 357-363.

RETC. 2009. RETC Model Version 6.02. https://www.pc-progress.com/en/Default.aspx?retc.

Ritchie, J. 1985. Description and performance of CERES wheat: A user-oriented wheat yield model. ARS wheat yield project: 159-175.

Roenneberg, T. and J. Rehman. 1996. Nitrate, a nonphotic signal for the circadian system. The FASEB journal 10: 1443-1447.

Ruget, F., N. Brisson, R. Delécolle and R. Faivre. 2002. Sensitivity analysis of a crop simulation model, STICS, in order to choose the main parameters to be estimated. Agronomie 22: 133-158. doi:10.1051/agro:2002009.

Rutan, J. and K. Steinke. 2017. Determining corn nitrogen rates using multiple prediction models. Journal of Crop Improvement 31: 780-800. doi:10.1080/15427528.2017.1359715.

Saglam M., S.H.Y., Bary A.I., Miles C.A., Ghimire S., Inglis D.A., Flury M. 2017. Modeling the effect of biodegradable paper and plastic mulch on soil moisture dynamics. Agricultural Water Management 193: 240-250. doi:http://dx.doi.org/10.1016/j.agwat.2017.08.011.

Sansoulet, J., E. Pattey, R. Kröbel, B. Grant, W. Smith, G. Jégo, R.L. Desjardins, N. Tremblay and G. Tremblay. 2014. Comparing the performance of the STICS, DNDC, and DayCent models for predicting N uptake and biomass of spring wheat in Eastern Canada. Field Crops Research 156: 135-150. doi:10.1016/j.fcr.2013.11.010.

Sawyer, J., E. Nafziger, G. Randall, L. Bundy, G. Rehm and B. Joern. 2006. Concepts and rationale for regional nitrogen rate guidelines for corn. Iowa State University-University Extension, Ames, Iowa.

Scheible, W.-R., R. Morcuende, T. Czechowski, C. Fritz, D. Osuna, N. Palacios-Rojas, D. Schindelasch, O. Thimm, M.K. Udvardi and M. Stitt. 2004. Genome-wide reprogramming of primary and secondary metabolism, protein synthesis, cellular growth processes, and the regulatory infrastructure of Arabidopsis in response to nitrogen. Plant physiology 136: 2483-2499.

Sechley, K., T. Yamaya and A. Oaks. 1992. Compartmentation of nitrogen assimilation in higher plants. International review of cytology. Elsevier. p. 85-163.

Setiyono, T.D., H. Yang, D.T. Walters, A. Dobermann, R.B. Ferguson, D.F. Roberts, D.J. Lyon, D.E. Clay and K.G. Cassman. 2011. Maize-N: A Decision Tool for Nitrogen Management in Maize. Agronomy Journal 103. doi:10.2134/agronj2011.0053.

Shanahan, J., N. Kitchen, W. Raun and J.S. Schepers. 2008. Responsive in-season nitrogen management for cereals. Computers and electronics in agriculture 61: 51-62.

Shock, C., A. Akin, L. Unlenen, E. Feibert, K. Nelson and A. Tschida. 2003. A comparison of soil water potential and soil water content sensors. Special Report 1048: 235-240.

Sierra, J., N. Brisson, D. Ripoche and C. Noël. 2003. Application of the STICS crop model to predict nitrogen availability and nitrate transport in a tropical acid soil cropped with maize. Plant Soil 256: 333-345.

Sinclair, T.R. 1986. Water and nitrogen limitations in soybean grain production I. Model development. Field Crops Research 15: 125-141.

Sinclair, T.R. and R.C. Muchow. 1995. Effect of Nitrogen Supply on Maize Yield: I. Modeling Physiological Responses. Agronomy Journal 87: 632-641. doi:10.2134/agronj1995.00021962008700040005x.

Singels, A. and J. De Jager. 1991. Refinement and validation of the PUTU wheat crop growth model 3. Grain growth. South African Journal of Plant and Soil 8: 73-77.

Slabbers, P.J. 1980. Practical prediction of actual evapotranspiration. Irrigation Science 1: 185-196. doi:10.1007/bf00270883.

Spaeth, S.C. and T.R. Sinclair. 1985. Linear Increase in Soybean Harvest Index during Seed-Filling1. Agronomy Journal 77: 207-211. doi:10.2134/agronj1985.00021962007700020008x.

Spedding. 1976. Editorial. Agricultural Systems 1: 1-3.

Stanford, G. 1973. Rationale for Optimum Nitrogen Fertilization in Corn Production 1. Journal of Environmental Quality 2: 159-166.

Stitt, M. 1999. Nitrate regulation of metabolism and growth. Current opinion in plant biology 2: 178-186.

Thomson, S.J. and C.F. Armstrong. 1987. Calibration of the Watermark model 200 soil moisture sensor. Appl. Eng. Agric 3: 186-189.

Valbuena, R., A. Hernando, J.A. Manzanera, E.B. Görgens, D.R.A. Almeida, C.A. Silva and A. García-Abril. 2019. Evaluating observed versus predicted forest biomass: R-squared, index of agreement or maximal information coefficient? European Journal of Remote Sensing 52: 345-358. doi:10.1080/22797254.2019.1605624.

Van Dyne, G. and J. Anway. 1976. A research program for and the process of building and testing grassland ecosystem models. Rangeland Ecology & Management/Journal of Range Management Archives 29: 114-122.

van Ittersum, M.K., P.A. Leffelaar, H. Van Keulen, M.J. Kropff, L. Bastiaans and J. Goudriaan. 2003. On approaches and applications of the Wageningen crop models. European journal of agronomy 18: 201-234.

Vellidis, G., M. Tucker, C. Perry, C. Kvien and C. Bednarz. 2008. A real-time wireless smart sensor array for scheduling irrigation. Computers and electronics in agriculture 61: 44-50.

Vellidis, G., M. Tucker, C. Perry, D. Reckford, C. Butts, H. Henry, V. Liakos, R. Hill and W. Edwards. 2013. A soil moisture sensor-based variable rate irrigation scheduling system. Precision agriculture'13. Springer. p. 713-720.

Vos, J., P. Van Der Putten and C. Birch. 2005. Effect of nitrogen supply on leaf appearance, leaf growth, leaf nitrogen economy and photosynthetic capacity in maize (Zea mays L.). Field Crops Research 93: 64-73.

Walch-Liu, P., I.I. Ivanov, S. Filleur, Y. Gan, T. Remans and B.G. Forde. 2005. Nitrogen regulation of root branching. Annals of botany 97: 875-881.

Wang, R., K. Guegler, S.T. LaBrie and N.M. Crawford. 2000. Genomic analysis of a nutrient response in Arabidopsis reveals diverse expression patterns and novel metabolic and potential regulatory genes induced by nitrate. The Plant Cell 12: 1491-1509.

Wang, R., M. Okamoto, X. Xing and N.M. Crawford. 2003. Microarray analysis of the nitrate response in Arabidopsis roots and shoots reveals over 1,000 rapidly responding genes and new linkages to glucose, trehalose-6-phosphate, iron, and sulfate metabolism. Plant physiology 132: 556-567.

Wang, R., X. Xing and N. Crawford. 2007. Nitrite acts as a transcriptome signal at micromolar concentrations in Arabidopsis roots. Plant Physiology 145: 1735-1745.

Whitmore, A. 1991. Method for assessing the goodness of computer simulation of soil processes. Journal of Soil Science 42: 289-299.

Wilkinson, S., M.A. Bacon and W.J. Davies. 2007. Nitrate signalling to stomata and growing leaves: interactions with soil drying, ABA, and xylem sap pH in maize. Journal of Experimental Botany 58: 1705-1716.

Williams, J., C. Jones, J. Kiniry and D.A. Spanel. 1989. The EPIC crop growth model. Transactions of the ASAE 32: 497-0511.

Williams, J., K. Renard and P. Dyke. 1983. EPIC: A new method for assessing erosion's effect on soil productivity. Journal of Soil and water Conservation 38: 381-383.

Williams, J. and V. Singh. 1995. The EPIC Model, Computer Models of Watershed Hydrology. Water Resources Publications, Highlands Ranch, Colorado: 909-1000.

Willmott, C.J. 1981. ON THE VALIDATION OF MODELS. Physical Geography 2: 184-194. doi:10.1080/02723646.1981.10642213.

Worthington, E.B. 1975. The evolution of IBPCambridge University Press Cambridge.

Xu, G., X. Fan and A.J. Miller. 2012. Plant nitrogen assimilation and use efficiency. Annual review of plant biology 63: 153-182.

Yang, H., A. Dobermann, J.L. Lindquist, D.T. Walters, T.J. Arkebauer and K.G. Cassman. 2004. Hybrid-maize—a maize simulation model that combines two crop modeling approaches. Field Crops Res. 87: 131-154.

Yang, J., G.A. Wadsworth, D.L. Rowell and I.G. Burns. 1999. Evaluating a crop nitrogen simulation model, N_ABLE, using a field experiment with lettuce. Nutrient Cycling in Agroecosystems 55: 221-230. doi:10.1023/a:1009818101373.

APPENDIX A

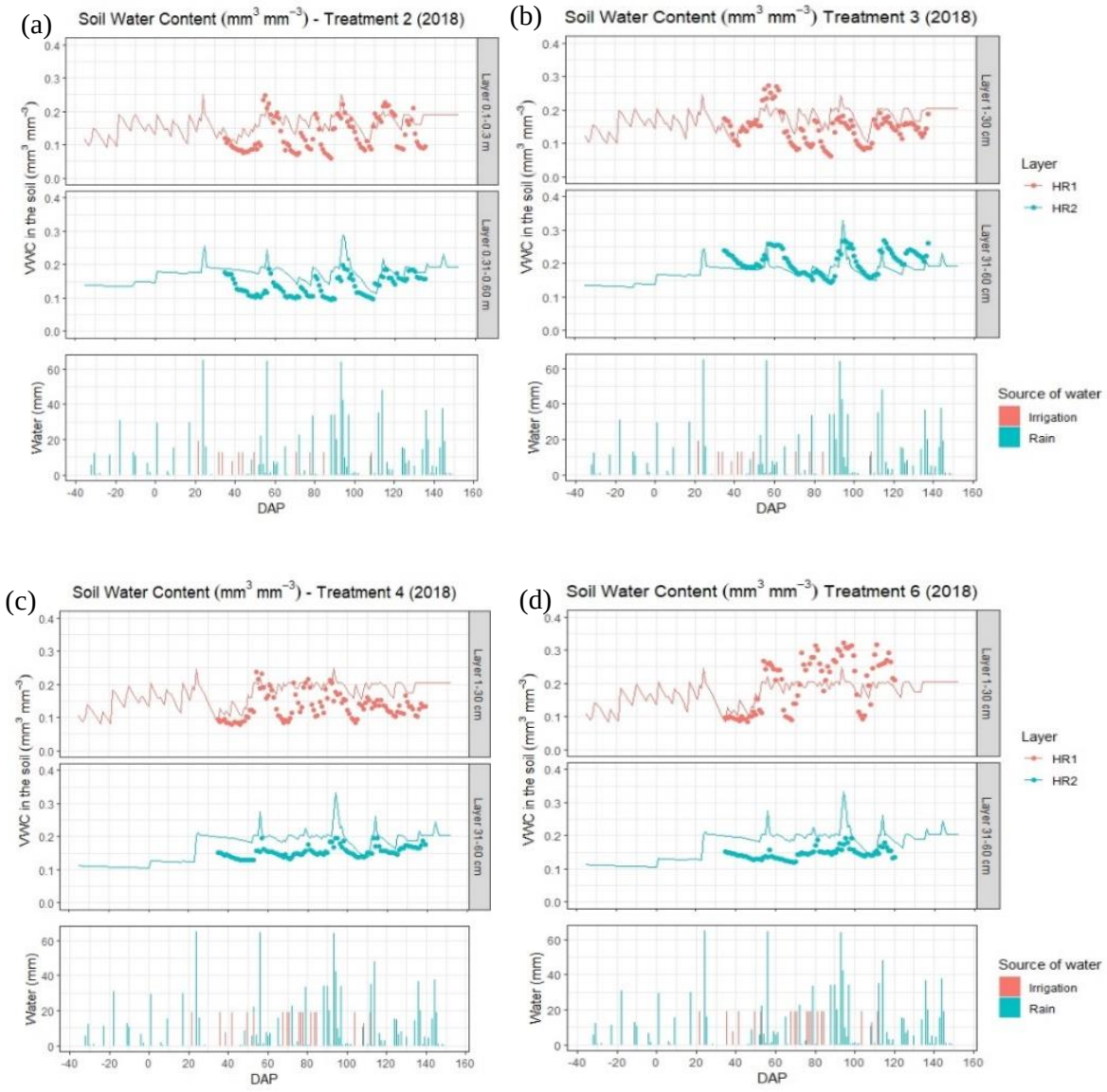
(a)
Soil Water Content (mm3 mm−3) - Treatment 2 (2018)
(b)
Soil Water Content (mm3 mm−3) Treatment 3 (2018)
(c)
Soil Water Content (mm3 mm−3) - Treatment 4 (2018)
(d)
Soil Water Content (mm3 mm−3) Treatment 6 (2018)
VWC in the soil (mm3 mm−3)
Layer 0.1-0.3 m
Layer 0.31-0.60 m
Layer 1-30 cm
Layer 31-60 cm
Water (mm)
DAP
Layer
HR1
HR2
Source of water
Irrigation
Rain

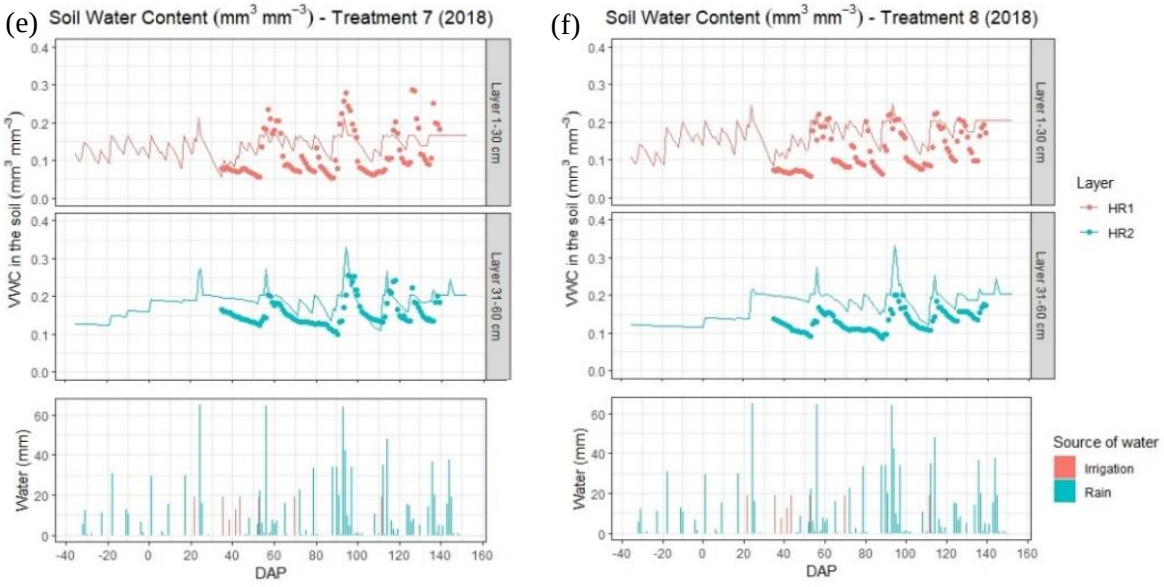

Figure A.1 Dynamics of measured (dots) and simulated (lines) SWC during the growing season expressed as DAP for treatments 2 (a), 3 (b), 4 (c), 6 (d), 7 (e) and 8 (f) of 2018. The bar graphs show irrigation in red and rain in blue expressed in mm over the same x axes

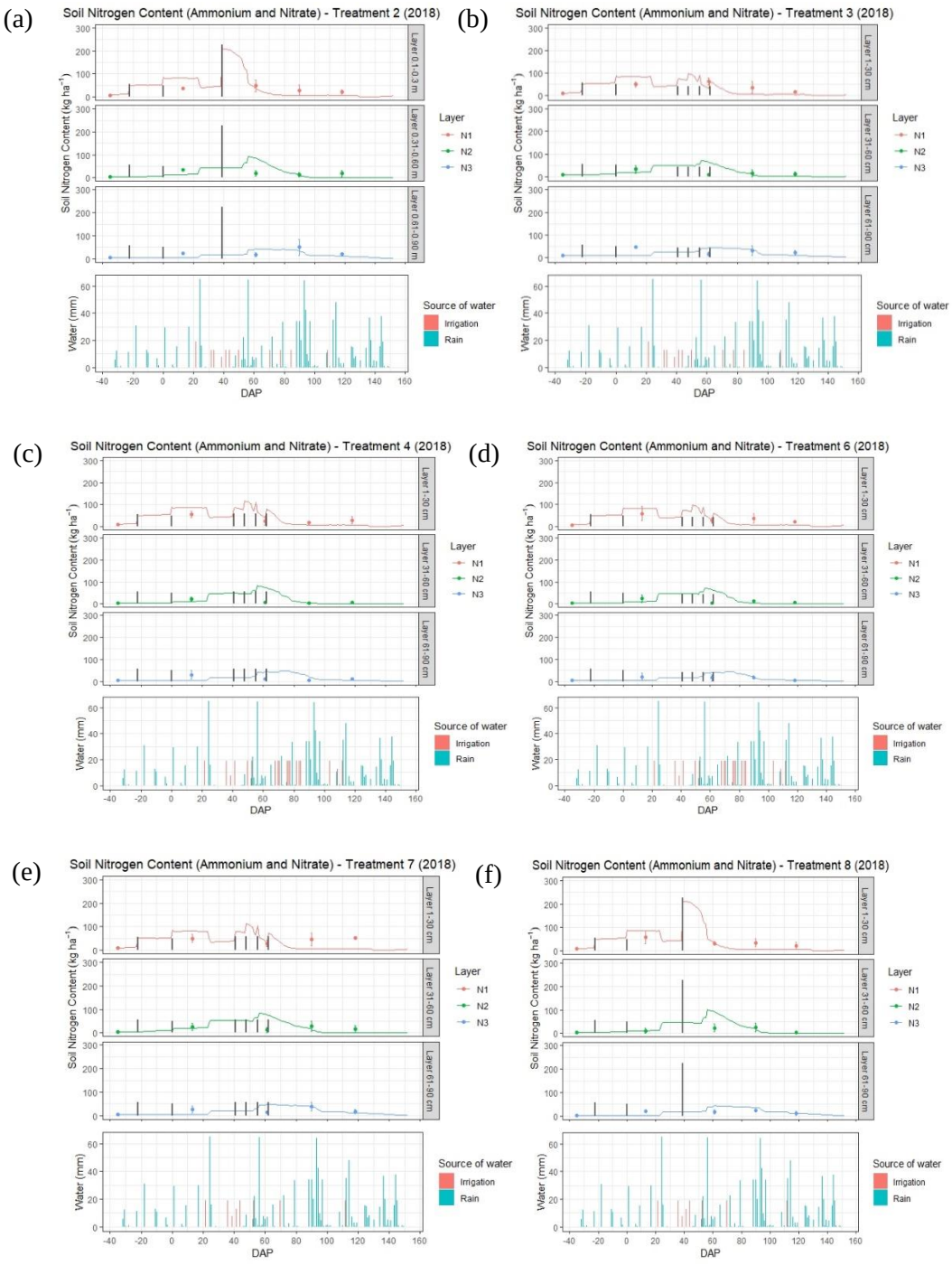

Figure A.2 Dynamics of measured (dots) and simulated (lines) N in the soil during the growing season expressed as DAP for treatments 2 (a), 3 (b), 4 (c), 6 (d), 7 (e) and 8 (f) of 2018. Black bars represent fertilizer applications in kg N ha^{-1}. The bar graphs show irrigation in red and rain in blue expressed in mm over the same x axes

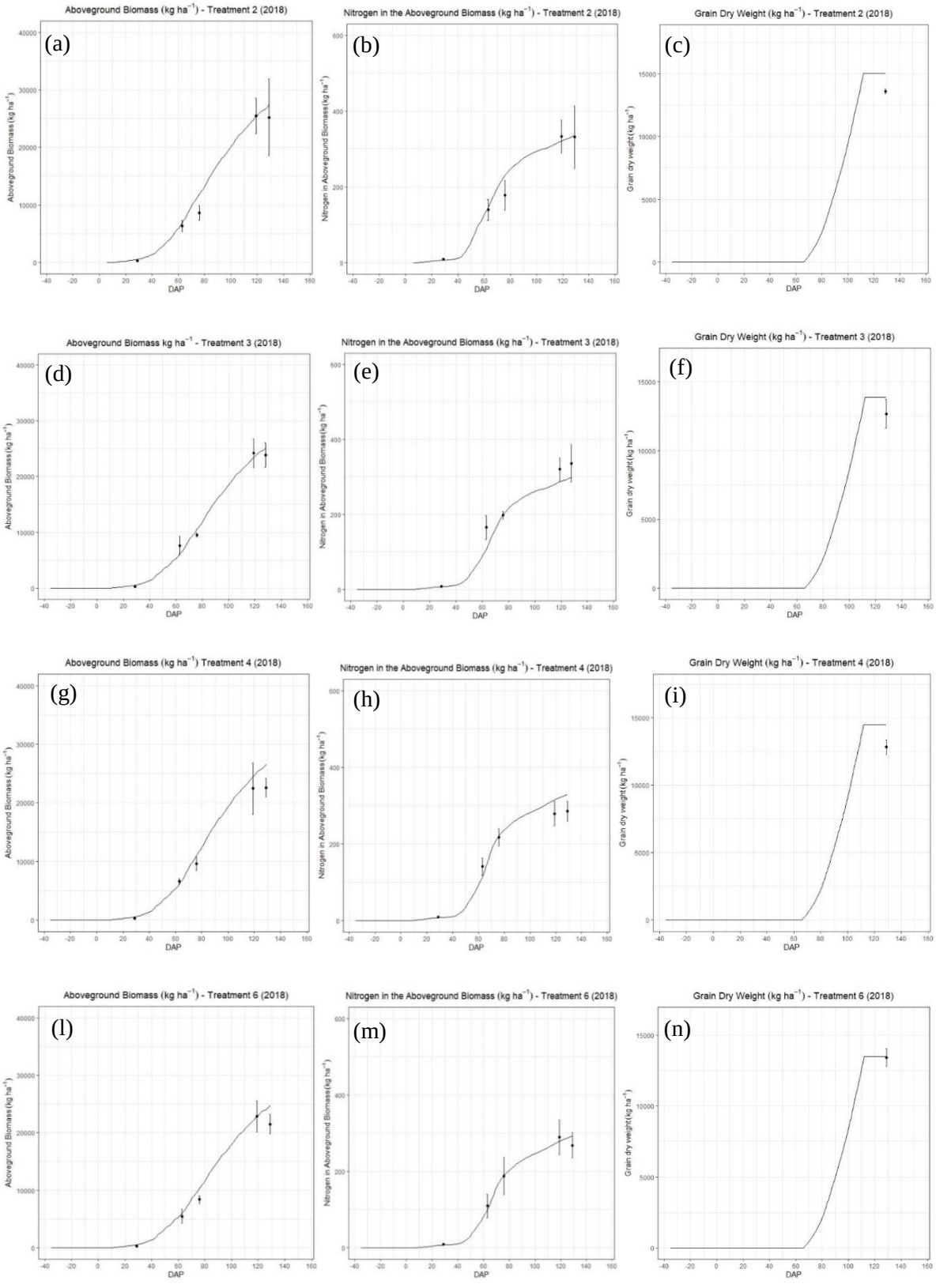
Aboveground Biomass (kg ha^{-1}) - Treatment 2 (2018)
(a)
Aboveground Biomass (kg ha^{-1})
DAP
Nitrogen in the Aboveground Biomass (kg ha^{-1}) - Treatment 2 (2018)
(b)
Nitrogen in Aboveground Biomass (kg ha^{-1})
DAP
Grain Dry Weight (kg ha^{-1}) - Treatment 2 (2018)
(c)
Grain dry weight (kg ha^{-1})
DAP
Aboveground Biomass kg ha^{-1} - Treatment 3 (2018)
(d)
Aboveground Biomass (kg ha^{-1})
DAP
Nitrogen in the Aboveground Biomass (kg ha^{-1}) - Treatment 3 (2018)
(e)
Nitrogen in Aboveground Biomass (kg ha^{-1})
DAP
Grain Dry Weight (kg ha^{-1}) - Treatment 3 (2018)
(f)
Grain dry weight (kg ha^{-1})
DAP
Aboveground Biomass (kg ha^{-1}) Treatment 4 (2018)
(g)
Aboveground Biomass (kg ha^{-1})
DAP
Nitrogen in the Aboveground Biomass (kg ha^{-1}) - Treatment 4 (2018)
(h)
Nitrogen in Aboveground Biomass (kg ha^{-1})
DAP
Grain Dry Weight (kg ha^{-1}) - Treatment 4 (2018)
(i)
Grain dry weight (kg ha^{-1})
DAP
Aboveground Biomass (kg ha^{-1}) - Treatment 6 (2018)
(l)
Aboveground Biomass (kg ha^{-1})
DAP
Nitrogen in the Aboveground Biomass (kg ha^{-1}) - Treatment 6 (2018)
(m)
Nitrogen in Aboveground Biomass (kg ha^{-1})
DAP
Grain Dry Weight (kg ha^{-1}) - Treatment 6 (2018)
(n)
Grain dry weight (kg ha^{-1})
DAP

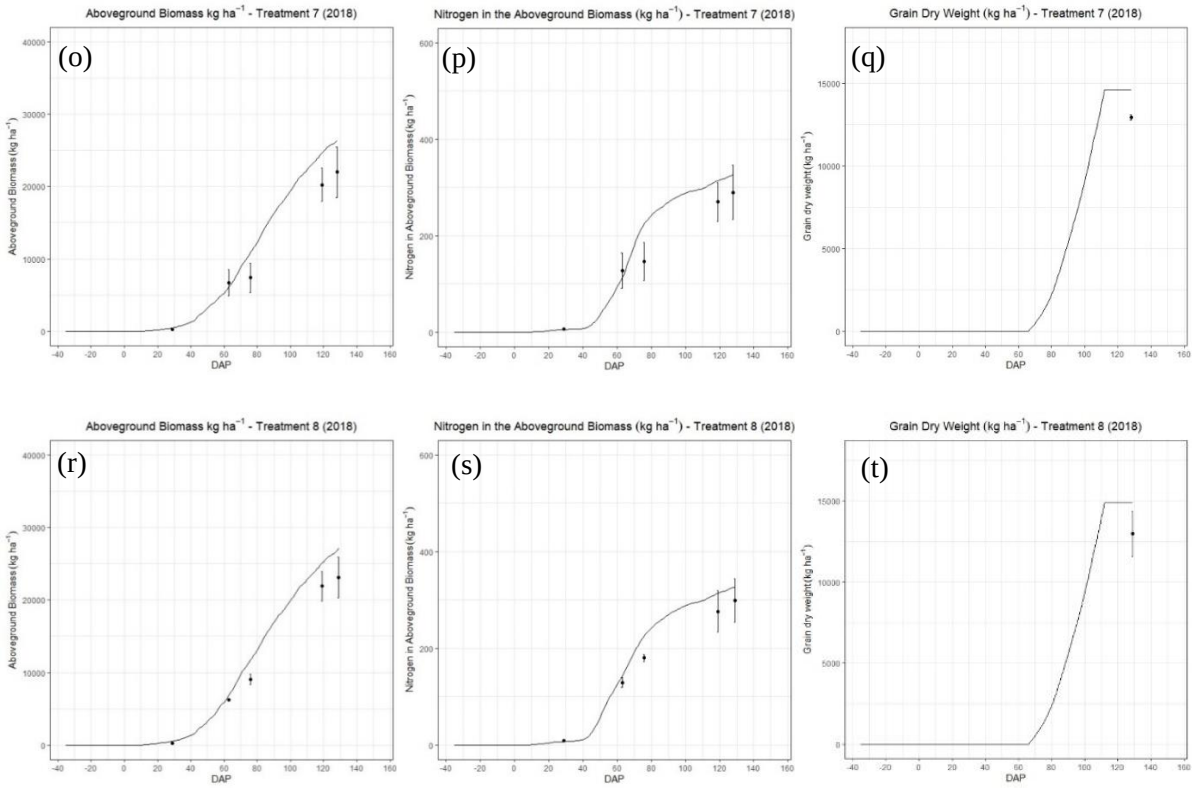

Figure A.3 Dynamics of measured (dots) and simulated (lines) aboveground biomass, N in aboveground biomass and grain dry weight during the growing season expressed as DAP for treatments 2 (a, b, c), 3 (d, e, f), 4 (g, h, i), 6 (l, m, n), 7 (o, p, q) and 8 (r, s, t) of 2018

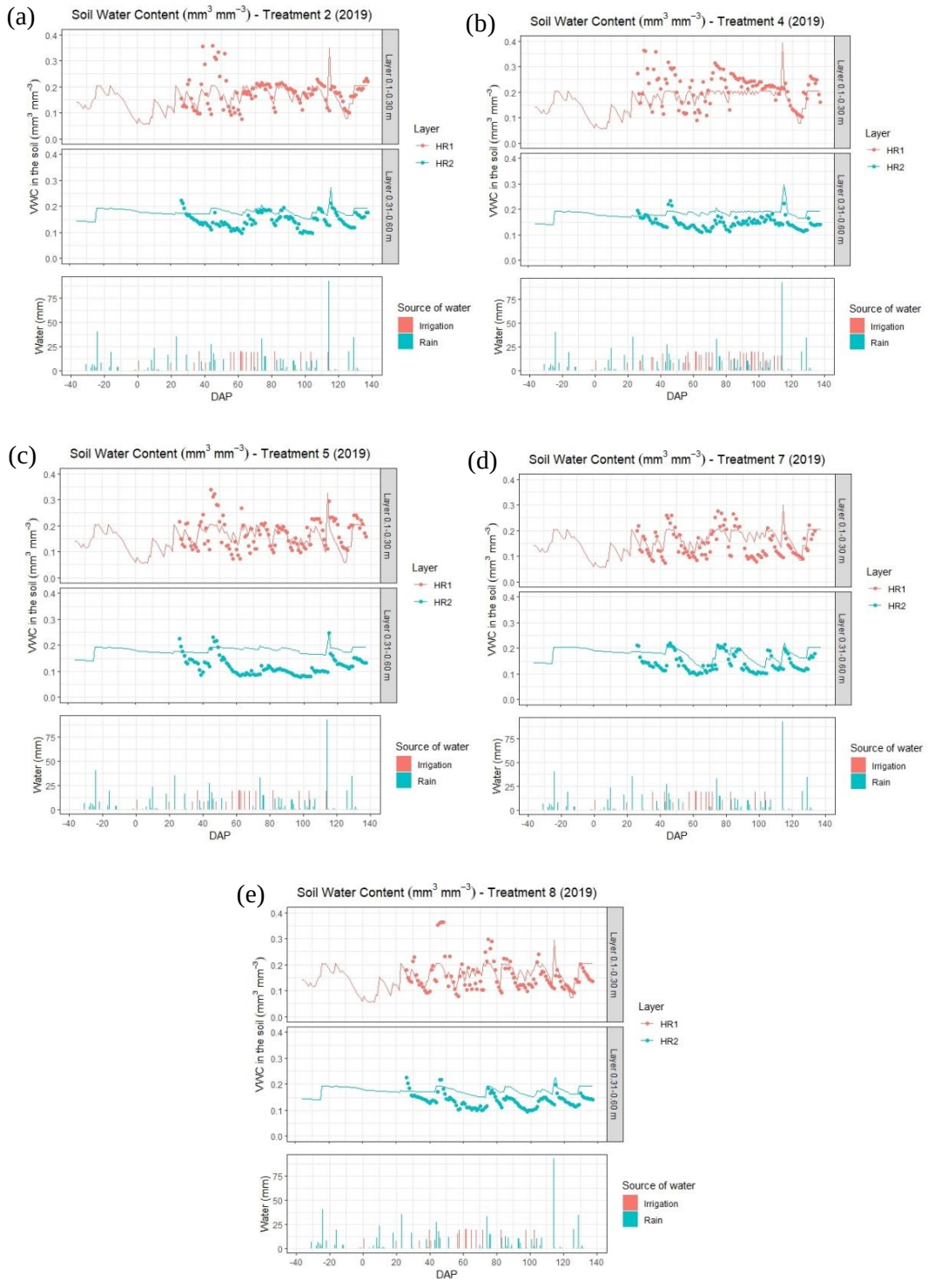

Figure A.4 Dynamics of measured (dots) and simulated (lines) SWC during the growing season expressed as DAP for treatments 2 (a), 4 (b), 5 (c), 7 (d) and 8 (e) of 2019. The bar graphs show irrigation in red and rain in blue expressed in mm over the same x axes

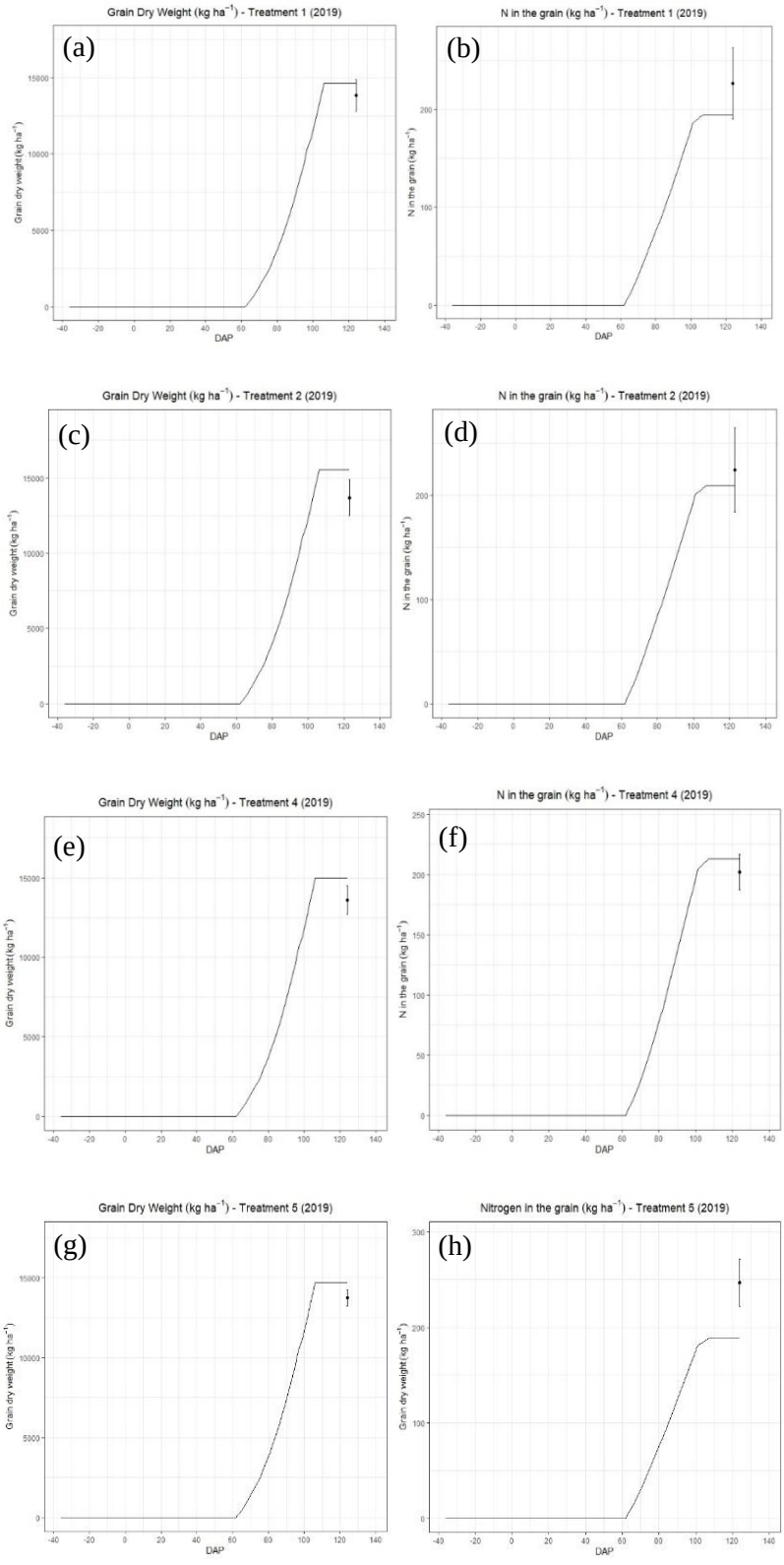
Grain Dry Weight (kg ha^{-1}) - Treatment 1 (2019)
(a)
Grain dry weight(kg ha^{-1})
DAP
N in the grain (kg ha^{-1}) - Treatment 1 (2019)
(b)
N in the grain (kg ha^{-1})
DAP
Grain Dry Weight (kg ha^{-1}) - Treatment 2 (2019)
(c)
Grain dry weight(kg ha^{-1})
DAP
N in the grain (kg ha^{-1}) - Treatment 2 (2019)
(d)
N in the grain (kg ha^{-1})
DAP
Grain Dry Weight (kg ha^{-1}) - Treatment 4 (2019)
(e)
Grain dry weight(kg ha^{-1})
DAP
N in the grain (kg ha^{-1}) - Treatment 4 (2019)
(f)
N in the grain (kg ha^{-1})
DAP
Grain Dry Weight (kg ha^{-1}) - Treatment 5 (2019)
(g)
Grain dry weight(kg ha^{-1})
DAP
Nitrogen in the grain (kg ha^{-1}) - Treatment 5 (2019)
(h)
Grain dry weight(kg ha^{-1})
DAP

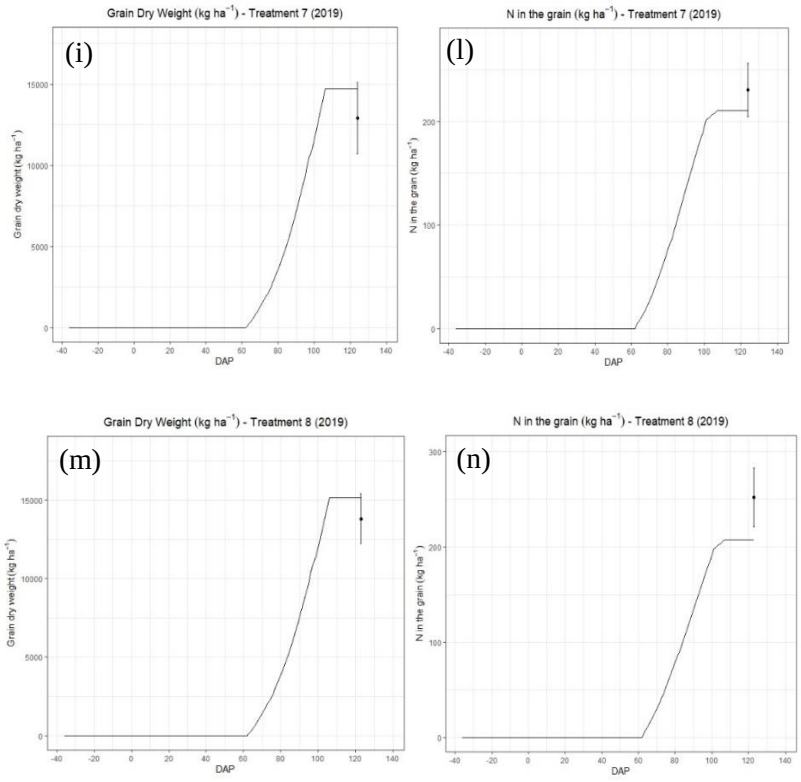

Figure A.5 Validation of grain dry weight and N in the grain of treatments 1 (a, b), 2 (c, d), 4 (e, f), 5 (g, h), 7 (i, l) and 8 (m, n) of 2019. Lines represent the model simulations and dots the observed values at different successive soil layers over time expressed as days after planting (DAP)